Simplified Design of Fire Exposed Concrete Beams and Columns

An Evaluation of Eurocode and Swedish Building Code Against Advanced Computer Models

Johan Rigberth

Department of Fire Safety Engineering
Lund University, Sweden

Brandteknik
Lunds Tekniska Högskola
Lunds Universitet

Report 5063, Lund 2000

Simplified Design of Fire Exposed Concrete Beams and Columns
An Evaluation of Eurocode and the Swedish Building Code Against Advanced Computer Models

Johan Rigberth

Lund 2000

Simplified Design of Fire Exposed Concrete Beams and Columns
An Evaluation of Eurocode and the Swedish Building Code Against Advanced Computer Models

Johan Rigberth

Report 5063
ISSN: 1402-3504
ISRN: LUTVDG/TVBB--5063--SE

Number of pages: 88

Keywords
Eurocode, BKR, Swedish building code, Danish building code, fire-exposed concrete structures, concrete beams, concrete columns, strength reduction of concrete cross-sections, structural fire design, the 500°C-method, Hertz's method, second order effects, Temperature Calculation & Design, TCD, SUPER-TEMPCALC, C-Beam, CONFIRE.

Abstract
In this report the simplified methods for fire design of concrete beams and columns in Eurocode and BKR were evaluated against advanced computer models. The 500°C- (BKR) and Hertz's (Eurocode) method for calculating strength reduction of fire-exposed concrete were evaluated against a finite element model, by calculating the moment capacity of normal-reinforced beams at a cross-sectional level. The stress-strain relationship of steel in over-reinforced beams exposed to fire was also studied with the 500°C-method. The methods in Eurocode and BKR for calculating the load-bearing capacity of fire-exposed columns were evaluated against a finite element model for structural member analysis of fire exposed concrete structures. The evaluation of columns was extended with a method developed by Hertz, which is expected to be adopted in the Danish code. The reliability of the finite element model for structural member analysis of fire exposed concrete structures was also analysed.

Brandteknik
Lunds Tekniska Högskola
Lunds Universitet
Box 118
221 00 Lund

brand@brand.lth.se
http://www.brand.lth.se

Telefon: 046 - 222 73 60

Department of Fire Safety Engineering
Lund University
P.O. Box 118
SE-221 00 Lund
Sweden

brand@brand.lth.se
http://www.brand.lth.se/english

Telephone: Int + 46 - 46 - 222 73 60

SUMMARY

This report is an evaluation of the simplified design methods in Eurocode and the Swedish building code for fire exposed concrete beams and columns. For columns the evaluation is extended with a method developed by Christian Hertz, which is expected to be adopted in the Danish code. The stress-strain relationship of reinforcement at high temperatures is also studied for over-reinforced beams. Moreover the already existing minimum widths for the 500^{o}C-method at different fire-exposures is evaluated.

Instead of evaluating the simplified methods against real tests, advanced computer models have been used. Cross-sectional analysis was assumed to be sufficient for beams, while member analysis was necessary for columns.

The heat flow analysis of the structural members was performed at a cross-sectional level with a finite element model, which solves the non-linear two-dimensional heat flow equation. The temperature field, of a cross-section, as a function of time was then assumed to be constant along the length of the structural members.

For beams, the 500^{o}C-method (BKR) and Hertz's method (EC) were compared to a Finite Element Model, which from the temperature field as a function of time calculates the moment capacity of reinforced cross-section. The 500^{o}C-method is based on the assumption that all concrete with a temperature over 500^{o}C has lost all strength and below 500^{o}C has the same strength as at 20^{o}C. Hertz's method reduces the cross-section based on a distribution of strength and stiffness dependent of the temperature field. The varied parameters were cross-sectional geometry, strength of concrete and steel, reinforcement, fire exposure and boundary condition of fire exposure.

For columns, the stiffness method in BKR, the stiffness method in Eurocode and Hertz's method based on curvature were compared to a non-linear finite element model for structural analysis of fire exposed concrete structures. The finite element model is based on the constitutive laws in chapter 2 and it calculates time to failure for loaded structures. Instead of using the 500^{o}C-method with the stiffness method in BKR, Hertz's method was used. The reasons being that the input should be the same in the evaluation and that Hertz's method takes stiffness into account, which the 500^{o}C-method does not. The varied parameters were slenderness and reinforcement ratio since they have great influence of second order effects.

The following conclusions were made:

<u>Beams (reduction of cross-sections)</u>

- The 500^{o}C- and Hertz's method give very good results for cross-sections with fire exposed tension zones.
- Both methods give good results for cross-sections with the compression zones exposed to the ISO-834 standard fire. For natural fires the results are conservative, especially for the 500^{o}C-method.
- Hertz's method for reduction of cross-sections can take any strength-reduction curve into account because it is based on strength and stiffness distribution of a fire-exposed cross-section.
- The 500^{o}C-method is originally developed for ordinary siliceous concrete but it could be modified for other types of concrete.

- For over-reinforced cross-sections with fire exposed tension zones the 2%-limit of strain i.e related strength-temperature curve could be applied for strains down to 1,3% with acceptable deviation (<10%).
- The deviation in moment capacity is acceptable for cross-sections, which turn from normal- into over-reinforced due to fire exposed compression zone. The reason is that the deviation is acceptable for strains down to 1,3% and the penetration of damaged concrete is slow for normal time periods and cross-sections.

<u>Columns (second order effects)</u>

- The stiffness methods in BKR and Eurocode over-estimate the load bearing capacity of fire exposed columns and are unsafe to use.
- There have been indications that the stiffness method in BKR could take transient load into account by reducing the reinforcement area with 0,5 for columns with only corner bars. This study shows that this is not possible.
- Hertz's method gives good results for columns with slenderness, which after a cross-section reduction should not exceed approximately 25. Above 25 the method gives very conservative results and the method which takes transient load into account needs to be modified.
- In general, simplified design methods developed for normal temperatures must be considered as unsafe if they are not complemented with a procedure, which takes the transient load into account.

Having analysed the results of this report, I will not recommend any further development and research of simple hand methods. I think it is time to leave them to educational purpose only and develop a general, computer based, model for fire-exposed structures. As early as in 1986, Forsén proved it to be possible when he created CONFIRE, a program for structural analysis of fire exposed concrete structures. It is remarkable that the development has not got any further since then, especially considering that CFD-modelling of enclosure fires is in rapid advance for commercial use. Used together, they would optimise the design of fire-exposed structures and always guarantee a high level of safety.

ACKNOWLEDGEMENTS

I would like to thank Dr. Yngve Anderberg at Fire Safety Design AB and Dr. Björn Karlsson at the department of Fire Safety Engineering, who initiated this thesis about simplified design of fire exposed concrete structures. It has been an instructive work since I in the beginning had poor knowledge about fire exposed concrete structures and computer modelling.

I would also like to thank the rest of the staff at Fire Safety Design AB for making my time with them interesting and fun. A special thank to Sebastian Jeansson for his guidance through the work and will of sharing knowledge.

Office space, computer and software as well as most of the literature were supplied by Fire Safety Design AB.

Finally, thanks to everybody who has assisted me in any way during the work.

Lund, August 2000

Johan Rigberth

CONTENTS

1 INTRODUCTION

1.1 BACKGROUND

There are considerable differences between the building codes in the EU-countries. This situation makes it difficult for companies in the building sector, to get approval outside their native countries. The European committee for Standardisation (CEN), works for establishing a set of harmonised technical rules, that could be used as an alternative to the different rules in the member states of EU. These rules are named Eurocodes and should in the future replace all national building codes. At the moment there are nine Eurocodes under development, which deals with different areas of structural and geotechnical design of buildings and civil engineering works. Some of them are already accomplished and some are pre-standards with a lifetime of three years. After two years CEN members are invited to submit their comments on the pre-standards. These comments will be taken into account in the further development of the pre-standards. In order to accept the final results it is important that the member states participate in the development and compare their codes with the pre-standards.

1.2 OBJECTIVES

The main purpose of this work is to compare and evaluate simplified design rules for fire exposed concrete beams and columns in Eurocode 2: *Design of concrete structures* – Part 1 (EN 1992-1, 1999) and Part 1-2 (ENV 1992-1-2, 1995) with the Swedish building code (BKR, 1999). Both codes are based on the idea of reducing the cross-section of fire exposed concrete structures. BKR uses the 500^{o}C-method (Anderberg, Pettersson, 1992) and Eurocode the Hertz-method (Hertz, 1999). The evaluation of design methods for fire exposed concrete beams is focused on the strength reduction of cross-sections. For columns it is focused on second order effects. The evaluation of columns is also extended with a method developed by Hertz, which is expected to be adopted by the Danish code.

Beside the main purpose above, the stress-strain relationship of reinforcement at high temperatures is studied for over-reinforced beams. Moreover the already existing minimum widths for the 500^{o}C-method at different fire-exposures is evaluated.

1.3 WORK METHODOLOGY

Instead of evaluating the simplified methods against real tests, advanced computer models have been used. It is assumed that cross-sectional analysis is sufficient for beams, while it is necessary with structural member calculations for columns.

The temperature field of the analysed members were calculated over time with the finite element program *TCD* (FSD, 1999), which solves the non-linear two-dimensional heat flow equation. Since the program is 2-dimensional, the temperature field is calculated at cross-sectional level and is assumed to be constant along the length.

For beams the 500^{o}C-method and Hertz's method were evaluated against a sub program in TCD, which calculates the moment capacity as a function of time.

For columns the stiffness method in BKR, the stiffness method in Eurocode and Hertz's method based on curvature were evaluated against a finite element model named CONFIRE (Forsén, 1986). It is a non-linear finite element model, which analyses the behaviour of fire-exposed concrete structures and calculates their time to failure at specific loads.

1.4 LIMITATIONS AND ASSUMPTIONS

- Analysis of beams at a cross-sectional level is assumed to be sufficient. External forces causing shear are excluded.
- All columns are based on one cross-section exposed to the ISO-834 standard fire (1975). Slenderness and reinforcement ratio were varied because they have great influence on second order effects.
- No temperature gradient along the length of the structural members has been accounted for.
- No real tests of beams or columns were performed.
- Only ordinary siliceous concrete is analysed.
- The effect of spalling is not considered.

1.5 REPORT DISPOSITION

Chapter 7 *GENERAL CONCLUSIONS* presents the general conclusions of the study.

Chapter 6 *COLUMNS* presents the conclusions of the analysed columns. It also describes the simplified hand-methods and the computer model for calculating the load-bearing capacity.

Chapter 5 *BEAMS* presents the conclusions of the analysed beams. It also describes the simplified hand-methods and the computer model for calculating the moment capacity.

Chapter 4 *HEAT FLOW ANALYSIS* describes the heat-flow theory in the program TCD (FSD, 1999). It also presents the fire exposures that have been used.

Chapter 3 *THERMAL PROPERTIES* describes the thermal properties of concrete and steel used in the heat-flow analysis.

Chapter 2 *MECHANICAL PROPERTIES* describes the mechanical behaviour of heated concrete and steel used in the study.

2 MECHANICAL PROPERTIES

This chapter describes the mechanical properties of heated concrete and steel. It is based on Eurocode and the material models (constitutive models) in the program CONFIRE (Forsén, 1986) used for the structural member analysis of fire exposed columns.

2.1 CONCRETE

A brief description of the deterioration of concrete exposed to heating can be made as follows:
When siliceous concrete is heated the free water in it evaporates, and above approximately 150°C the chemically bound water in the hydrated calcium silicates starts being released. In some cases the surface of the concrete is not able to resist the pressure of the water and steam, which leads to spalling. The release of water causes shrinkage of the hydrated cement paste, while the aggregate and reinforcement are subjected to a thermal expansion. This leads to stresses in the composite material and from approximately 300°C micro cracks will occur in the concrete. These cracks cause reduction of the tensile strength and modulus of elasticity, and unloaded specimen will be subjected to an irreversible expansion. At about 400-535°C the concrete starts weakening rapidly because the calcium hydroxide decomposes into calcium oxide and water. At 710°C the rate of decomposition of the remaining calcium silicates reaches its maximum and at about 900°C the volumes of quartz aggregates become unstable. Above 1150°C, concrete containing feldspar will melt. (Hertz, 1999)

2.1.1 Relative Ultimate Strength

The relative ultimate strength curve of siliceous ordinary concrete is shown in figure 2.1.

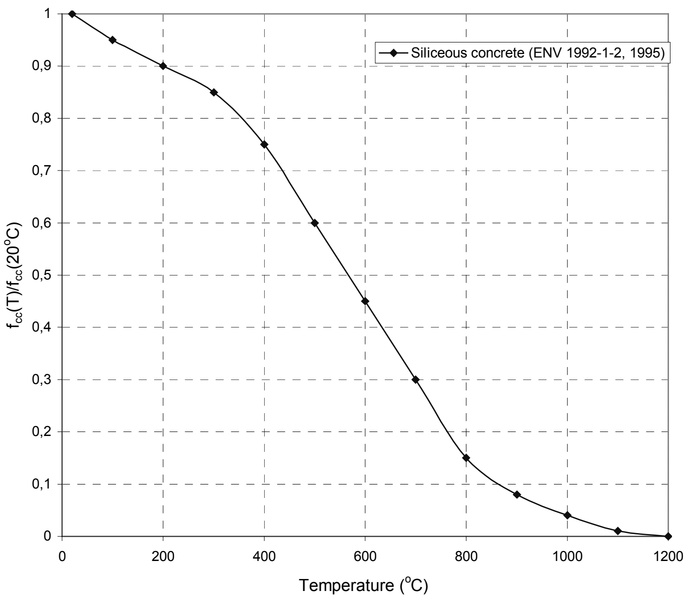

Figure 2.1 Strength of siliceous concrete as a function of temperature (ENV 1992-1-2, 1995).

2.1.2 Constitutive Model

The constitutive model (material model) describes the behaviour of heated and loaded concrete in mathematical terms. It is based on the stress-strain relationships of heated concrete and is the sum of four terms (Anderberg, Thelandersson, 1976), see equation 2.1. Each of the terms are briefly described in this section.

$$\varepsilon_{tot} = \varepsilon_{\sigma}(\overline{\sigma},\sigma,T) + \varepsilon_{th}(T) + \varepsilon_{cr}(\sigma,T,t) + \varepsilon_{tr}(\sigma,T) \qquad (2.1)$$

where

ε_{tot}	is the total strain [-].
ε_{σ}	is the stress-related strain [-].
ε_{th}	is the thermal strain [-].
ε_{cr}	is the creep strain [-].
ε_{tr}	is the transient strain [-].
T	is the temperature [^{o}C].
t	is the time [s].
σ	is stress [MPa].
$\overline{\sigma}$	is stress history [MPa].

2.1.2.1 Stress-Related Strain

The stress-strain relationship of compressed siliceous concrete is shown in figure 2.2.

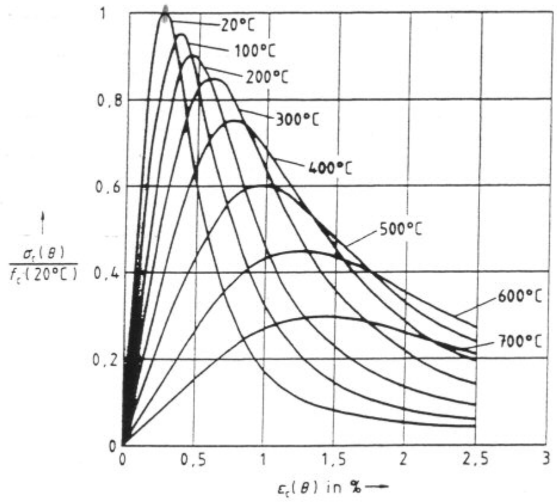

Figure 2.2 Stress-strain relationship of siliceous concrete at different temperatures Eurocode (ENV 1992-1-2, 1995).

The theoretical model of the stress-strain relationship is shown in figure 2.3 (Anderberg, 1976). On the compression side, the curve consists of a parabolic branch followed by a linear descending slope until crushing occurs. On the tension side, the curve consists of a decreasing linear slope until maximum tension is reached, thereafter it increases linearly until cracking occurs.

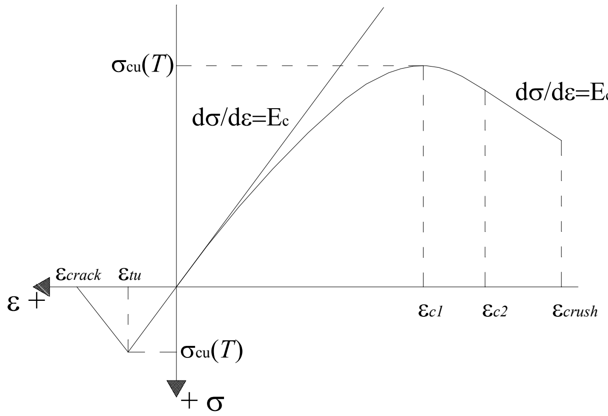

Figure 2.3 Theoretical model of the stress-strain relationship of concrete (Anderberg, 1976).

where

$\sigma_{cu}(T)$	is the ultimate compressive stress [MPa].
ε_{c1}	is the ultimate compressive strain at σ equal to $\sigma_{cu}(T)$ [-].
ε_{c2}	is the strain at the transition between parabolic and linear descending branch [-].
$E_c(T)$	is the elastic modulus of the parabolic curve[MPa].
$E_c{}^*(T)$	is the elastic modulus of the descending branch [^{o}C].
$\sigma_{tu}(T)$	is the ultimate tension strength of concrete [MPa].
ε_{tu}	is the ultimate tension strain at σ equal to $\sigma_{tu}(T)$ [-].
ε_{crack}	is the cracking strain [-].
ε_{crush}	is the crushing strain [-].

The stress-strain curve in figure 2.3 is mathematical described by equation 2.2-2.7.

Equations 2.2 and 2.3 describe the parabolic branch:

$$\sigma_c(T) = \sigma_{cu}(T) \times \frac{\varepsilon}{\varepsilon_{c1}} \times \left(2 - \left(\frac{\varepsilon}{\varepsilon_{c1}}\right)\right) \qquad 0 > \varepsilon > \varepsilon_{c2} \qquad (2.2)$$

$$E_c(T) = \alpha \times \frac{\sigma_{cu}(T)}{\varepsilon_{c1}} \qquad (2.3)$$

For ordinary siliceous concrete the coefficient α is found to be 2 (Anderberg, Thelandersson, 1976).

The linear descending branch is given by equations 2.4 and 2.5:

$$\sigma_c(T) = E_c{}^*(T) \times \varepsilon + \sigma^*(T) \qquad \varepsilon_{c2} > \varepsilon > \varepsilon_{crush} \qquad (2.4)$$

$$\sigma_c{}^*(T) = \sigma_{cu}(T) \times \left(1 - \frac{E_c{}^*(T)}{E_c(T)}\right)^2 \qquad (2.5)$$

On the tension side the stress-strain curve is defined by equations 2.6 and 2.7:

$$\sigma_t(T) = E_c(T) \times \varepsilon \qquad 0 < \varepsilon < \varepsilon_{tu} \qquad (2.6)$$

$$\sigma_t(T) = E_c(T) \times \varepsilon_{tu} \times \frac{(\varepsilon_{crack} - \varepsilon)}{(\varepsilon_{crack} - \varepsilon_{tu})} \qquad \varepsilon_{tu} < \varepsilon < \varepsilon_{crack} \qquad (2.7)$$

where

ε_{tu} is the strain when the maximum tensile stress is reached and $\varepsilon_{tu} = \dfrac{\sigma_{tu}(T)}{E_c(T)}$ [-].

With equation 2.2-2.7, it is possible to describe the stress-strain relationship of concrete by defining four parameters as a function of temperature:

- ultimate compressive stress, $\sigma_{cu}(T)$,
- ultimate compressive strain, $\varepsilon_{cu}(T)$,
- slopes of descending branch, $E_c{*}(T)$ and
- ultimate tension stress, $\sigma_{tu}(T)$.

Ultimate compressive stress $\sigma_{cu}(T)$

The ultimate stress is dependent on parameters such as temperature, load history, aggregate, etc. However it is clearly shown that for a specific concrete type, the ultimate stress is almost only dependent on temperature and the load history may be neglected (Anderberg, Thelandersson, 1976). The relative temperature dependence of siliceous concrete is seen in figure 2.1.

Ultimate compressive strain $\varepsilon_{cu}(T)$

The ultimate compressive strain is dependent on both temperature and prehistory of stress. The dependence of temperature and prehistory are shown in figure 2.4.

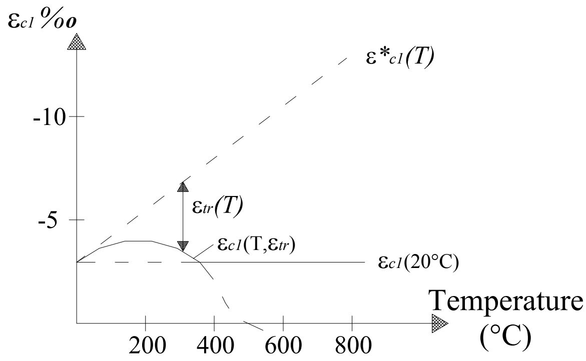

Figure 2.4 Theoretical model of ultimate strain (Anderberg, Thelandersson, 1976).

where

$\varepsilon^*_{c1}(T)$	is the ultimate strain at zero load history [-].
$\varepsilon_{c1}(20^oC)$	is the ultimate strain at 20 ^oC [-].
$\varepsilon_{tr}(T)$	is the accumulated transient strain [-].
$\varepsilon_{c1}(T,\ \varepsilon_{tr})$	is the ultimate strain [-].

Figure 2.4 can also be described by equation 2.8.

$$\varepsilon_{c1}\left(T, \varepsilon_{tr}\left(T\right)\right) = \min\ \left(\varepsilon_{c1}(20^o C),\ \varepsilon^*_{c1}(T) - \varepsilon_{tr}\left(T\right)\right) \tag{2.8}$$

The slope for the temperature dependent part of the ultimate strain, $\varepsilon^*_{c1}(T)$, is set to 0,008. The reason is that it correlates well with experimental data for ordinary siliceous concrete (Anderberg, Thelandersson, 1976) and tabulated values in Eurocode (ENV 1992-1-2, 1995).

The transient strain, $\varepsilon_{tr}(T)$, will be discussed further in section 2.1.1.4.

Slopes of descending branch, E-Modulus $E_c*(T)$

There is poor knowledge of the descending branch of the stress-strain curve. However it is not an important parameter for the behaviour of concrete since it already has passed its ultimate strain and is about to break. For ordinary siliceous concrete it is given the constant value of 880 MPa, independent of both temperature and stress history (Anderberg, 1976).

Ultimate tension stress $\sigma_{tu}(T)$

The tensile stress is assumed to be zero since it has very little influence on reinforced structures.

Cracking strain ε_{crack}

The cracking strain is assumed to be 0,04%, independent of temperature, because it has shown good agreement with experimental curves (Anderberg, 1976).

2.1.2.2 Thermal Strain

Thermal strain during heating is a simple function of temperature and its theoretical curve is plotted in figure 2.5. The theoretical curve also includes drying shrinkage, but despite this, the curve is justified for rapid heating during fire (Anderberg, 1976).

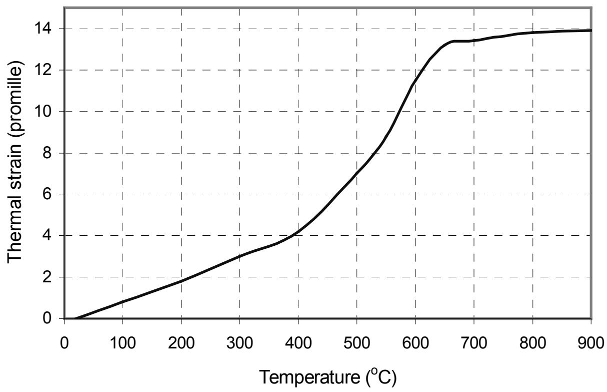

Figure 2.5 Thermal strain for ordinary siliceous concrete (Anderberg, 1976).

2.1.2.3 Creep Strain

The creep strain depends on concrete, the load, the temperature and the time. The following expression is used to describe the creep for ordinary siliceous concrete (Anderberg, Thelandersson, 1976):

$$\varepsilon_{cr}(\sigma, T, t) = -530 \cdot 10^{-6} \times \frac{\sigma}{\sigma_{cu}(T)} \times \sqrt{\frac{\Delta t}{3}} \times e^{\frac{3,04(T-20)}{1000}} \quad (2.5)$$

where

$\varepsilon_{cr}(\sigma,T,t)$ is creep strain [-].
σ/σ_{cu}(T) is the ratio between the actual compressive strength of the concrete [-].
T is the temperature in concrete [°C].
Δt is the time interval [h].

It is seen that even at a stress ratio equal to 1, the duration should be at least 10-20 h, for the creep strain to be comparable to the thermal strain at temperature levels below 500^{o}C. Creep strains are therefore mostly important for applications of concrete in industry and reactor technology, where sustained high temperatures occur (Hertz, 1999). For fire exposed concrete structures creep strains may be important for calculation of the time dependent deflections during the cooling phase.

2.1.2.4 Transient Strain

Transient stress is the hindered part of thermal expansion for loaded concrete structures exposed to heating. It is an irreversible process and occurs only during the first heating. The transient stress is found to be proportional to the thermal expansion and to the ratio between the compressive stress and strength at 20^{o}C (Anderberg, Thelandersson, 1976), see equation 2.6.

$$\varepsilon_{tr}(\sigma, T) = -2{,}35 \times \frac{\sigma}{f_{cc20^o C}} \times \varepsilon_{th} \tag{2.6}$$

where

$\varepsilon_{tr}(\sigma,T)$ is the transient strain [-].
σ / f_{cc20} is the ratio between the compressive stress and compressive strength of the concrete at 20^{o}C [-].
ε_{th} is the thermal expansion [-].

2.2 STEEL

Reinforcement is used to compensate the low tensile strength of concrete. Therefore knowledge about mechanical properties of reinforcement is important, especially when it has a primary load bearing capacity as for beams and slender columns. In order to gain maximum moment capacity at ordinary temperatures, reinforcement are placed close to the surface. During a fire the opposite effect occurs since the temperature close to surface increases fast and the relative strength of steel is very sensitive to temperature.

2.2.1 Relative Yield Strength

Hot rolled, cold worked and prestressed steel must be separated when their strength properties are described. Their relative yield strengths, dependent on temperature, are shown in figure 2.6.

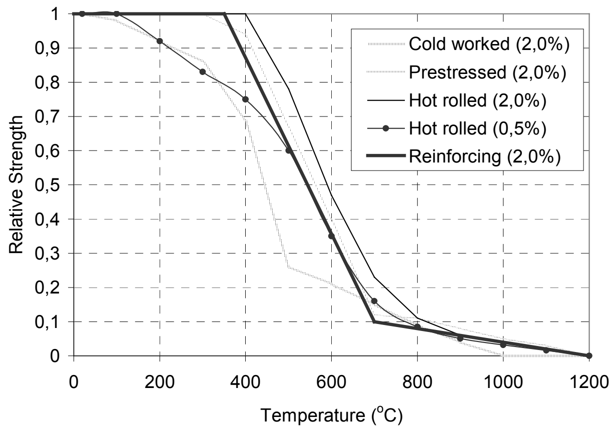

Figure 2.6 Relative yield strength of steel (ENV 1992-1-2, 1995).

2.2.2 Constitutive Model

The constitutive model (material model) describes the behaviour of heated and loaded steel in mathematical terms. Since transient strain does not exist for steel the model is simpler than for concrete and is described as the sum of three terms, see equation 2.7. Each of the terms are briefly described in this section.

$$\varepsilon_{tot} = \varepsilon_\sigma(\sigma,T) + \varepsilon_{th}(T) + \varepsilon_{cr}(\sigma,T,t) \tag{2.7}$$

where

ε_{tot}	is the total strain [-].
$\varepsilon_\sigma(\sigma,T)$	is the stress-related strain [-].
$\varepsilon_{th}(T)$	is the thermal strain [-].
$\varepsilon_{cr}(\sigma,T,t)$	is the creep strain [-].
T	is the temperature [^{o}C].
t	is the time [s].
σ	is stress [MPa].

2.2.2.1 Stress-Related Strain

Figure 2.7 describes the stress-strain relationships for structural steel at various temperatures. From these curves a theoretical model based on linear interpolation of both temperature and strain, was developed for the program CONFIRE (Forsén, 1986). The model is shown schematically in figure 2.8.

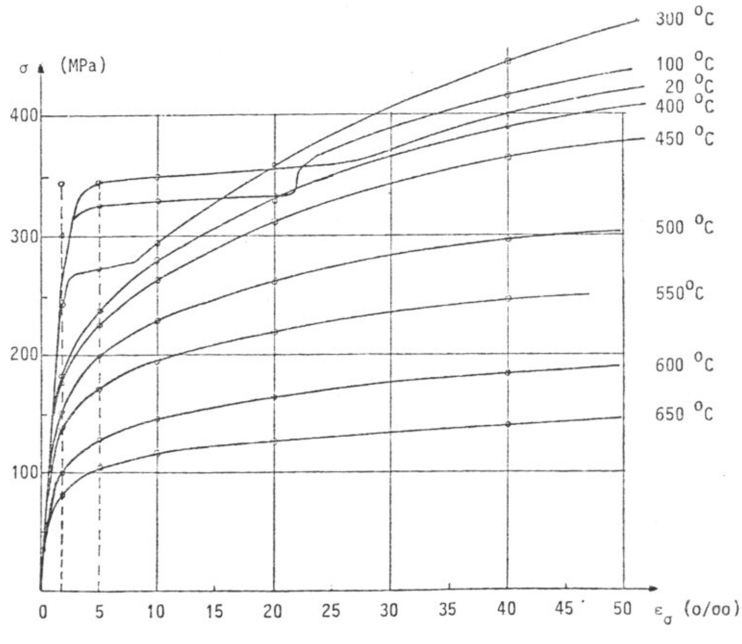

Figure 2.7 Experimental stress-strain curves for structural steel, St52, at various temperatures (Thor, 1972).

In the model the elasticity of modulus is given a smooth course, with respect to strain by introducing the parameter ξ. The parameter ξ is set to 1 in the structural analysis of columns, see figure 2.8.

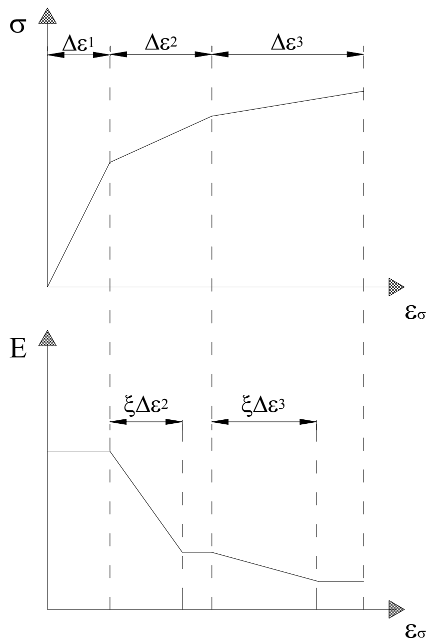

Figure 2.8 Stress-strain relationship and corresponding elasticity modulus as a function of strain (Forsén, 1982).

2.2.2.2 Thermal Strain

The thermal strain is normally the largest strain and is therefore an important factor when calculating the total deformation or load-bearing capacity of concrete structures exposed to fire. The thermal strain, $\Delta l/l$, is expressed as the length change due to temperature rise. Equation 2.8 describes this for reinforcing and prestressing steel (Anderberg, 1976).

$$\Delta l/l = -2{,}379 \cdot 10^{-4} + 1{,}169 \cdot 10^{-5}T + 0{,}5128 \cdot 10^{-8}T^2 \qquad (2.8)$$

where

- l is the length at room temperature for reinforced/prestressed steel [mm].
- Δl is the temperature induced elongation for reinforced/prestressed steel [mm].
- T is the temperature in steel [°C].

Similar expressions are found in Eurocode (ENV 1992-1-2, 1995), equation 2.9-2.12, and they give almost the same results as equation 2.8.

Reinforcing steel:

$\Delta l/l = -2{,}416 \cdot 10^{-4} + 1{,}2 \cdot 10^{-5}T + 0{,}4 \cdot 10^{-8}T^2$	$20^{o}C < T < 750\,^{o}C$	(2.9)
$\Delta l/l = 11{,}0 \cdot 10^{-3}$	$750^{o}C < T < 860\,^{o}C$	(2.10)
$\Delta l/l = -6{,}2 \cdot 10^{-3} + 2{,}0 \cdot 10^{-5}T$	$860^{o}C < T$	(2.11)

Prestressed steel:

$\Delta l/l = -2{,}016 \cdot 10^{-4} + 1{,}0 \cdot 10^{-5}T + 0{,}4 \cdot 10^{-8}T^2$	$20^{o}C < T < 1200\,^{o}C$	(2.12)

2.2.2.3 Creep Strain

During fire, creep becomes significant around 400°C and rapidly increases with temperature. It is therefore important to include the influence of creep in structural analysis (Anderberg, 1976). The used model considers the effects of both variable temperature and stress. It neglects creep below 200°C and is identical for both tension and compression. Figure 2.9 principally describes it. The model can be divided into two separate phases, a primary phase having a parabolic curve and a secondary linear phase (Dorn, 1954).

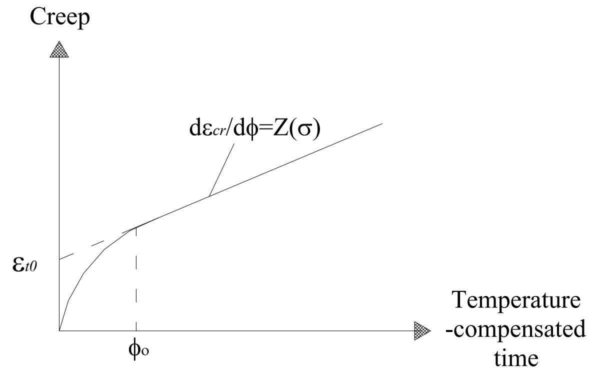

Figure 2.9 Principal creep curve for steel (Dorn, 1954).

Figure 2.9 can also be described by equation 2.13-2.14.

$$\phi = \int_0^t e^{\frac{-\Delta H\, dt}{RT}} \tag{2.13}$$

where

$\Delta H/R$ = 45000K	is the activation energy of creep divided with the gas constant [K].
t	is the time [h].
T	is the temperature in steel [K].

$$\varepsilon_t(T,\sigma) = \varepsilon_{t0}(\sigma) \times \left(2 \times \sqrt{\frac{Z(\sigma)\times\phi}{\varepsilon_{t0}(\sigma)}} \right) \qquad 0 < \phi \le \phi_0 \tag{2.14a}$$

$$\varepsilon_t(T,\sigma) = \varepsilon_{t0}(\sigma) \times \left(1 + \frac{Z(\sigma)\times\phi}{\varepsilon_{t0}(\sigma)} \right) \qquad \phi > \phi_0 \tag{2.14b}$$

where the following parameters is for steel Ks 40 (Krakau, 1975).

$\varepsilon_{t0}(\sigma) = 2{\cdot}62 \cdot 10^{-6} \cdot \sigma^{1,0365}$ [-].

$Z(\sigma) = 140 \cdot 10^{4} \cdot \sigma^{4,7}$ $\quad 0 < \sigma < 8$ kPa $\quad$ [h^{-1}].
$Z(\sigma) = 258 \cdot 10^{16} \cdot e^{0,00443 \cdot \sigma}$ $\quad \sigma > 8$ kPa

2.2.3 Stress Related Strain According to Eurocode

The steel model in figure 2.10 is used in the simplified calculations when the reinforcement strain is below the yield point. The model is similar to the one in section 2.2.2.1 and describes the stress-strain relationship of steel at elevated temperatures.

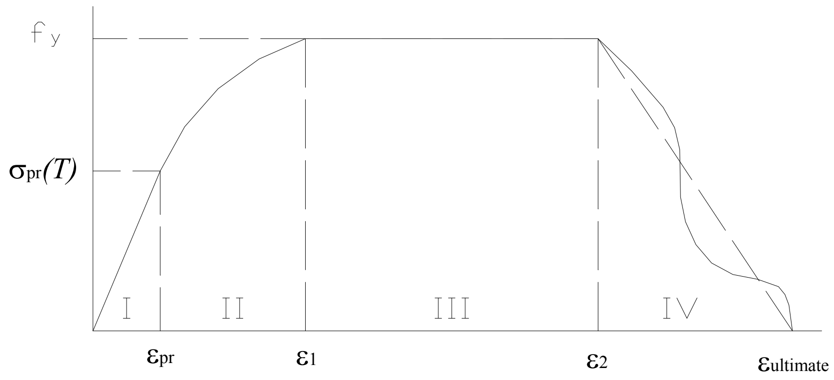

Range I elastic	$\sigma(T) = E(T) \times \varepsilon_s \qquad \varepsilon_{pr} = \sigma_{pr}(T)/E(T)$ (2.15)
Range II Non-linear	$\sigma(T) = b/a \times \sqrt{a^2 - (\varepsilon_1 - \varepsilon(T))^2} + \sigma_{pr}(T) - c$ (2.16) $E(T) = (b \times (\varepsilon_1 - \varepsilon(T))) \Big/ \left(a \times \sqrt{a^2 - (\varepsilon_1 - \varepsilon(T))^2}\right)$ (2.17) with $\varepsilon_1 = 0{,}02$ $a^2 = (E(T) \times (\varepsilon_1 - \varepsilon_{pr})^2 + c \times (\varepsilon_1 - \varepsilon_{pr}))/E(T)$ $b^2 = E(T) \times (\varepsilon_1 - \varepsilon_{pr}) \times c + c^2$ $c = (f_y(T) - \sigma_{pr}(T))^2 / (2 \times (\sigma_{pr}(T) - f_y(T)) + E(T) \times (\varepsilon_1 - \varepsilon_{pr}))$
Range III plastic	$\sigma(T) = f_y(T)$ (2.18) $E(T) = 0$ (2.19)
Range IV	For numerical purposes a descending branch should be adopted. Linear and non-linear models are permitted.

Figure 2.10 stress-strain relationships for steel (ENV 1992-1-2, 1995).

For a given steel temperature, the stress-strain curves in figure 2.10 are defined by three parameters:

- the slope of the linear elastic range *E(T)* for reinforcement and prestressing steels,
- the proportional limit $\sigma_{pr}(T)$ and
- the maximum stress level $f_y(T)$.

Values for each one of the three parameters are given for cold worked, hot rolled and prestressed steel in table 2.1-3.

Temperature (°C)	$E(T)/E(20^oC)$	$\sigma_{pr}(T)/\sigma_{0,2}(20^oC)$	$f_y(T)/\sigma_{0,2}(20^oC)$
20	1,00	1,00	1,00
100	1,00	0,96	1,00
200	0,87	0,92	1,00
300	0,72	0,81	1,00
400	0,56	0,63	0,94
500	0,40	0,44	0,67
600	0,24	0,26	0,40
700	0,08	0,08	0,12
800	0,06	0,06	0,11
900	0,05	0,05	0,08
1000	0,03	0,03	0,05
1100	0,02	0,02	0,03
1200	0,00	0,00	0,00

Table 2.1 Cold worked reinforcing steel.

Temperature (°C)	$E(T)/E(20^oC)$	$\sigma_{pr}(T)/\sigma_{0,2}(20^oC)$	$f_y(T)/\sigma_{0,2}(20^oC)$
20	1,00	1,00	1,00
100	1,00	1,00	1,00
200	0,90	0,81	1,00
300	0,80	0,61	1,00
400	0,70	0,42	1,00
500	0,60	0,36	0,78
600	0,31	0,18	0,47
700	0,13	0,07	0,23
800	0,09	0,05	0,11
900	0,07	0,04	0,06
1000	0,04	0,02	0,04
1100	0,02	0,01	0,02
1200	0,00	0,00	0,00

Table 2.2 Hot rolled reinforcing steel.

Temperature (°C)	$E(T)/E(20^oC)$	$\sigma_{pr}(T)/\sigma_{0,2}(20^oC)$	$f_y(T)/\sigma_{0,2}(20^oC)$
20	1,00	1,00	1,00
100	0,76	0,77	0,98
200	0,61	0,62	0,92
300	0,52	0,58	0,86
400	0,41	0,52	0,69
500	0,20	0,14	0,26
600	0,15	0,11	0,21
700	0,10	0,09	0,15
800	0,06	0,06	0,09
900	0,03	0,03	0,04
1000	0,00	0,00	0,00
1100	0,00	0,00	0,00
1200	0,00	0,00	0,00

Table 2.3 Prestressing steel (bars).

3 THERMAL PROPERTIES

Chapter 3 briefly describes the thermal properties of steel and ordinary siliceous concrete. These properties are used in the heat flow analysis of the cross-sections.

3.1 CONCRETE

Concrete is considered an isotropic material in temperature calculations and its thermal properties could be described by three different material properties: thermal conductivity, specific heat and density. Since concrete is a composite material these properties are a compromise between the composites. For example cement mortar has lower thermal conductivity than ballast in concrete.

3.1.1 Thermal Conductivity

The thermal conductivity for siliceous concrete is a function of temperature and is expressed by equation 3.1 or graphically shown in figure 3.1 (ENV 1992-1-2, 1995).

$$\lambda_c = 2 - 0{,}24\frac{T}{120} + 0{,}012\left(\frac{T}{120}\right)^2 \tag{3.1}$$

where

λ_c is thermal conductivity [W/(mK)].
T Is temperature [^{o}C].

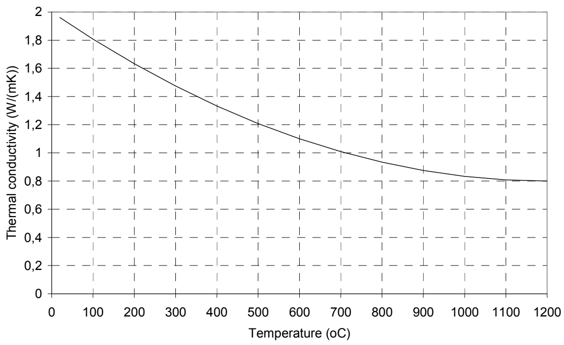

Figure 3.1 Thermal conductivity as a function of temperature (ENV 1992-1-2, 1995).

3.1.2 Specific Heat and Thermal Capacitivity

The specific heat is a function of temperature and is expressed by equation 3.2. According to Eurocode it is valid for both siliceous and calcareous concrete (ENV 1992-1-2, 1995).

$$c_c = 900 + 80\frac{T}{120} - 4\left(\frac{T}{120}\right)^2 \tag{3.2}$$

where

c_c is specific heat [J/(kgK)].
T is temperature [^{o}C].

Due to steam generation of water in heated concrete, the curve described by equation 3.2 needs to be modified. The shape of the modification is not known but it is modelled as a peak between 100 and 200^{o}C with a top at 120^{o}C. In this study, concrete with a density of 2300kg/m^3 and 2% of water content by weight is used. According to Eurocode the value of the specific heat peak is then 1875 J/(kgK) (ENV 1992-1-2, 1995). Figure 3.3 graphically shows equation 3.2 with the specific heat.

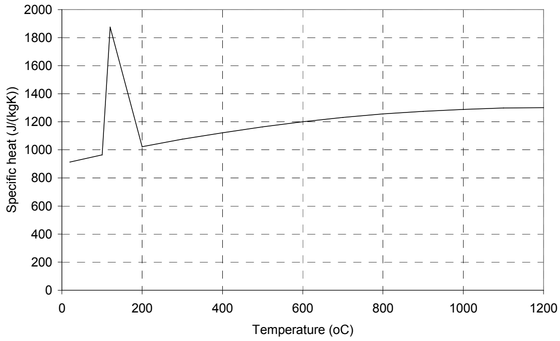

Figure 3.2 Specific heat for ordinary siliceous concrete (ENV 1992-1-2, 1995).

3.2 STEEL

Steel is just like concrete considered an isotropic material in temperature calculations and its thermal properties could be described by two different material properties: thermal conductivity and capacitivity, which is the product of specific heat and density. The thermal properties of steel are shown in figures 3.3 and 3.4.

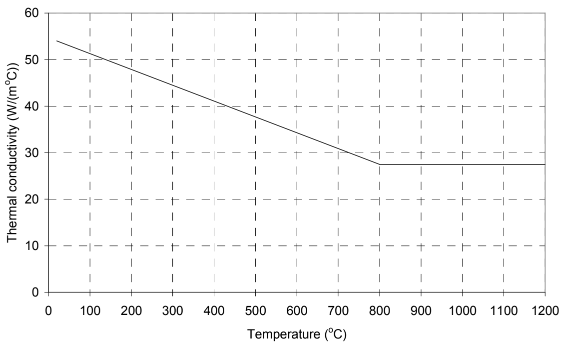

Figure 3.3 Thermal conductivity of steel as a function of temperature (ENV 1993-1-2, 1995).

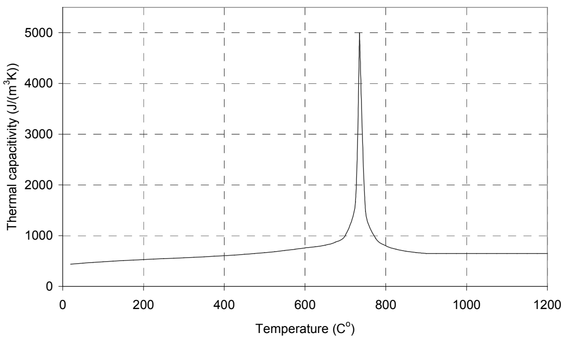

Figure 3.4 Thermal capacitivity of steel as a function of temperature (ENV 1993-1-2, 1995).

4 HEAT FLOW ANALYSIS

This chapter describes the theory and assumptions of the heat flow calculations. It also contains the fire exposures used in the analysis.

4.1 COMPUTER CALCULATION

The sub-program SUPER-TEMPCALC in the program package *Temperature Calculation and Design* (FSD, 1999) is used in the heat-flow analysis. SUPER-TEMPCALC solves Fourier's non-linear heat flow equation for two dimensions and the result has shown good agreement with experiments. A further description of the program package *Temperature Calculation and Design* is found in appendix F.

The temperature calculations are done without taking reinforcement into account. The reason is that the temperature in homogenous concrete approximately equals the temperature at the central point of the reinforcement (Ehm, 1967). This is due to a lower thermal conductivity of the reinforcement as well as variations in heat transfer coefficients on the surface of the reinforcement.

4.1.1 SUPER-TEMPCALC

The temperature field in a concrete cross-section is given by the differential equation for two-dimensional heat flow, equation 4.1. It is derived from the conservation of energy, describing the fact that total inflow per unit time equals the total outflow per unit time.

$$\rho c_p \frac{\partial T}{\partial t} - \frac{\partial}{\partial x}\left(\lambda_c \frac{\partial T}{\partial x}\right) - \frac{\partial}{\partial y}\left(\lambda_c \frac{\partial T}{\partial y}\right) - \dot{Q} = 0 \qquad (4.1)$$

where

$\dot{Q}$	is the amount of heat supplied to the body per unit volume and time [J/(m^{3}s)].
c_p	is the thermal capacity [J/(kgK)].
t	is time [s].
x,y	is cartesian coordinates.
ρ	is the density [kg/m^3].
λ	is the thermal conductivity [W/(mK)].
T	is the temperature [^{o}C].

The boundary conditions are decided either by time dependent prescribed temperature or heat flux. The heat is based on convection and radiation according to equation 4.2.

$$\dot{q}'' = \alpha_c (T_g - T_b) + \varepsilon_r \sigma (T_g^4 - T_b^4) \qquad (4.2)$$

where

$\dot{q}''$	is the heat flow at boundary [W/m^2].
T_g	is the gas temperature [^{o}C].
T_b	is the boundary temperature [^{o}C].
α_c	is the convection coefficient [W/(m^{2o}C)].
ε_r	is the resulting emissivity [kg/m^3].
σ	is Stefan-Boltzman's constant [W/(m^{2}K^4)].

4.1.2 Heat Transfer Coefficients at Boundaries

The following resultant emissivity and convection factors in table 4-1 are used.

Emissivity / Convection	$\varepsilon_p[-]$	$\alpha_\chi[-]$
Unexposed surface	0,8 (Thelandersson, 1974)	9 (ENV 1991-2-2, 1994)
Exposed surface	0,56 (ENV 1991-2-2, 1994)	25 (ENV 1991-2-2, 1994)

Table 4.1 Resultant emissivity and convection factors for exposed and unexposed surfaces.

4.2 FIRE EXPOSURE

The fire resistance of structures is usually determined by exposing them to the ISO-834 standard fire (ISO-834, 1975) or natural fires (Magnusson, Thelandersson, 1970). Both methods are used in the analysis and they are presented below.

4.2.1 ISO-834 Standard Fire

Structures must carry their loads for a certain time when they are exposed to the ISO-834 standard fire. How long depends on the use of the structure and national building codes. The following classes are used to describe the fire resistance of structures:

R30 R60 R90 R120 R180 R240

where R stands for resistance and the number for how many minutes the structure should at least carry the load. The temperature-time relationship on the boundary member is defined in equation 4.3 and shown graphically in figure 1.1.

$$T_b = 345 \times \log_{10}(8t+1) + T_0 \qquad (4.3)$$

where

- t is time [min].
- T_0 is ambient temperature [^{o}C].
- T_b is boundary temperature [^{o}C].

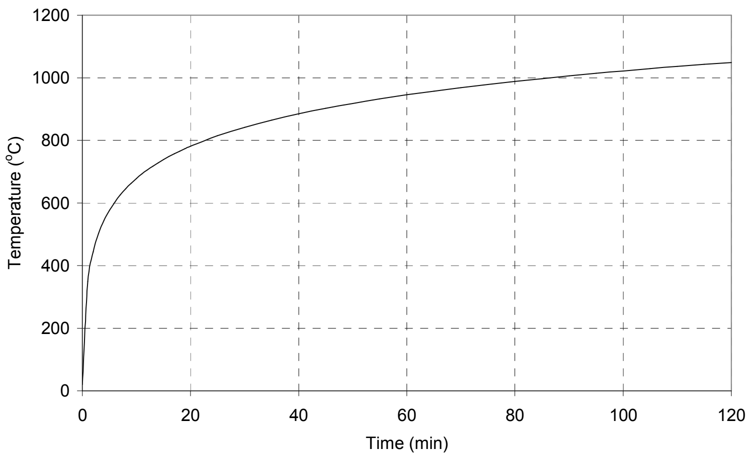

Figure 4.1 Temperature-time curve for the standard fire.

4.2.2 Natural Fires

At natural fires structures must carry their loads during the whole fire scenario and the cooling phase. How the temperature-time curve should be modelled should be decided by a certain analysis or from a compartment's fire-load density and opening factor. The analysis is limited to a standard compartment with opening factor 0,04m$^{1/2}$, which means that the heating phase is very similar to the ISO-834 standard fire. Figure 4.2 shows the temperature-time curves, which have been used in the analysis.

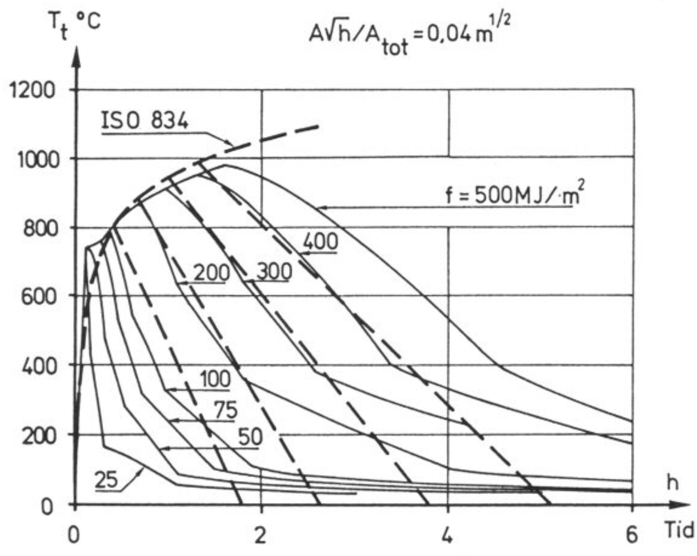

Figure 4.2 Time-temperature curves for different fire load densities at opening factor 0,04m$^{1/2}$ (Magnusson, Thelandersson, 1970).

5 CONCRETE BEAMS

This chapter contains the evaluation of the 500°C- and the Hertz-method, for reduction of concrete cross-sections and calculation of the moment capacity of fire exposed beams. It also contains an analysis of the stress-strain relationship of reinforcement at high temperatures for over-reinforced beams. Share forces are not considered in the calculations.

5.1 MECHANICAL BEHAVIOUR

Beams are structural elements carrying load that cause bending moments and shear forcec. The load-bearing capacity of a beam is dependent on the counteracted compression stress in the concrete, the tension stress in the reinforcement and the effective depth between these. The tension stress in concrete is negligible because it is very low compared to the one in reinforcement and the moment capacity usually gets higher if the concrete is allowed to crack in the tension zone. Figure 5.1 below graphically describes the stress-strain distribution in concrete beams.

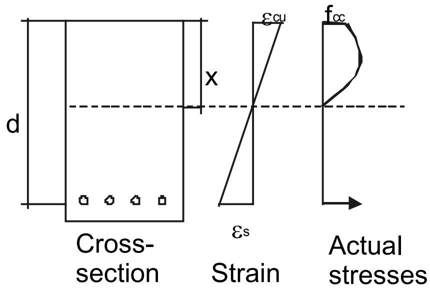

d	the effective depth of the beam (m)
x	the depth of the compression zone (m)
ε_{cu}	the ultimate compressive strain in concrete
ε_s	the tension strain in reinforcement
f_{cc}	the concrete compression strength (MPa)

Figure 5.1 Principal strains and stresses in reinforced concrete beams (Park, 1975).

As can be seen above the stresses are not uniform in the compression zone. In simplified calculations the stress is often assumed to be uniform with a reduced depth less than x (Nilsson, 1997) and in BKR (1999) it is reduced to 0,8x.

Three types of failures are identified for beams: normal-reinforced-, over-reinforced- and balanced-reinforced failure. They occur when the load increases over the load-bearing capacity or as in our case the load-bearing capacity decreases under the load as an effect of increasing temperature. Normal-reinforced failure is defined by the tension reinforcement yielding before the concrete reaches its maximum strength. Over-reinforced failure is defined by the compressed concrete reaches its maximum strength before the steel yields. Balanced failure is when the tensioned reinforcement yields at the same time as the concrete reaches its maximum strength.

For failures caused by fire it is very hard to draw a clear line between the failures since the stress-strain relationships of concrete and steel changes with temperature. Most failures are normal-reinforced since over-reinforced beams, in most cases, turn into normal-reinforced due to heating. The reason is that the ultimate stress for steel decreases much faster with temperature than the ultimate stress for concrete.

The following assumptions have been made:

- Plane cross-sections remain plane.
- The tensile strength of concrete is disregarded.
- Since the reinforcement areas are small, it is assumed that the temperature and strain is uniform over the reinforcement area, also se section 4.1.

5.2 PARAMETER CONFIGURATION

This section presents the cross-sections that are analysed. Since the analysis is done on cross-sectional level, external factors like length and boundary conditions don’t need to be identified. The following parameters need to be defined:

- Cross-sections geometry
- Reinforcing cross-sections and position of bars
- Fire exposure and boundary conditions
- Material properties

Section 5.2.1 shows the chosen cross-sections, material properties and boundary conditions for the fire exposure. Section 5.2.2 lists the fire exposures and calculation methods, which are used for each cross-section

5.2.1 Cross-Sectional Geometry and Material Properties

The analysed cross-sections are shown in figure 5.2. Cross-sections A-D are normal reinforced (strain over 2%) and E-F are over reinforced (strain below 2%).

<table>
<tr><th>Name</th><th>Cross-section (The thicker lines of the geometry’s are the sides exposed to fire).</th><th>Material properties</th></tr>
<tr><td>A.1</td><td>I-beam
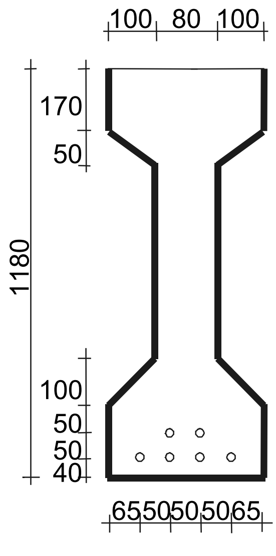
</td><td>Concrete: f_{cc} = 35,4 MPa

Prestressing steel, ϕ 13*:
f_y = 1870 MPa

*ϕ 13, effective area = 100e^{-6}m</td></tr>
</table>

<table>
<tr><td>B.1</td><td>T-Beam
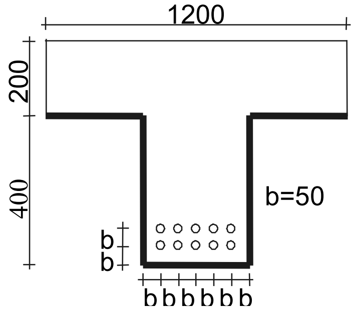
</td><td>Concrete: f_{cc} = 29,6 MPa

Reinforcing steel, ϕ25:
f_y = 370 MPa</td></tr>
<tr><td>C.1</td><td>R-beam (280x1180)
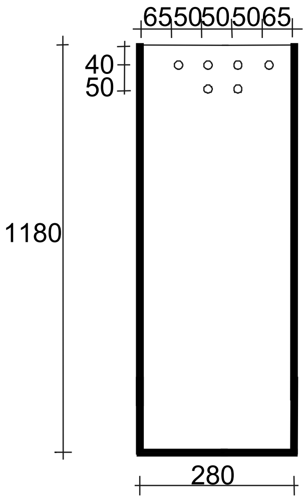
</td><td>Concrete: f_{cc} = 35,4 MPa

Prestressing steel, ϕ 13*:
f_y = 1870 MPa

*ϕ 13, effective area = 100e^{-6}m</td></tr>
<tr><td>D.i</td><td>R-Beam (bx1000)
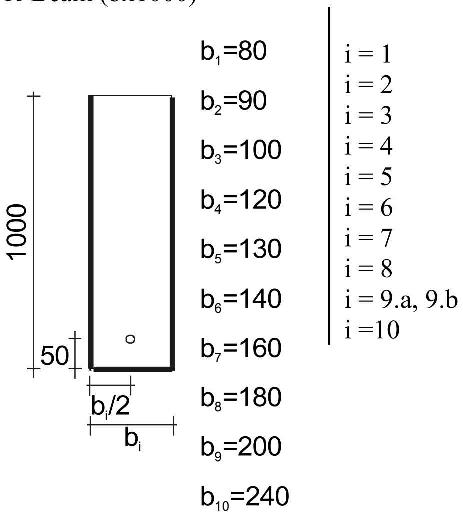
</td><td>Concrete: f_{cc} = 40 MPa

i = 1-8, 9a, 10
Reinforcing steel, ϕ 25:
f_{st} =f_y = 220 MPa

i = 9b
Tripled reinforcement area</td></tr>
</table>

E.i	R-Beam (300x500) i = 1.a, 1.b, 1.c 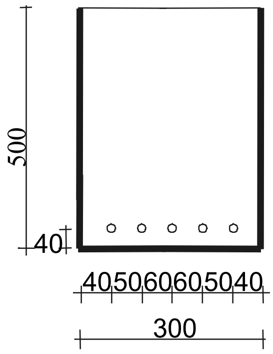	R-Beam (400x750) i = 2a, 2.b, 2.c 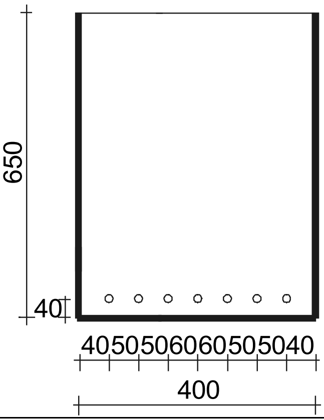	Concrete: f_{cc} = 29,4 MPa i = 1a, 2a Hot rolled steel, ϕ 25, f_y = 370 MPa i = 1b, 2b Doubled reinforcement area i = 1c, 2c Tripled reinforcement area
F.i	R-Beam (280x500) 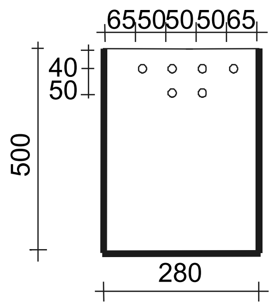	i = 1a, 1b i = 2a, 2b, 2c	Concrete: f_{cc} = 35,4 MPa i = 1a Cold worked steel, ϕ 16,8: f_y = 370 MPa i = 1b ϕ 23,8 i =2a Prestressing steel, ϕ 8: $f_{0,2\%} = f_y$ = 1670 MPa i =2b ϕ 10 i =2c ϕ 13

Figure 5.2 Analysed cross-sections.

5.2.2 Fire Exposures and Performed Calculations

This section lists the fire exposures and calculation methods, which are used at each cross-section. Table 5.1 lists the normal reinforced cross-sections and table 5.2 lists the over-reinforced.

Method	ISO-834							Fire load (MJ/m^2) at opening factor = 0,04m$^{1/2}$					Notes
	30	60	90	120	180	240	300	200	300	400	600	800	
A.1													
500°C	x	x	x	x				x	x	x			
Hertz	x	x	x	x				x	x	x			
Computer model	x	x	x	x				x	x	x			
B.1													
500°C	x	x	x	x				x	x	x			
Hertz	x	x	x	x				x	x	x			
Computer model	x	x	x	x				x	x	x			
C.1													
500°C	x	x	x	x				x	x	x			
Hertz	x	x	x	x				x	x	x			
Computer model	x	x	x	x				x	x	x			
D.1													
500°C		x											

Computer model		x											
D.2													
500°C		x						x					
Computer model		x						x					
D.3													
500°C								x					
Computer model								x					
D.4													
500°C			x	x				x	x				
Computer model			x	x				x	x				
D.5													
500°C									x				
Computer model									x				
D.6													
500°C			x	x					x	x			
Computer model			x	x					x	x			
D.7													
500°				x	x					x			
Computer model				x	x					x			
D.8													
500°C					x								
Computer model					x								
D.9.a, b													
500°C					x	x	x				x		
Computer model					x	x	x				x		
Hertz					x	x	x						
D.10													
500°C												x	
Computer model												x	

Table 5.1 Calculation methods and fire exposures for cross-section A.1-D.10.

The 500°C-method is used in all calculations.	ISO-834							Fire load (MJ/m^2) at opening factor = 0,04m$^{1/2}$			Notes
E.1a, b, c-E.2a, b, c	30	60	90	120	180	240	300	200	300	400	
Stress-strain relationship of steel is accounted	x	x	x	x				x	x	x	
Steel strain assumed over 2%	x	x	x	x				x	x	x	
F.1a, b-F.2a, b, c											
Stress-strain relationship of steel is accounted	x	x	x	x	x	x	x				
Steel strain assumed over 2%	x	x	x	x	x	x	x				

Table 5.2 Calculation methods and fire exposures for cross-section E.1-F.2.

5.3 COMPUTER CALCULATION

Computer calculations are performed for cross-sections A.1-D.10. Cross-section E.1-F.2 are not analysed with the computer model since they are over-reinforced and the computer model does not take strain into account, see equation 5.1.

5.3.1 Calculation Procedure

The principal calculation procedure for calculating the moment capacity in TCD is described in figure 5.3.

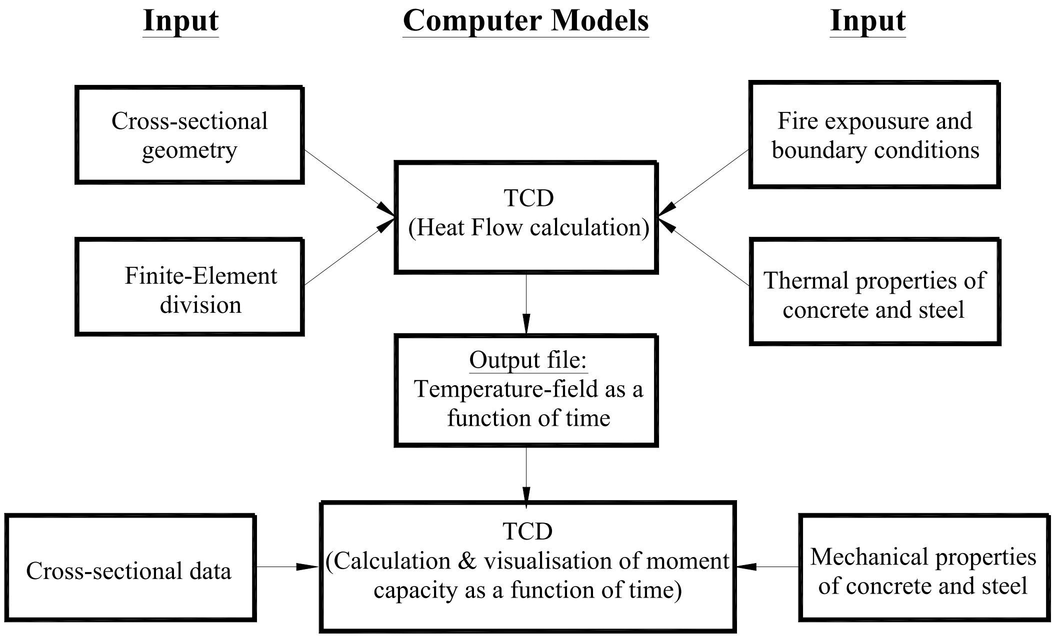

Figure 5.3 Principle calculation procedure in TCD.

The needed input in TCD, for calculating the moment capacity of concrete beams, are the one in the boxes the arrows start from.

5.3.2 C-Beam

The finite elements' temperature as a function of time, which are calculated with SUPER-TEMPCALC, are transferred to the sub program C-Beam, which calculates the moment capacity. The moment capacity is calculated by summarising the forces in each section of the concrete until they are equal to the summarised steel force, see equation 5.1. Equation 5.1 also determines the height of the compression zone and consequently even the lever arms needed for calculation of moment capacity in equation 5.2. Figure 5.4 shows a principal sketch of the procedure.

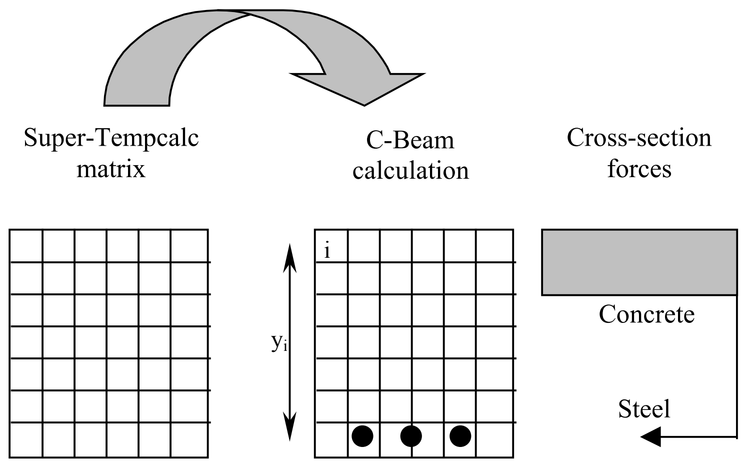

Figure 5.4 Principal description of the working procedure for calculating moment capacity in TCD.

$$\sum_i \left(f_{st,i}(T_i)\times A_{s,i}\right)-\sum_j\left(f_{cc,j}(T_j)\times A_{c,j}\right)=0 \qquad (5.1)$$

$$M_{cap}=\sum_j\left(f_{cc,j}(T_j)\times A_{c,j}\times y_j\right) \qquad (5.2)$$

where

M_{cap}	is the moment capacity for a given cross-sectional temperature field [kNm].
$f_{cc,j}(T_j)$	is the compression strength of concrete element j at temperature T_j [MPa].
T_j	is the temperature of element j [°C].
$A_{c,j}$	is the area of element j within the compression zone [m^2].
$f_{st,i}$	is the tension strength of reinforcement bar i with temperature T_i [MPa].
T_j	is the temperature of reinforcement bar i [°C].
$A_{s,i}$	is the area of reinforcement bar i [m^2].
y_j	is the lever arm of resultant force in concrete compression element j [m]. It is determined by equation 5.1.

A description of the program package TCD is found in appendix F.

5.4 SIMPLIFIED CALCULATIONS

This section describes the two simplified methods for reduced cross-sections and how to calculate the moment capacity. BKR recommends the 500°C-method (Anderberg, Pettersson, 1992) and Eurocode recommends the Hertz-method (Hertz, 1999).

5.4.1 Calculation Procedure

The principal calculation procedure for both methods is briefly described below.

1. Determine the temperature field of the cross-section at a specific time.
2. Reduce the concrete cross-section.
3. Determine the temperatures in reinforcement.
4. Reduce the strength of reinforcement due to temperatures.
5. Use a design method at normal temperature and calculate moment capacity with the reduced properties.
6. Compare the capacity with the design load.

5.4.2 Reduction of Cross-Section

5.4.2.1 The 500°C-method

It is assumed that concrete with a temperature over 500°C has no compression strength left and that under 500°C it has full strength. In reality this is not true, but empirical experiments with different loads and fire exposures have verified its legality for ordinary siliceous concrete (Anderberg, 1978). Figure 5.5 shows how the area of the 500°C-isoterm for cross-sections is simplified. The main principle is that the surfaces, which occur by the intersection of the 500°C-isotherm and the simplified isotherm, should be equal inside and outside the simplified isotherm.

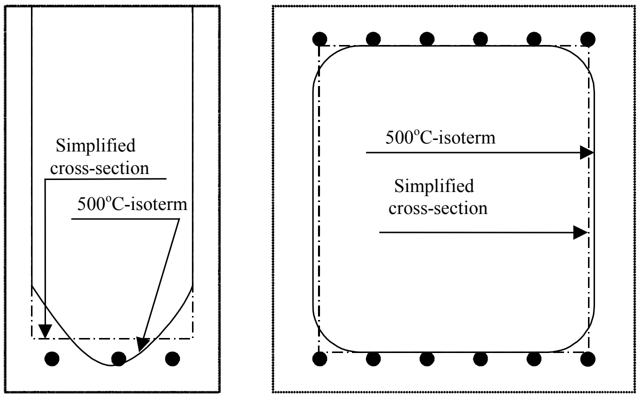

Figure 5.5 Simplification of the 500°-isotherm area.
A) Three sided fire exposure
B) Four sided fire exposure

5.4.2.2 Hertz-method

This section is based on the description in Eurocode (ENV 1992-1-2, 1995). It is assumed that isotherms in the compression zone of a rectangular cross-section are parallel with the sides. The fire damaged cross-section is represented by a reduced cross-section by ignoring a damaged zone of thickness a_z at the fire exposed sides, see figure 5.6. For a rectangular cross-section exposed to fire on one face only, the width is assumed to be w, see figure 5.6c. When two opposites sides are exposed to fire the width is assumed to be $2w$, see figure 5.6a, b, d, e and the web of f. The flange of figure 5.6f is related to the equivalent wall in figure 5.6d, and the web to the equivalent wall in figure 5.6a.

For bottoms and ends of rectangular members exposed to fire, where the width is less than the height, the value a_z is assumed to be the same as the calculated values for the sides, see figure 5.6b, e and f.

The compressive strength and the elasticity of modulus of the reduced cross-section are assumed to be constant and equal to that calculated for the point M. M corresponds to any point in the middle of the plane of the equivalent wall.

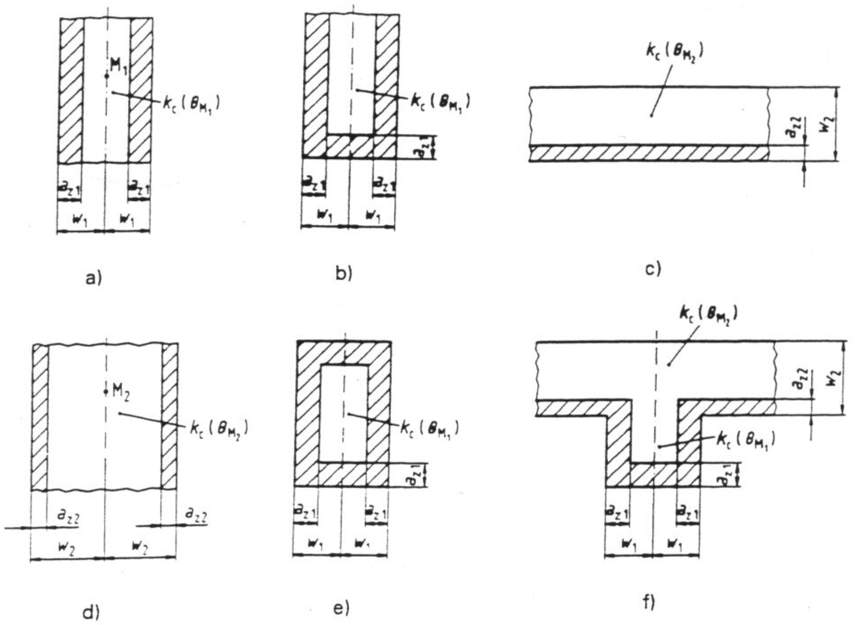

Figure 5.6 Reduction of strength and cross-sections found by means of equivalent walls exposed to fire from sides (ENV 1992-1-2, 1995).

The reduced compressive strength $f_{cc}(T)$ at the point M in a member exposed to fire from both sides is calculated with equation 5.3 where T is the temperature at point M.

$$f_{cc}(T) = k_c(T) \times f_{cc}(20^o C) \tag{5.3}$$

The reduced short time modulus of elasticity at this point is calculated by equation 5.4.

$$E_{cc}(T) = (k_c(T))^2 \times E_{cc}(20^o C) \tag{5.4}$$

The damaged zone, a_z, is estimated as follows for an equivalent wall exposed on both sides:

- The half thickness of the wall is divided into n parallel zones of equal thickness, where $n >= 3$, see figure 5.7. In this report n is determined so that the equal thickness always is 1 cm.
- The temperature is calculated for the middle of each zone.
- The corresponding reductions, $k_{ci}(T_i)$, of the compressive strength are determined.

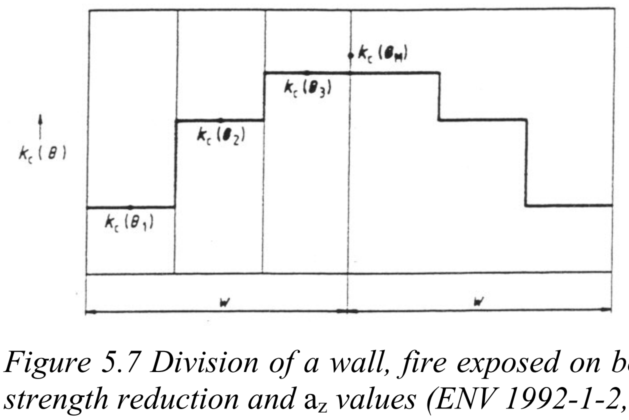

Figure 5.7 Division of a wall, fire exposed on both sides, into zones for use in calculation of strength reduction and a_z *values (ENV 1992-1-2, 1995).*

– The mean reduction coefficient incorporating a factor (1-0,2/n), which allows for the variation of temperature within each zone, is calculated by equation 5.5.

$$k_{c,m} = \frac{(1-0{,}2/n)}{n} \times \sum_{i=1}^{n} k_c(T_i) \tag{5.5}$$

– The width of damaged zone for beams is calculated with equation 5.6a. For walls and columns, where second order effects must be considered, equation 5.6b is used.

$$a_z = w \times \left(1 - \frac{k_{c,m}}{k_c(T_M)}\right) \tag{5.6a}$$

$$a_z = w \times \left(1 - \left(\frac{k_{c,m}}{k_c(T_M)}\right)^{1,3}\right) \tag{5.6b}$$

5.4.3 Mechanical Calculation

Figure 5.8 shows the geometrical parameters, which need to be defined when calculating the moment capacity of beams. b' is defined by one of the methods in section 5.4.2 *Reduction of Cross-Section*, d is given by the geometry and x is calculated in this section.

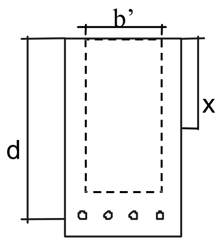

b’ = New width after fire exposure (m)
d = Effective depth (m)
x = Depth of compression zone (m)

Figure 5.8 Necessary parameters for calculating the moment capacity of a single reinforced beam.

When the geometrical parameters are defined, the strength of the material must also be defined. Thereafter equation 5.7 and 5.8 are used to calculate the moment capacity.

$$\sum_i \left(f_{st,i}(T_i, \varepsilon_i) \times A_{s,i}\right) - f_{cc}(T) \times 0{,}8 \times b' \times x = 0 \tag{5.7}$$

$$M_{cap} = \sum_j \left(f_{st,i}(T_i, \varepsilon_i) \times A_{s,i} \times (d - 0{,}4 \times x)\right) \tag{5.8}$$

where

M_{cap}	is the moment capacity for a given cross-sectional temperature field [kNm].
$f_{ccj}(T)$	is the compression strength of concrete [MPa].
T	is the temperature of concrete [^{o}C].
b'	is the width of the compression zone [m].
x	is the depth of compression zone [m].
$f_{st,i}(T_i, \varepsilon_i)$	is the tension strength of reinforcement bar i with temperature T_i [MPa].

T_i	is the temperature of reinforcement bar i [^oC].
$A_{s,i}$	is the area of reinforcement bar i [m^2].
d	is the effective depth [m].

The normal procedure when designing a concrete beam is to assume that it is normal-reinforced (the steel strain is above 2%). Then $f_{st,i}(T_i, \varepsilon_i)$ is simplified to $f_{st,i}(T_i)$ and the moment capacity does not need to be iterated with respect to both temperature and strain. It makes the calculation procedure simple but it must be verified that the steel strain is above 2%. This is done with equation 5.9, were the strain for ultimate compressive concrete strength is set to 0,35% (BKR 99, 1999). The relationship of the parameters in equation 5.9 is graphically explained in figure 5.1.

$$\varepsilon_s = \varepsilon_{cu} \times (d - x)/x \tag{5.9}$$

5.5 RESULTS

Section 5.5.1 contains the results of the comparison of the 500^{o}C-method and the Hertz-method with the computer model. Section 5.5.2 contains a control of minimum widths of beams, for use of the 500^{o}C-method, at different fire exposures. Section 5.5.3 contains the results of the analysis of the stress-strain relationship of reinforcement for over-reinforced beams.

The results, which are not presented, in this section can be studied in Appendix A.

5.5.1 Comparison of Results Between Simplified Methods and Computer Model

This section is based on cross-section A.1, B.1, C.1 and D.9a. The analysis shows that the Hertz- and 500^{o}C-method are both good methods, see figure 5.9 and 5.10. As the middle of a cross-section has reached 500^{o}C, which exceeds the application area of the 500^{o}C-method, the Hertz-method continues to give good results, see figure 5.11.

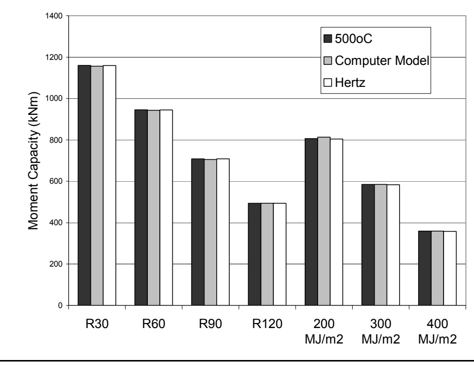

A.1 (I-Beam)

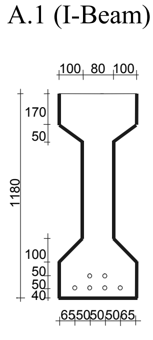

Concrete: f_{cc} = 35,4 MPa

Prestressing steel:
f_y = 1870 MPa, ϕ 13*

* ϕ 13, effective area = 100e^{-6}m

Figure 5.9 A.1 (I-Beam), comparison of simplified methods with computer model when the tension zone is three-sided exposed to fire.

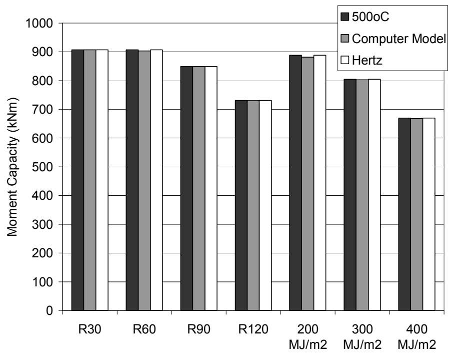

B.1 (T-Beam)

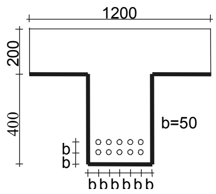

Concrete: f_{cc} = 29,6 MPa

Reinforcing steel:
f_y = 370 MPa, ϕ25

Figure 5.10 B.1 (T-Beam), comparison of simplified methods with computer model when the tension zone is three-sided exposed to fire.

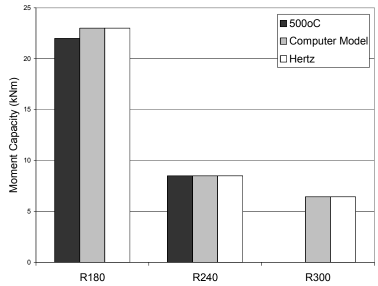

At R300 the temperature in the middle of the cross-section is 610°C.

D.9 R-Beam (200x1000)

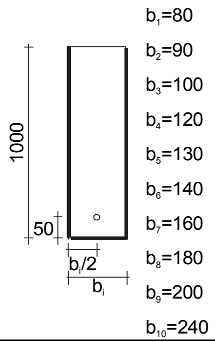

Concrete: f_{ck} = 40 MPa

Reinforcing steel:
f_{st} =f_y = 220 MPa, ϕ 25

Figure 5.11 D.9 (R-Beam), comparison of the Hertz-method with computer model when the temperature is just below or has reach over 500°C in the middle of the cross-section.

Both methods show good agreement with the computer model for cross-sections with compression-zone exposed to the ISO-834-fire from three sides. For natural fires both methods tend to be conservative, especially the 500°C-method, see figure 5.12. The reason being that the methods have different ways of calculating the penetration of short sides.

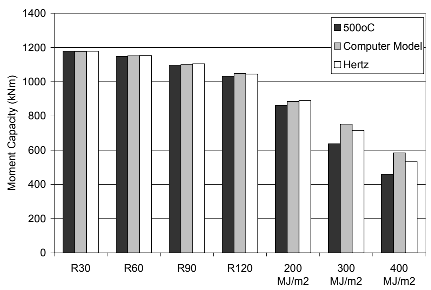

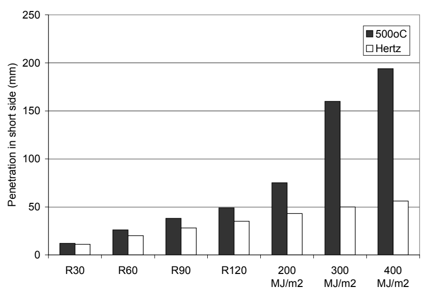

C.1 R-beam (280x1180)

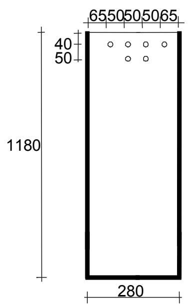

Concrete: f_{cc} = 35,4 MPa

Prestressing steel:
f_y = 1870 MPa, ϕ 13*

*ϕ 13, effective area = $100e^{-6}$m

Figure 5.12 C.1 (R-Beam), comparison of simplified methods with computer model when the compression zone is three-sided fire exposed.

5.5.2 *500°C-Method, Minimum Widths of Fire Exposed Cross-Sections*

The recommended minimum widths turned out to be quite relevant. Some of them may be changed since they were too thin or too thick. Table 5.3 shows the old values, table 5.4 the new values for the standard fire and table 5.5 the new values for natural fires at opening factor 0,04m$^{1/2}$. The results are based on calculation D.1-10. The temperature-time curves for fire load 600MJ/m^2 and 800MJ/m^2 were never found and therefore their values have not been evaluated.

Fire resistance	R 60	R 90	R 120	R 180	R 240
Fire load density (MJ/m^2)	200	300	400	600	800
Minimum width of cross-section (mm)	80	120	160	200	240

Table 5.3 Minimum width of cross-sections as a function of fire resistance and fire load density (Anderberg Y, 1992).

Fire resistance	R 60	R 90	R 120	R 180	R 240
Minimum width of cross-section (mm)	90	120	160	180	200

Table 5.4 New minimum width of cross-sections exposed to an ISO-834 fire.

Fire load density (MJ/m^2) Opening factor = 0,04m$^{1/2}$	200	300	400	600	800
Minimum width of cross-section (mm)	100	140	160	?	?

Table 5.5 New minimum width of cross-sections exposed to natural fires at opening factor = 0,04m$^{1/2}$.

5.5.3 *Study of Over-Reinforced Cross-Sections with the 500°C-Method*

This section is based on calculations of cross-sections E.1-2 and F.1-2. They differ from the rest since they are over-reinforced and steel strain must be taken into account in the calculations. The 500°C-method has been used since the computer model does not take steel strain into account and it gives more conservative results than the Hertz-method for fire-exposed compression zones.

It is seen from figure 5.13, 5.14 and 5.15 that the deviation in moment capacity is acceptable (less than 10%) for cross-sections as long as the steel strain is greater than 1,3% (equation 5.9). The difference between the proportionality and yield strength in table 2.1, 2.2 and 2.3 also support this.

Figure 5.14 and 5.15 also show that the deviation in moment capacity is acceptable for normal reinforced cross-sections, which turns into over-reinforced cross-section due to fire exposed compression zone. The reason is that the deviation is acceptable for strains down to 1,3% and the penetration of damaged concrete is slow for normal time periods and cross-sections.

i = 2a

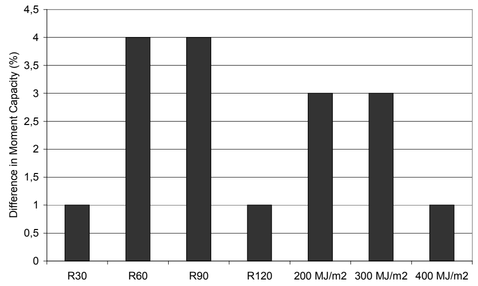

Strain (%)	1,17	1,19	1,33	1,67	1,31	1,38	1,65
$T_{ave.}$ (°C)	156	345	478	576	379	481	566

R-Beam (400x750)

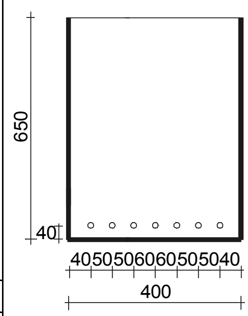

Concrete: f_{cc} = 29,4 MPa

Hot rolled steel:
f_y = 370 MPa

i = 2a , ϕ 25

i = 2b, doubled reinforcement area

i = 2c, tripled reinforcement

i = 2b

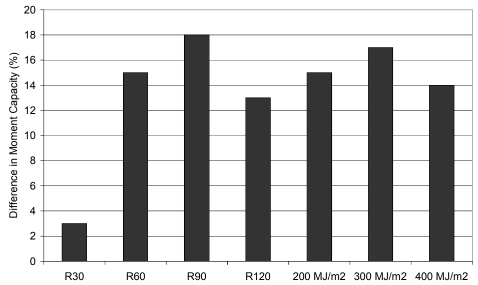

Strain (%)	0,44	0,53	0,64	0,81	0,61	0,66	0,80
$T_{ave.}$ (°C)	156	345	478	576	379	481	566

i = 2c

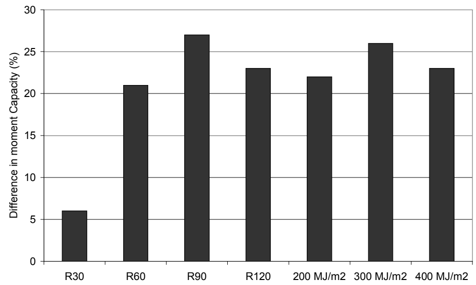

Strain (%)	0,18	0,30	0,40	0,52	0,36	0,42	0,51
$T_{ave.}$ (°C)	156	345	478	576	379	481	566

Figure 5.13 E.2 (R-Beam, hot rolled), difference in moment capacity when the stress-strain relationship of steel is taken into account contra it is assumed the steel is yielded.

i =1a

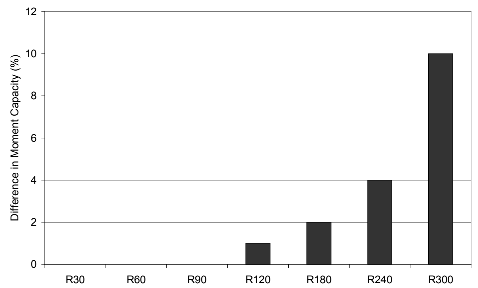

Strain (%)	1,94	1,69	1,48	1,31	1,02	0,9	0,73
$T_{ave.}$ (°C)	33	68	113	158	241	333	417

i =1b

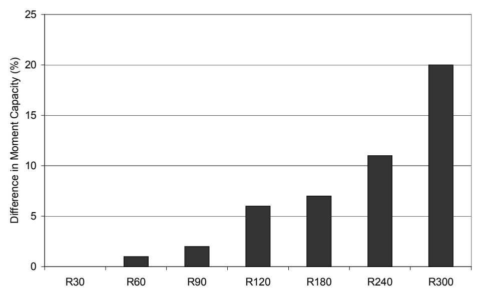

Strain (%)	0,79	0,68	0,59	0,52	0,38	0,34	0,30
$T_{ave.}$ (°C)	33	68	113	158	241	333	417

R-Beam (280x500)

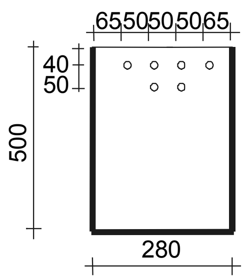

Concrete:
f_{cc} = 35,4 MPa

Cold worked steel:
f_y = 370 MPa

i =1a, ϕ 12

i = 1b, ϕ 17

Figure 5.14 F.1 (R-Beam, cold worked), difference in moment capacity when the stress-strain relationship of steel is taken into account contra it is assumed the steel is yielded.

i = 2a

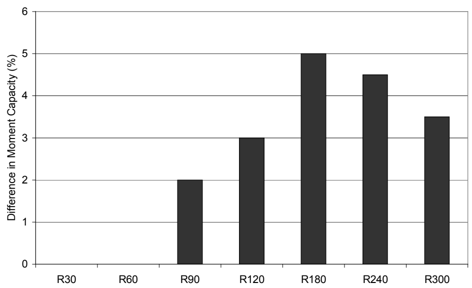

Strain (%)	1,93	1,73	1,58	1,49	1,42	1,5	1,55
$T_{ave.}$ (°C)	33	68	113	158	241	333	417

R-Beam (280x500)

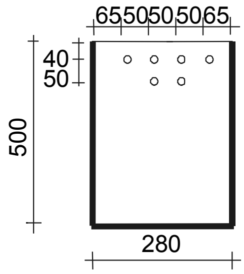

Concrete:
f_{cc} = 35,4 MPa

Prestressing steel:
$f_{0,2\%}$= f_y = 1670 MPa

i =2a,ϕ 8

i = 2b, ϕ 10

i =2c, ϕ 13

i = 2b

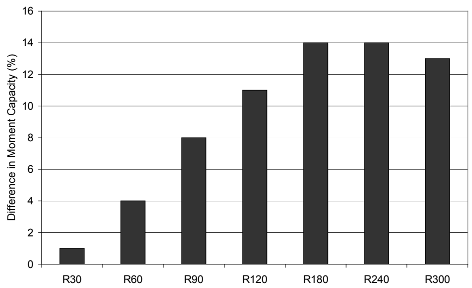

Strain (%)	1,27	1,18	1,12	1,07	1,03	1,09	1,13
$T_{ave.}$ (°C)	33	68	113	158	241	333	417

i = 2c

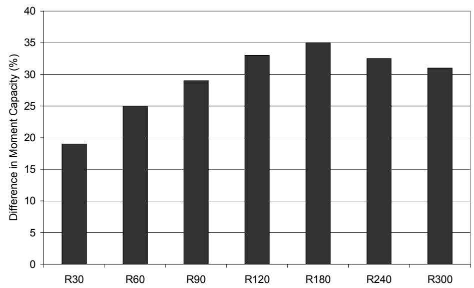

Strain (%)	0,72	0,69	0,65	0,63	0,60	0,63	0,64
$T_{ave.}$ (°C)	33	68	113	158	241	333	417

Figure 5.15 F.2 (R-Beam, prestressed), difference in moment capacity when the stress-strain relationship of steel is taken into account contra it is assumed the steel is yielded.

5.6 CONCLUSIONS

The study shows that the Hertz-method and 500°C-method give very good results for fire-exposed tension zones. The deviation of the results for the two methods compared to the computer model is negligible. For cross-sections where the lowest temperature is above 500°C the Hertz-method continues to give good results. The results can be studied in section 5.5.1.

When the compression-zone of a cross-section is exposed to fire (ISO-834) from three sides, both methods give somewhat safer results (<1%) compared to the computer model. For natural fires the results are more conservative (especially the 500°C-method). The deviation from the computer model for the Hertz-method is less than 10% for all calculations. For a fire load at 300MJ/m^2, with an opening factor of 0,04$m^{1/2}$, the results of the 500°C-method are conservative (>15%) for cross-sections with a width of 280mm. The results can be studied in section 5.5.1.

The minimum widths, for use of the 500°C-method, of fire-exposed cross-sections can be changed for some fire exposures. The results can be studied in section 5.5.2.

The Hertz-method can take into account any strength-reduction curve because it is based on strength and stiffness distribution in a fire-exposed cross-section (Hertz, 1999). The 500°C-method is originally developed for ordinary siliceous concrete but can be modified for other concrete qualities (Anderberg, Pettersson, 1992). This has been done for high performance concrete, i.e. the load-bearing capacity, with which the 500°C-method is calculated, is reduced by a factor of 0,95 for beams in bending and 0,90 for columns axially loaded (Tómasson, 1998).

The 2%-limit of steel strain, i.e the related strength-temperature curve, could be applied for over-reinforced cross-sections for steel strains down to 1,3% with an acceptable deviation (<10%). The result can be studied in section 5.5.3.

The deviation in moment capacity is acceptable for normal reinforced cross-sections, which turns into over-reinforced cross-sections due to fire exposed compression zone. The reason is that the deviation is acceptable for steel strains down to 1,3% and the penetration of damaged concrete is slow for normal time periods and cross-sections. The results can be studied in section 5.5.3.

6 CONCRETE COLUMNS

This chapter contains the evaluation of simplified methods for calculating the load-bearing capacity of fire exposed concrete columns. The simplified methods are evaluated against a computer based non-linear finite element model and it is focused on the second order effects.

6.1 MECHANICAL BEHAVIOUR

A column is a structural element, which primarily carries axial loads. When columns are loaded, a horizontal deflection occurs which causes an extra bending moment. This extra moment is also known as second order effects and increases when columns are fire-exposed. For short columns the second order effects are negligible but for slender columns it has a considerable influence on the load-bearing capacity.

6.1.1 Slenderness

The slenderness, λ, is defined by equation 6.1 and it takes the critical load (the lowest load which causes permanent deformations), the length, stiffness and cross-section dimensions into account.

$$\lambda = \frac{l_c}{i} \tag{6.1}$$

where

l_c	is the critical length [m].
$i = h/12^{0,5}$	is the radius of inertia [m], where *h* is equal to the height of the cross-section [m].

The critical length is theoretically defined by equation 6.2.

$$l_c = \pi\sqrt{\frac{EI}{N_{cr}}} \tag{6.2}$$

where

EI	is the flexural rigidity, which should allow for the effects of cracking, creep and non-linearity of the stress-strain curve [Nm^2].
N_{cr}	is the critical load, which is the load where the first permanent deformation occurs [N].

Critical length could also be defined by equation 6.3, which is a function of the columns' geometrical length and its mechanical boundary conditions.

$$l_c = \alpha \times l \tag{6.3}$$

where

l	is the geometrical length of column [m].
α	is the buckling length factor [-].

The buckling length factor takes the degree of lateral and rotational restraint at the ends of the columns into account. According to Eurocode (ENV 1992-1-1, 1999) the buckling length factor, α, could be chosen from figure 6.1.

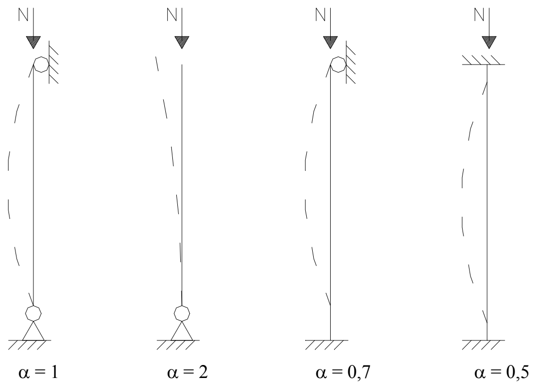

Figure 6.1 Examples of different buckling modes and corresponding buckling length factors for isolated members.

6.1.2 Second Order Effects

For a column exposed to an axial force, N, with the eccentricity e, a moment $N \cdot e$ occurs and causes bending. The bending then causes an additional eccentricity, Δ, and the total moment is increased to $N \cdot (e + \Delta)$. This phenomenon is also known as second order effects and is illustrated in figure 6.2.

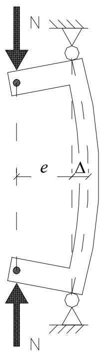

Figure 6.2 Loading and deflection of an eccentrically loaded column (Mårtensson, 1997).

The relation between the force and the additional moment is non-linear since Δ increases more than force. For short columns the additional moment is negligible but for slender columns the load-bearing capacity is directly dependent on it. This is illustrated in figure 6.3, which also shows a principal interaction diagram of the cross-section of a column. A column can carry any combination of load and eccentricity that can be plotted within the interaction diagram.

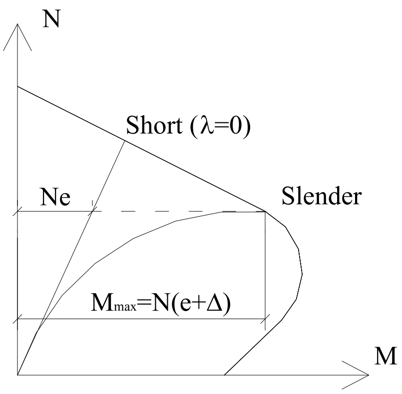

Figure 6.3 Interaction diagram for an eccentrically loaded column (Mårtensson, 1997).

An interaction diagram can be created with the equations 6.4 and 6.5, which are the equilibrium equations for an eccentrically loaded cross-section, see figure 6.4.

$$N_U = f_{cc}(T) \times 0{,}8 \times x \times b + \sum\left(A'_s \times f'_s(\varepsilon', T')\right) - \sum\left(A_s \times f_s(\varepsilon, T)\right) \qquad (6.4)$$

$$M = N_U \times e' = f_{cc}(T) \times 0{,}8 \times x \times b \times (d - 0{,}4x) + \sum\left(A'_s \times f'_s(\varepsilon, T) \times (d - d')\right) \qquad (6.5)$$

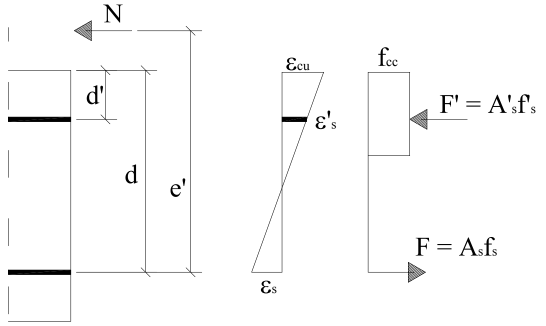

Figure 6.4 Principle strains, stresses and forces for an eccentrically loaded cross-section (Mårtensson, 1997).

6.1.3 Behaviour at High Temperatures

Forces and moments that interact on fire exposed concrete columns are often varied during a fire scenario. These variations are often caused by direct changes in mechanical behaviour of the fire-exposed column or by interacting continuous constructions. For concrete columns the following factors usually influence the structural behaviour at high temperatures (Forsén, 1982).

- Additional shear forces and moments due to dilation of adjacent horizontal members.
- Additional axial forces may occur due to restrained thermal elongation.
- Restraint moments and forces from adjacent members can be transferred by stiff connections.
- Second order moment may prove to be significant due to increased transversal displacement.

Longitudinal reinforcement in a column is often placed near the surface as it increases the moment of inertia of the cross-section. For fire-exposed columns this means that the strength reduction will occur fast for the reinforcing steel and the load-bearing capacity might get independent of the steel (Hertz, 1999).

The fast heating of slender cross-sections and the large reduction of elasticity of modulus make slender concrete columns susceptible to special fire hazards. It increases the risk of buckling failure compared to the risk of compression failure and it is therefore important to take weakening concrete in a precise manner into account (Hertz, 1999).

6.2 PARAMETER CONFIGURATION

Five different columns have been analysed, based on one rectangular cross-section. The following factors must be defined before the analysis:

- Cross-sectional geometry
- Fire exposure
- Material properties
- Structural factors

Cross-sectional geometry means the height and the width of the cross-section as well as the reinforcement topology etc. Structural factors include slenderness, initial out of straightness, load eccentricity and boundary conditions. Fire exposure includes fire exposure, time of heat exposure and boundary conditions. Tables 6.1 lists the parameter setup and figure 6.5 shows the boundary condition for the heat flow analysis and figure 6.6 for the structural member analysis.

	Column number				
	1	**2**	**3**	**4**	**5**
Concrete cross-section (mm^2)	300x300				
Reinforcement diameter (mm)	4ϕ25	4 ϕ16	4 ϕ12	4ϕ25	4ϕ25
Geometrical reinforcement ratio	0,022	0,010	0,005	0,022	0,022
Concrete cover (mm)	40				
Column length (mm)	8000			12000	4000
Initial slenderness	27	27	27	40	13
Initial out of straightness, e_a (mm)	20				
Structural boundary condition (α).	1				
Fire exposure	ISO-834				
Boundary conditions for temperature analysis	4-sided exposure				
Time of maximum load (minutes)	30, 60, 90 and 120				

Table 6.1 Geometrical and structural parameters for column calculations.

As it can be seen in table 6.1, natural fires are excluded from the analysis of concrete columns. The reason is that the analysis of the ISO-834 standard fire shows that the simplified methods are unsafe and deviates huge from the computer model. Since natural fires are much more complex than the ISO-834 standard fire nothing speaks for the results of natural fires would be any different.

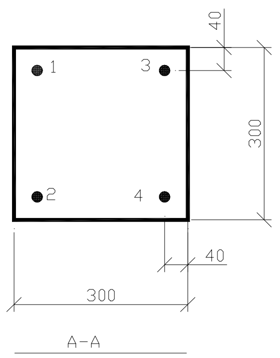

(mm)

Concrete:
f_{cc} = 29,6 MPa
f_{ct} = 0 MPa

Reinforcement:
f_y = 370 MPa

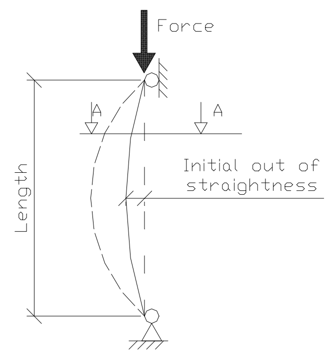

Figure 6.5 Boundary condition for heat flow analysis and position of reinforcement.

Figure 6.6 Structural boundary conditions, the whole line shows the initial conditions and the dashed line the deflections.

The initial out of straightness, in figure 6.6, is set to account for imperfections during the manufacturing of columns. It is modelled by using a half sinus curve with the amplitude 0,02m, see table 6.1. The amplitude is fixed for the columns and it is calculated according to the Swedish building code (BKR, 1999) for the eight meter tall columns.

6.3 COMPUTER CALCULATION

This section describes the calculation procedure and the computer model.

6.3.1 Calculation Procedure

The principal calculation procedure for calculating the load-bearing capacity of fire exposed columns with CONFIRE is described in figure 6.7.

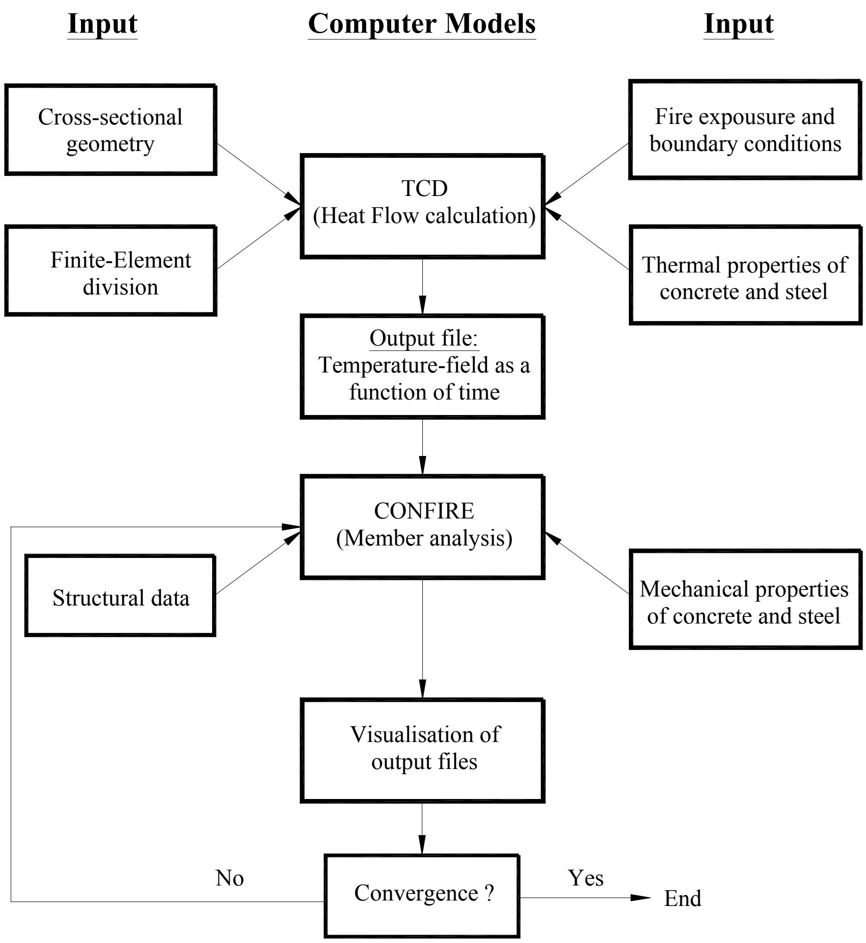

Figure 6.7 Principal calculation procedure for calculating fire-exposed columns´ time to failure with CONFIRE.

6.3.2 CONFIRE

CONFIRE is a program for analysing plane concrete frames subjected to inplane loading and temperatures varying with time. The analysis is based on a non-linear displacement formulation of the finite element method using two dimensional beam elements. The non-linear geometric effects are taken into account by updating the nodal coordinates of the structure during deformation. The non-linear temperature field, calculated with SUPER-TEMPCALC, takes temperature dependent material properties, into account. The material models (constitutive models), which are used by CONFIRE, is defined in chapter 2. In the model the total strain, ε_{tot}, is restricted to vary linearly in the lateral (Bernoulli-Navier hypothesis) and longitudinal directions for each element. Furthermore the strain is restricted to be constant over the width of the cross-sections (Forsén, 1982 & 1986). The program requires several kinds of input data; cross-sectional measures, mechanical data for concrete and reinforcement, load and eccentricities, structural data including topology, boundary conditions including information on supports as well as about the incremental iteration process and time increments. A principal model of the analysed columns in CONFIRE is shown in figure 6.8.

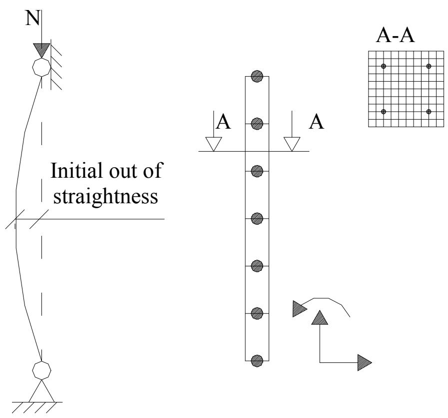

Figure 6.8 Simplified structure model and cross-section used in CONFIRE.

6.4 SIMPLIFIED CALCULATIONS

Three simplified methods for calculating the second order effects and load capacities of columns are analysed. The methods are: the stiffness method recommended by BKR, the stiffness method in Eurocode and a method developed by Hertz, which is expected to be adopted by the Danish code.

Independent of the choice of method, all cross-sections and material properties are reduced with Hertz's method in chapter 5. The reason is that the second order effect should be calculated with the same parameters and the method takes stiffness into account, which the 500^{o}C-method does not.

6.4.1 Stiffness Method in BKR

The Swedish building code says that the cross-section of the column should be reduced with the 500^{o}C-method but as already mentioned Hertz's method will be used in the analysis. Thereafter the maximum centric axial load should be calculated. If the load is eccentric the second order moment should be calculated and compared to an interaction diagram of the cross-section.

The centric load is calculated with equation 6.6.

$$N_{uT} = \left(k_c \times A_c \times f_{cc}\right) / \left(1 + 1{,}0 \times k_\varphi\right) + k_s \times A_s \times \sigma_{0.5}(T_m) \quad (6.6)$$

where

A_c is the reduced cross section of concrete [m^2].
A_s is the reinforcements area [m^2].
k_c, k_φ, k_s are coefficients dependent on the ratio l_c/h (slenderness), strength classes of concrete and reinforcement. l_c is the buckling length and h is the width for rectangular cross sections [-].
T_M is the average temperature of reinforcement [^oC].
$\sigma_{0,5}(T_M)$ is the stress at 0,5% strain [MPa].

The coefficients k_c, k_φ, and k_s are chosen from table 6.2 below where the strength classes are taken from the Swedish building code.

Strength class	l_c/h						Coefficient
	0	10	20	30	40	50	
K16	1	0,90	0,77	0,63	0,45	0,29	k_c
K30	1	0,89	0,73	0,55	0,36	0,20	
K50	1	0,88	0,69	0,48	0,27	0,13	
K80	1	0,87	0,65	0,40	0,19	0,09	
K16	0	0,02	0,10	0,29	0,60	0,90	k_φ
K30	0	0,04	0,16	0,48	0,87	1,00	
K50	0	0,05	0,24	0,71	0,99	1,00	
K80	0	0,06	0,35	0,90	1,00	1,00	
K16	1	0,79	0,50	0,23	0,19	0,15	k_s $220<f_{yd}\leq400$MPa
K30	1	0,81	0,52	0,33	0,22	0,19	
K50	1	0,82	0,62	0,37	0,27	0,22	
K80	1	0,82	0,70	0,41	0,31	0,24	
K16	1	0,72	0,35	0,15	0,13	0,10	k_s $400<f_{yd}<600$MPa
K30	1	0,72	0,35	0,21	0,15	0,13	
K50	1	0,74	0,41	0,24	0,18	0,15	
K80	1	0,77	0,47	0,28	0,21	0,16	

Table 6.2 Coefficients k_c, k_φ, and k_s used in equation 6.6.

The total moment is calculated by dividing the first order of moment with the *c*-value, see equation 6.7. The *c*-value is given in table 6.3.

N/N_{uT}	K16-K40				K45-K80			
	l_c/h				l_c/h			
	0	10	20	>30	0	10	20	>30
0	1	1,00	1,00	1,00	1	1,00	1,00	1,00
0,2	1	0,86	0,62	0,62	1	0,78	0,56	0,56
0,4	1	0,77	0,52	0,47	1	0,68	0,44	0,41
0,6	1	0,67	0,42	0,32	1	0,57	0,33	0,26
0,8	1	0,56	0,32	0,21	1	0,45	0,24	0,14
1,0	1	0,35	0,25	0,13	1	0,25	0,17	0,08

Table 6.3 c values for calculating total moment with equation 6.7.

$$M_{Tot} = M_0 / c \tag{6.7}$$

where

M_{Tot} is the total moment acting on the cross-section[kNm].
M_0 is the moment caused by load and initial eccentricity, $N \cdot e_0$ [kNm].
c is a coefficient which takes second order effects into account [-].

The interaction diagram is calculated with the equilibrium equations 6.4 and 6.5.

6.4.2 Stiffness Method in Eurocode

According to Eurocode the cross-section of the column should be reduced with Hertz's method. Then the second order moment should be calculated and compared to an interaction diagram of the critical cross-section.

The second order effect is calculated with equation 6.8, which is a function of the first order moment, the critical load and the load acting on the column.

$$M_{Ed} = M_{0Ed} \times \left(1 + \beta / \left(N_B / N_{Ed} - 1\right)\right) \tag{6.8}$$

where

M_{0Ed} is the first order moment [kNm].
β is π^2/c_0 and $c_0 = 8$ for a constant first order moment [-].
N_{Ed} is the design value of axial load [kN].
N_B is the buckling load based on reduced stiffness [kN].

The buckling load (N_B) is calculated with equation 6.2 and the stiffness (EI), which is needed in equation 6.2, with equation 6.9.

$$EI = K_e \times K_\varphi \times E_{cd} \times I_c + K_s \times E_{sd} \times I_s \tag{6.9}$$

where

E_{cd} is the design value of the modulus of elasticity of concrete [MPa].
I_c is the moment of inertia of concrete cross section [m^4].
E_{sd} is the design value of the modulus of elasticity of reinforcement [MPa].

I_s is the moment of inertia of reinforcement referred to CG of concrete [m^4].
K_e is the correction factor for the effects of cracking [-].
K_ϕ is the correction factor for the effects of creep [-].
K_s is the correction factor for the contribution of reinforcement [-].

The correction factor for the effects of cracking and contribution of reinforcement are decided by the reinforcement ratio, A_s/A_c.

- if $A_s/A_c>0{,}01$: $K_e = 0{,}4$ and $K_s = 0$
- if $A_s/A_c>0{,}005$: $K_e = 0{,}2$ and $K_s = 1$

K_ϕ is calculated with equation 6.10. The value of the creep coefficient, ϕ_{ef}, is estimated to 0,9 from figure 3.1 in Eurocode (EN 1992-1-1, 1999). It correlates to a column with 30 days of ageing before loading.

$$K_\phi = 1/(1+\phi_{ef}) \quad (6.10)$$

The interaction diagram is calculated with the equilibrium equations 6.4 and 6.5.

6.4.3 Hertz's Method for Calculating Columns' Load Capacities

The cross-section of the column should be reduced with Hertz's method in chapter 5. Thereafter the maximum load should be calculated as follows (Hertz, 1999):

1. Calculate the critical load with the extended Rankine formula.
2. Estimate the transient load and calculate the thermal eccentricity.
3. Calculate the load-bearing capacity of the uncracked cross-section.
4. Calculate the load-bearing capacity of the cracked cross-section.
5. The final load-bearing capacity is decided whether the cross-section is uncracked or cracked.

Critical load

The critical force is calculated with the Rankine formula (equation 6.11), which is derived from the critical load (equation 6.2).

$$F_{cr} = \frac{1}{\dfrac{1}{(F_{cu}(T)+F_{sc}(T))} + \dfrac{1}{(N_{ccr}(T)+N_{scr}(T))}} \quad (6.11)$$

where

$F_{cu}(T)$ is the maximum compression load of concrete [kN].
$F_{sc}(T)$ is the maximum compression load of reinforcement [kN].
$N_{ccr}(T)$ is the critical load of concrete [kN].
$N_{scr}(T)$ is the critical load of reinforcement [kN].

$F_{cE}(T)$ is calculated with equation 6.12 and $F_{sE}(T)$ with 6.13. The moment of inertia, $I \cdot E(T)$, are referred to the neutral axis of concrete for both materials.

$$F_{cE}(T) = \left(\pi^2 \times I_c \times E_c(T)\right) / l_c^2 \qquad (6.12)$$

$$F_{sE}(T) = \left(\pi^2 \times I_s \times E_s(T)\right) / l_c^2 \qquad (6.13)$$

$F_{cu}(T)$, is calculated with equation 6.14 and $F_{sc}(T)$, with 6.15.

$$F_{cu}(T) = f_{cc}(T) \times A_c \qquad (6.14)$$

$$F_{sc}(T) = \sum \left(f_{sc}(T) \times A_s\right) \qquad (6.15)$$

<u>Transient load and additional thermal eccentricity</u>

Cause of heating a transient load is applied. It is done by estimating a transient moment from the critical load and the initial out of straightness of the column, see equation 6.16.

$$M_{transient} = \frac{F_{cr}}{2} \times e_0 \qquad (6.16)$$

The transient moment is used to calculate the concrete stresses, σ_{c1} and σ_{c2}, in figure 6.9 below.

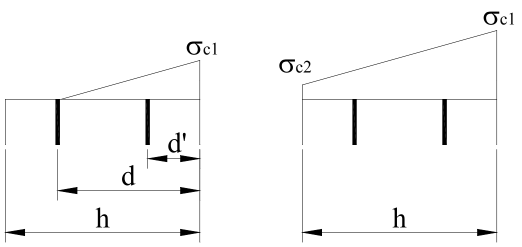

Figure 6.9 Principle stresses for cross-sections with tension and compression and compression only.

σ_{c1} and σ_{c2} are calculated from equation 6.17 to 6.20.

$$\sigma_{c1} = \sigma_0 + \Delta\sigma \qquad (6.17)$$

$$\sigma_{c2} = \sigma_0 - \Delta\sigma \qquad (6.18)$$

$$\sigma_0 = \frac{\left(F_{cr} / 2 \times E_c(T)\right)}{\left(E_s(T) \times A_s + A_c \times E_c(T)\right)} \qquad (6.19)$$

$$\Delta\sigma = \frac{E_c(T) \times h \times M_{transient}}{2 \times \left(E_s(T) \times I_s + I_c \times E_c(T)\right)} \qquad (6.20)$$

were h is the thickness of the reduced cross section.

σ_{c1} and σ_{c2} are used to calculate the transient factors k_{tr1} and k_{tr2} with equation 6.21 and 6.22. These factors are necessary for calculating the additional eccentricity caused by thermal exposure.

$$k_{tr1} = \left(1 - 2{,}35 \times \sigma_{c1} / f_{cc20}\right) \geq 0 \qquad (6.21)$$

$$k_{tr2} = \left(1 - 2{,}35 \times \sigma_{c2} / f_{cc20}\right) \geq 0 \qquad (6.22)$$

For cross-section with compression the additional eccentricity is calculated with equation 6.23 and for cross-section with compression and tension equation 6.24 is used.

$$e_{th1} = \frac{\left(1{,}1 \cdot 10^{-5} \times \left(k_{tr2} \times T_2 - k_{tr1} \times T_1\right)\right)}{h} \times l_c^{\ 2} \tag{6.23}$$

$$e_{th2} = \frac{\left(1{,}1 \cdot 10^{-5} \times \left(T_s - k_{tr1} \times T_1\right)\right)}{\left(8 \times d\right)} \times l_c^{\ 2} \tag{6.24}$$

where d is the effective width of the reduced cross section (see figure 6.9), T_s is the average steel temperature calculated with equation 6.25, T_1 and T_2 are concrete temperature at the border of the damaged zone.

$$T_s = \sum \left(k_{si}(T_{si}) \times A_{si} \times T_{si}\right) / \sum \left(k_{si}(T_{si}) \times A_{si}\right) \tag{6.25}$$

Load-bearing capacity of uncracked cross-section

The load-bearing capacity for an uncracked cross-section is calculated with equation 6.26.

$$F_{\max,uncracked} = F_R \times \left(1 - 2\left(\left(e_0 + e_{th1}\right)/h\right)\right)^P \qquad h \le 2\cdot(e_0 + e_{th1}) \tag{6.26a}$$

$$F_{\max,uncracked} = 0 \qquad h > 2\cdot(e_0 + e_{th1}) \tag{6.26b}$$

where

h is the thickness of the cross section.

$P = 1 + l_c/(25h)$

Load-bearing capacity of cracked cross-section

In order to calculate the load-bearing capacity of a cracked cross-section (equation 6.30), the difference in strength between compression and tensioned steels (equation 6.27), the moment of steel bars (equation 6.28), the deflection of the cracked column (equation 6.29) and the parameter b (equation 6.31) must be calculated.

$$F_{so} = \sum F_{sc}(T_s) - \sum F_{st}(T_s) \approx 0 \tag{6.27}$$

$$M_s = d \times F_{sc}(T_s) - d' \times F_{sc}(T_s) \tag{6.28}$$

$$e_{cracked} = 0{,}10 \times l_c^{\ 2} \times \left(\frac{0{,}0035}{k_c(T_M)} + \frac{f_s(20^o)}{E_s(20^o)}\right) \bigg/ \left(8 \times d'\right) \tag{6.29}$$

$$F_{\max,cracked} = \frac{-b + \sqrt{b^2 - 4 \times F_{so}^2 + 8 \times h \times M_s \times f_{cc}(T)}}{2} \tag{6.30}$$

Final load-bearing capacity, cracked or uncracked cross-section

If the condition in equation 6.31 is fulfilled the cross-section is considered to be cracked.

$$e_0 > \frac{d + 2 \times d'}{6} \qquad (6.31)$$

6.5 RESULTS

This section contains the results of the analysed columns. It also contains a statistical evaluation of the reliability of CONFIRE. Results that are not presented here, such as interaction diagrams, deformations and strains are found in appendix B-E.

6.5.1 Statistical Evaluation of CONFIRE's Reliability

Since CONFIRE is a non-linear model there are many true solutions for a specific column and load, depending on how the time increments and convergence criteria are chosen. Therefore a study of CONFIRE's reliability compared to real tests was done. It was done from a report where twelve real tests were simulated (Anderberg, Holmberg, 1993). Three of them were excluded because the fire exposure and material properties differed between the tests and simulations. The fourth was excluded since the results differed hugely and the reason is believed to be a fault in the simulation. The statistical analysis of the remaining eight tests gives an average deviation of **0** minutes to failure and a standard deviation of **6,6** minutes. The time range for failure was between 50 and 120 minutes with a mean time of 71 minutes.

6.5.2 Comparison of Results Between BKR and Computer Model

Earlier tests have indicated that it is possible to take transient load into account by reducing the steel area with 0,5 for columns with reinforcement in the corners. Calculations have been done for both cases, no reduction of steel area and reduction with 0,5.

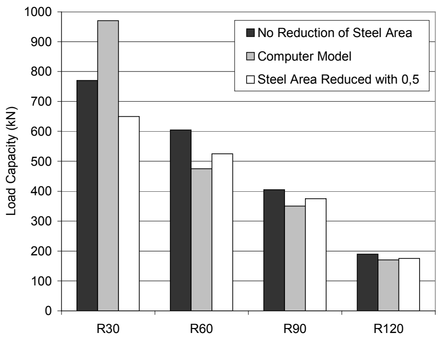

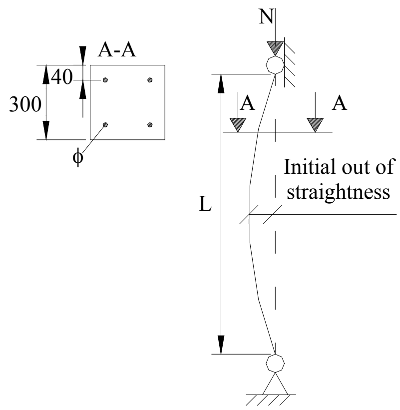

Figure 6.10 Column 1. L = 8m, ϕ = 25mm, λ_0=27→ λ_{120}=38.

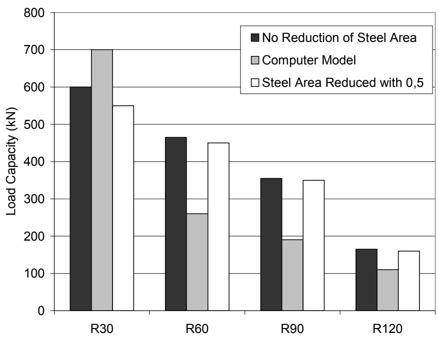

Figure 6.11 Column 2. L = 8m, ϕ = 16 mm, λ_0=27→ λ_{120}=38.

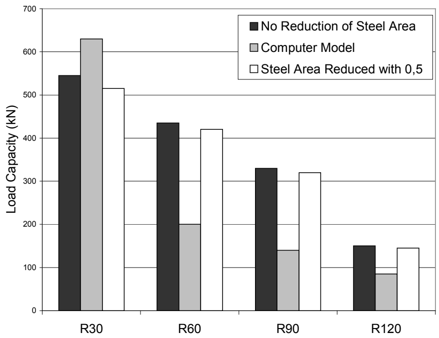

Figure 6.12 Column 3. L = 8m, ϕ = 12mm, λ_0=27→ λ_{120}=38.

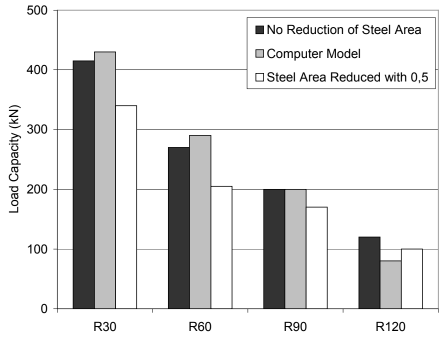

Figure 6.13 Column 4. L = 12m, ϕ = 25mm, $\lambda_0=40 \rightarrow \lambda_{120}=57$.

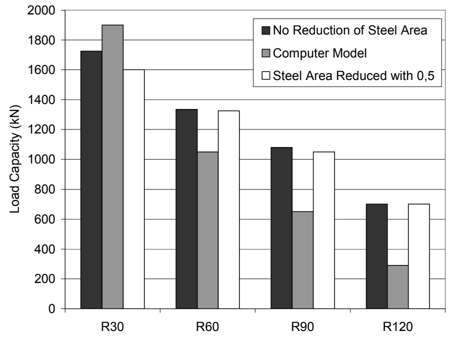

Figure 6.14 Column 5. L = 4m, ϕ = 25mm, $\lambda_0=13 \rightarrow \lambda_{120}=19$.

The results show that BKR gives higher values than the advanced computer model. The good agreement for column 4 is a coincidence caused by slenderness, which is too high for calculating maximum load. This can be seen in section 6.4.1 and appendix D.

6.5.3 Comparison of Results Between Eurocode and Computer Model

Since it is not clearly defined how the creep coefficient should be set in fire design a sensitive analysis is done with the values 0,9 and 0. 0,9 corresponds to a column loaded after 30 days and 0 corresponds to a column with no creep.

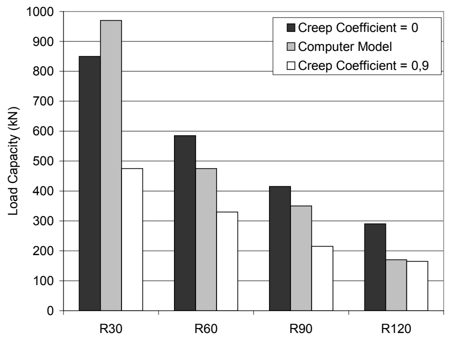

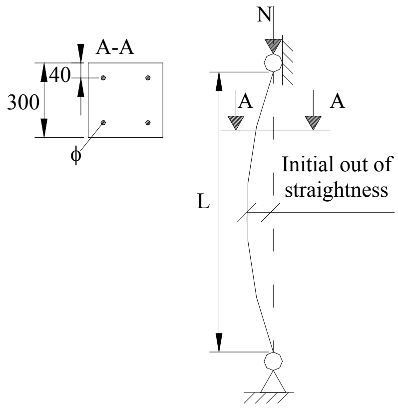

Figure 6.15 Column 1. L = 8m, ϕ = 25mm, $\lambda_0=27 \rightarrow \lambda_{120}=38$.

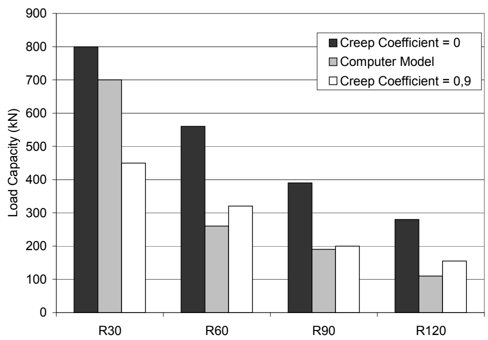

Figure 6.16 Column 2. L = 8m, ϕ = 16mm, $\lambda_0=27 \rightarrow \lambda_{120}=38$.

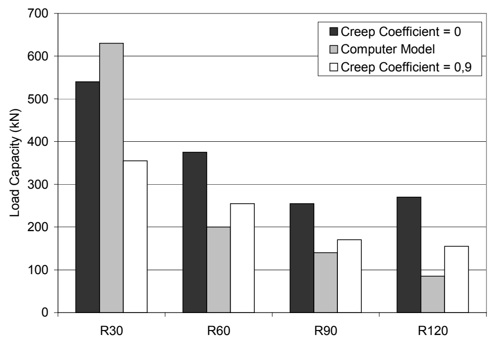

Figure 6.17 Column 3. L = 8m, ϕ = 12mm, $\lambda_0=27 \rightarrow \lambda_{120}=38$.

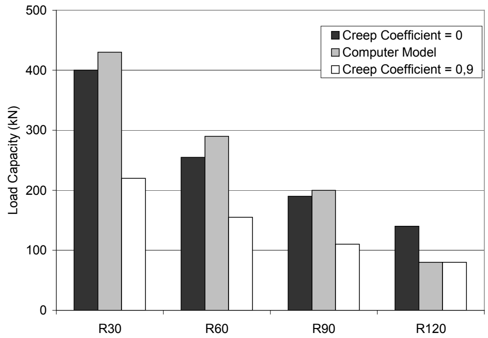

Figure 6.18 Column 4. L = 12m, ϕ = 25mm, λ_0=40$\rightarrow$ λ_{120}=57.

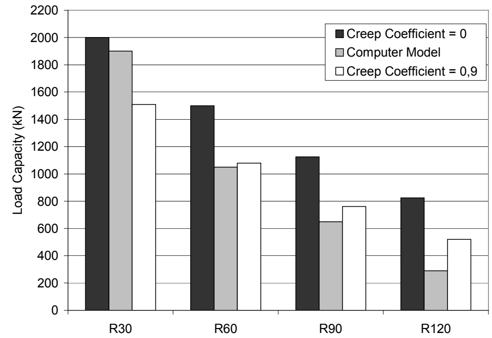

Figure 6.19 Column 5. L = 4m, ϕ = 25mm, λ_0=13$\rightarrow$ λ_{120}=19.

For column 3 the load-bearing capacity is bigger for 120 minutes than for 90. It is correct according to the equations and depends on the reinforcement ratio.

6.5.4 Comparison of Results Between Hertz's Method and Computer Model

Hertz has developed a method, based on curvature, for calculating the load-bearing capacity of columns. Since methods based on curvature tends to give conservative results at high slenderness, Hertz's method is modified by using the critical force, the initial and thermal eccentricity in equation 6.8.

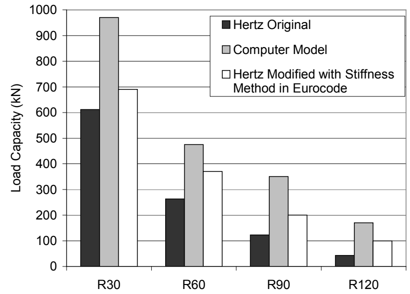

Figure 6.20 Column 1. L = 8m, ϕ = 25mm, λ_0=27$\rightarrow$ λ_{120}=38.

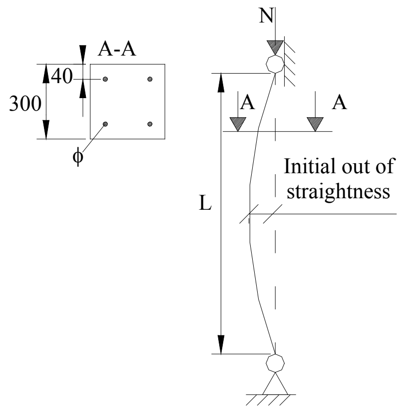

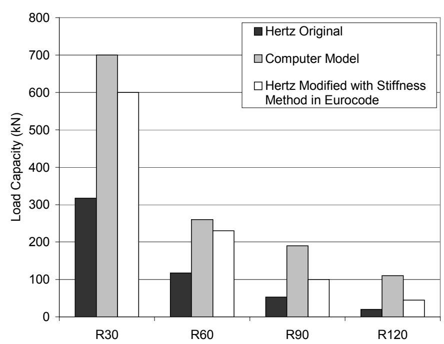

Figure 6.21 Column 2. L = 8m, ϕ = 16mm, λ_0=27$\rightarrow$ λ_{120}=38.

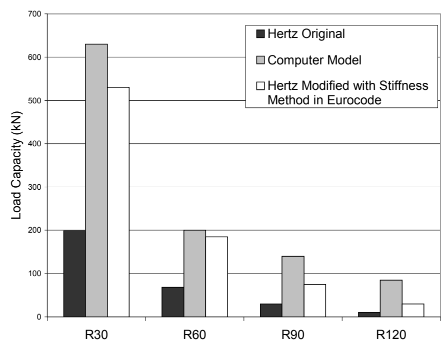

Figure 6.22 Column 3. L = 8m, ϕ = 12mm, λ_0=27$\rightarrow$ λ_{120}=38.

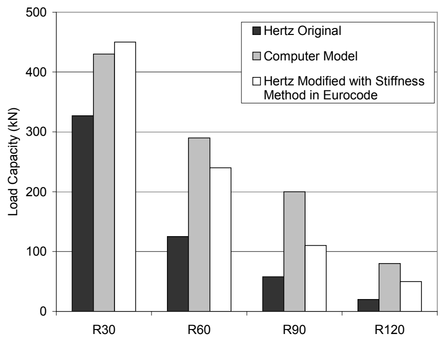

Figure 6.23 Column 4. L = 12m, ϕ = 25mm, λ_0=40$\rightarrow$ λ_{120}=57.

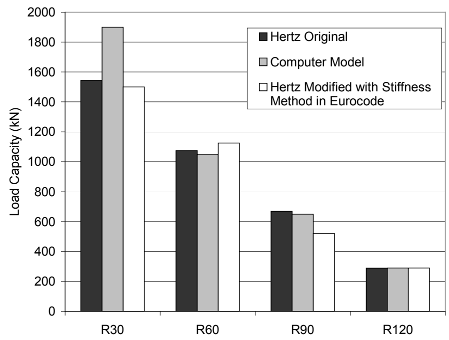

Figure 6.24 Column 5. L = 4m, ϕ = 25mm, λ_0=13$\rightarrow$ λ_{120}=19.

6.6 CONCLUSIONS

The statistical analysis of CONFIRE shows that the program and constitutive models in chapter 2 give a good picture of reality. Therefore the reliability of the performed calculations must be considered as high since the deflections of the columns have good convergence. The results can be studied in section 6.5.1 and appendix C.

The BKR-method gives unsafe results. Earlier calculations have indicated that it is possible to take transient load, for columns with only corner bars, into account by reducing the steel area with 0,5 (Anderberg, Holmberg, 1993). However the study shows that this is not possible. The results can be studied in section 6.5.2.

In general the stiffness-method in Eurocode gives unsafe results. The sensitivity analysis of the creep coefficient turned out to have a great influence on the results. It is still nothing that can be used in fire design since the creep is time dependent. The results can be studied in section 6.5.3.

Hertz's method gives good results for columns with slenderness up to approximately 25, after the reduction of cross-section. Over a slenderness of 25 the method tends to give conservative results, which is also supported by tests (Hertz, 1998). One possible reason is that the method is based on the curvature, which has a tendency to give conservative results at high slenderness. The results are better, but still conservative, when the method is combined with the stiffness method in Eurocode. The conclusion is that the equations for calculating the transient load must be modified for high slenderness. It may be possible by developing equation 6.16, which estimates the transient load. The results can be studied in section 6.5.4.

The general conclusion is that design-methods at normal temperature give unsafe results even if material strengths and cross-sections are reduced. They must be complemented with a procedure for taking transient load into account. Hertz's method of doing this, calculating a thermal deflection and adding it to the initial deflection, seems good and could be adopted by other methods. However, as already mentioned, it must be modified for high slenderness.

7 GENERAL CONCLUSIONS AND FURTHER WORK

After studying the results, I will not recommend further research and development of simple hand methods. Whether it is a method for strength reduction or structural member analysis; they all have limited usage areas that must be fulfilled. For columns it is obvious since all results, except Hertz's, are on the unsafe side. If instead structural member analysis was performed on beams and not on cross-sectional level, the result would probably be more or less unsafe, due to the boundary conditions of the members. A comparison of *tabulated data* in Eurocode (ENV 1992-1-2, 1995) with 45 tests by Hass (1986) shows that the assessments generally are on the unsafe side (Hertz, 1998). The comparison is not explained any further, but the result can be seen in figure 7.1. I therefore think it is time to ask the same question as Professor Ove Pettersson (Lund Institute of Technology) did twenty years ago at a defence of a Ph.D. thesis, "How could the existing knowledge and data about concrete structures be used for calculations"?

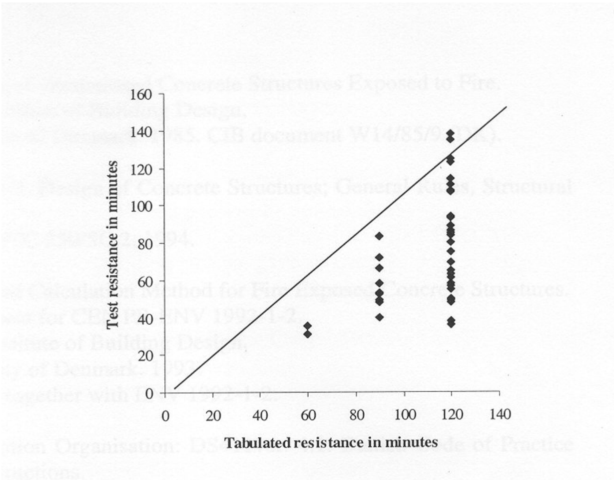

Average fire resistance at test, 74 minutes
Average deviation in minutes, –36,3 minutes (unsafe)
Standard deviation in minutes, 26,2

Figure 7.1 Tabulated data plotted against full-scale fire tests of concrete columns (Hertz, 1998).

Since then many people have answered the question and the answers have always been some kind of simplified hand calculation method. It is a logical answer since the practical use of advanced computer models always has been limited by computer capacity. However that's not the case any more and I think it is time to leave the simplified methods to educational purpose only and develop a general, computer based, model for fire-exposed structures. As early as in 1986, Forsén proved it to be possible when he created CONFIRE, a program for structural analysis of fire exposed concrete structures. It is remarkable that the development has not got any further since then, especially considering that CFD-modelling of enclosure fires is in rapid advance for commercial use. Used together, they would optimise the design of fire-exposed structures and always guarantee a high level of safety.

REFERENCES

Anderberg Y., (1976), *FIRE EXPOSED CONCRETE STRUCTURES – AN EXPERIMENTAL AND THEORETICAL STUDY*, Lunds Institute of Technology, Bulletin 55, Lund.

Anderberg Y., Thelandersson S., (1976), *STRESS AND DEFORMATION CHARACTERISTICS OF CONCRETE AT HIGH TEMPERATURES, 2. EXPERIMENTAL INVESTIGATION AND MATERIAL BEHAVIOUR MODEL*, Lunds Institute of Technology, Bullitn 54,Lund.

Anderberg Y,. (1978), *Analytical Fire Engineering Design of Reinforced Concrete Structures Based on Real Fire Characteristics*, FIP Eight Congress, Proceedings, Part I, London.

Anderberg Y., Forsén N.-E., (1982), *FIRE RESISTANCE OF CONCRETE STRUCTURES*, LUTVDG/(TVBB-3009), Lunds Institute of Technology, Lund.

Anderberg Y., Pettersson O., (1992), *Brandteknisk dimensionering av betongkonstruktioner (Del 1)*, Statens råd för byggnadsforskning, ISBN 91-540-5448-6, Stockholm.

Anderberg Y., (1992), *Temperaturbilagan*, Statens råd för byggnadsforskning, Stockholm.

Anderberg Y., Holmberg S., (1993), *CONCRETE STRUCTURES AND FIRE computer simulations and a design method for fire exposed concrete columns*, Fire Safety Design AB, Lund.

Anderberg Y., (1999), *Annex C*, CEN/TC250/SC2/PT 1-2 Doc 59, Fire Safety Design AB, Lund.

BBK-94, (1994), *Betongkonstruktioner, Band 1-konstruktion*, Boverket, Tryckeri Balder AB, Stockholm.

BKR-94, (1999), *Boverkets konstruktionsregler-99*, Boverket, Nordstedts tryckeri, Karlskrona.

BBR-94, (1993), *Boverkets byggregler–94 (föreskrifter och allmänna råd)*, Boverket och C E Fritzes AB, Nordstedts tryckeri, Stockholm.

Dorn J.E., (1954), *Some Fundamental Experiments on High Temperature Creep*, *Journal of Mechanics and Physics of Solids 3*, 35, London.

Ehm H., (1967), *Beitrag zur rechnerischen Bemessung von brandbeanspruchten balkenartigen Stahlbetonbautteilen*, Dissertation, Technische Universität Braunschweig.

EN 1992-1, (1999) *Design of concrete strucuters – Part1: General rules and rules for buildings*, European Committee for Standardization, Bryssel.

ENV 1991-2-2, (1994), *Basis of design and actions on structures, Part 2-2 Actions on structures exposed to fire*, European Committee for Standardization, Bryssel.

ENV 1992-1-2, (1995) *Design of concrete structures – Part 1-2: General rules – structural fire design*, European Committee for Standardization, Bryssel.

ENV 1993-1-2, (1995), *Design of steel structures – Part 1-2: General rules – structural fire design*, European Committee for Standardization, Bryssel.

Forsén N.-E., (1982), *A Theoretical Study of the Fire Resistance of Concrete Structures*, FCB-SINTEF, report STF65 A82062, Trondheim.

Forsén N.-E., (1986), *CONFIRE, NONLINEAR ANALYSIS OF PLANE, REINFORCED CONCRETE FRAMES EXPOSED TO FIRE, VERSION II REV.1*, MULTICONSULT AS, OSLO.

Hertz K., (1980), *Betongkonstruktioners brandtekniske egenskaber*, Report No. 140, Institute of Building Design, 210p in Danish, Technical University of Denmark.

Hertz K., (1985), *Analysis of Prestressing Concrete Structures Exposed to Fire*, Technical University of Denmark, Lyngby.

Hertz K., (1998), *Comments on simplified calculation method for fire exposed concrete columns – As found in ENV 1992-1-2 chapter 4.3 and in proposal for Danish code of Practice DS411 chapter 9*, Department of Building and Energy, Technical University of Denmark, Lyngby.

Hertz K., (1998), *Additional documentation for simplified design of fire exposed concrete columns*, Department of Building and Energy, Technical University of Denmark, Lyngby.

Hertz K., (1999), *Analyses of Concrete Structures Exposed to Fire*, Technical University of Denmark, Lyngby.

Ingasson H., (1987), *BETONG KONSTRUKTIONER UTSATTA FÖR BRAND – TEORETISK UNDERSÖKNING MED HJÄLP AV DATOR*, Byggnadstekniskt brandskydd, Lunds Tekniska Högskola.

ISO-834, (1975), *Fire Resistance Tests. Elements of Building Construction*, International Standards Organisation, Geneva.

FSD, (1999),*TCD 5.0 User's Manual* , Fire Safety Design AB, Lund.

Krakau S., (1975), *STÅLS EGENSKAPER VID HÖGA TEMPERATURER*, Lund Institute of Technology.

Magnusson S.E., Thelandersson S., (1970), *Temperature-Time Curves for the Complete Process of Fire Development – A Theoretical Study of Wood Fuels in Enclosed Spaces*, Acta Polytechnica Scandinavia, Ci 65, Stockholm.

Mårtensson A., (1997), *Betongkonstruktioner*, Lunds tekniska högskola, KF SIGMA AB, Lund.

Nilsson M., (1997), *Studiematerial, Konstruktionsteknik för BI*, Lunds tekniska högskola, KF SIGMA AB, Lund.

Park R., Paulay T., (1975), *Reinforced Concrete Structures*, John Wiley & Sons.

Thelandersson S., (1974), *Betong handboken, Material, Kapitel 25, brandbeständighet*, Svensk Byggtjänst AB, Stockholm.

Thor J., (1972), *Statiskt bestämda stålbalkars deformation och bärförmåga vid brandpåverkan – Experimentell och teoretisk undersökning*, Jernkontorets Forskning, Serie D-Nr.54, Stockholm.

Tómasson B., (1998), *HIGH PERFORMANCE CONCRETE – DESIGN GUIDE LINES*, Lunds Tekniska Högskola, Lunds Universitet, ISSN 1102-8246, Lund.

A. BEAMS, PARAMETER SETUP AND RESULTS

BEAM A.1

The thicker lines of the geometry's are the sides exposed to fire		Material properties
A.1	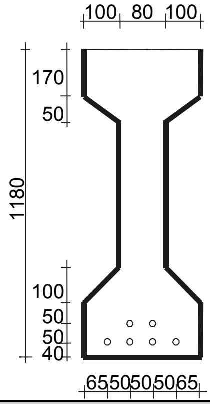	Concrete: f_{cc} =35,4 MPa Prestressing steel: $f_{st} = f_y$ = 1870 MPa, ϕ 13* * effective area = $100e^{-6}$m

A.1 (I-Beam 280x1180)	ISO-834				Fire load at opening factor 0,04$m^{1/2}$		
Moment capacity (kNm)	R 30	R 60	R 90	R 120	200 MJ/m^2	300 MJ/m^2	400 MJ/m^2
500°C	1160	946	708	493	807	585	359
Hertz	1159	945	708	493	804	583	358
Computer model	1156	943	706	493	813	585	359
Difference in relative moment capacity (%)							
500°C	0	0	0	0	0	0	0
Hertz	0	0	0	0	0	0	0
Penetration (mm)							
500°C	10	19	25	35	0	0	0
Hertz	11	20	28	35	12	14	14

BEAM B.1

The thicker lines of the geometry's are the sides exposed to fire		Material properties
B.1	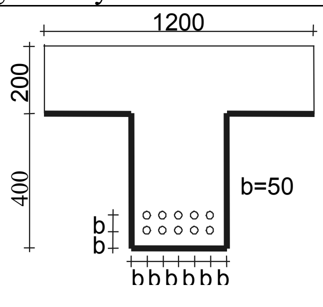	Concrete: f_{cc} = 29,6 MPa Reinforcing steel: f_y = 370 MPa , ϕ 25

B.1 (T-Beam 600x1200)	ISO-834				Fire load at opening factor 0,04$m^{1/2}$		
Moment capacity (kNm)	R 30	R 60	R 90	R 120	200 MJ/m^2	300 MJ/m^2	400 MJ/m^2
500°C	907	907	849	731	888	804	669
Hertz	907	907	849	731	888	804	669
Computer model	907	903	849	730	881	803	668
Difference in relative moment capacity (%)							
500°C	0	0	0	0	0	0	0
Hertz	0	0	0	0	0	0	0
Penetration (mm)							
500°C	5	10	14	18	0	0	14
Hertz	11	20	28	34	14	18	26

BEAM C.1

The thicker lines of the geometry's are the sides exposed to fire		Material properties
C.1	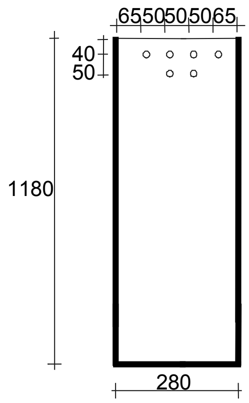	Concrete: f_{cc} = 35,4 MPa Prestressing steel: f_y = 1870 MPa, ϕ 13* * effective area = $100e^{-6}$m

C.1 (R-Beam 280x1180)	ISO-834				Fire load at opening factor $0{,}04m^{1/2}$		
Moment capacity (kNm)	R 30	R 60	R 90	R 120	200 MJ/m^2	300 MJ/m^2	400 MJ/m^2
500°C	1179	1148	1097	1032	862	637	459
Hertz	1179	1153	1105	1045	890	716	533
Computer model	1178	1152	1102	1048	885	752	584
Difference in relative moment capacity (%)							
500°C	0	0	0	0	-2,5	-15	-21,5
Hertz	0	0	0	0	0	-5	-9
Penetration (mm)							
500°C	12	26	38	49	75	160	194
Hertz	11	20	28	35	43	50	56
Reinforcement temperature (°C)							
1 & 4	<100	119	191	263	228	307	382
2, 3, 5 & 6	<100	<100	<100	110	129	188	258

BEAM D.1-D.10

The thicker lines of the geometry's are the sides exposed to fire		Material properties
D.i	R-Beam (bx1000) 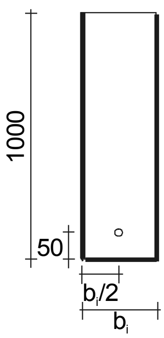 b_1=80 b_2=90 b_3=100 b_4=120 b_5=130 b_6=140 b_7=160 b_8=180 b_9=200 b_{10}=240 i = 1 i = 2 i = 3 i = 4 i = 5 i = 6 i = 7 i = 9 i =10	Concrete: f_{cc} = 40 MPa Reinforcing steel: f_y = 220 MPa, ϕ 25

D.1	Moment capacity (kNm)		Penetration of sides (mm)
Fire exposure	500°C	Computer model	
R 60	-		>40
D.2	Moment capacity (kNm)		Penetration of sides (mm)
Fire exposure	500°C	Computer model	

<table>
<tr><td>R 60</td><td colspan="2">54</td><td colspan="2">54</td><td colspan="2">28</td></tr>
<tr><td>F = 200 MJ/m^2</td><td colspan="2">-</td><td colspan="2"></td><td colspan="2">>45</td></tr>
<tr><th>D.3</th><th colspan="4">Moment capacity (kNm)</th><th colspan="2" rowspan="2">Penetration of sides (mm)</th></tr>
<tr><th>Fire exposure</th><th colspan="2">500^{o}C</th><th colspan="2">Computer model</th></tr>
<tr><td>F = 200 MJ/m^2</td><td colspan="2">47</td><td colspan="2">48</td><td colspan="2">25</td></tr>
<tr><th>D.4</th><th colspan="4">Moment capacity (kNm)</th><th colspan="2" rowspan="2">Penetration of sides (mm)</th></tr>
<tr><th>Fire exposure</th><th colspan="2">500^{o}C</th><th colspan="2">Computer model</th></tr>
<tr><td>R 90</td><td colspan="2">45</td><td colspan="2">45</td><td colspan="2">37</td></tr>
<tr><td>R 120</td><td colspan="2">-</td><td colspan="2"></td><td colspan="2">>60</td></tr>
<tr><td>F = 200 MJ/m^2</td><td colspan="2">63</td><td colspan="2">63</td><td colspan="2">18</td></tr>
<tr><td>F = 300 MJ/m^2</td><td colspan="2">-</td><td colspan="2"></td><td colspan="2">>60</td></tr>
<tr><th>D.5</th><th colspan="4">Moment capacity (kNm)</th><th colspan="2" rowspan="2">Penetration of sides (mm)</th></tr>
<tr><th>Fire exposure</th><th colspan="2">500^{o}C</th><th colspan="2">Computer model</th></tr>
<tr><td>F = 300 MJ/m^2</td><td colspan="2">47,5</td><td colspan="2">48</td><td colspan="2">46</td></tr>
<tr><th>D.6</th><th colspan="4">Moment capacity (kNm)</th><th colspan="2" rowspan="2">Penetration of sides (mm)</th></tr>
<tr><th>Fire exposure</th><th colspan="2">500^{o}C</th><th colspan="2">Computer model</th></tr>
<tr><td>F = 300 MJ/m^2</td><td colspan="2">56</td><td colspan="2">56</td><td colspan="2">33</td></tr>
<tr><td>F = 400 MJ/m^2</td><td colspan="2">-</td><td colspan="2"></td><td colspan="2">>70</td></tr>
<tr><th>D.7</th><th colspan="4">Moment capacity (kNm)</th><th colspan="2" rowspan="2">Penetration of sides (mm)</th></tr>
<tr><th>Fire exposure</th><th colspan="2">500^{o}C</th><th colspan="2">Computer model</th></tr>
<tr><td>R 120</td><td colspan="2">45</td><td colspan="2">45</td><td colspan="2">41</td></tr>
<tr><td>R 180</td><td colspan="2">-</td><td colspan="2"></td><td colspan="2">>80</td></tr>
<tr><td>F = 400 MJ/m^2</td><td colspan="2">28</td><td colspan="2">28</td><td colspan="2">61</td></tr>
<tr><th>D.8</th><th colspan="4">Moment capacity (kNm)</th><th colspan="2" rowspan="2">Penetration of sides (mm)</th></tr>
<tr><th>Fire exposure</th><th colspan="2">500^{o}C</th><th colspan="2">Computer model</th></tr>
<tr><td>R 180</td><td colspan="2">7,7</td><td colspan="2">10</td><td colspan="2">62</td></tr>
<tr><th>D.9</th><th colspan="4">Moment capacity (kNm)</th><th colspan="2">Penetration of sides (mm)</th></tr>
<tr><th>Fire exposure</th><th>500^{o}C</th><th colspan="2">Computer model</th><th>Hertz</th><th>500^{o}C</th><th>Hertz</th></tr>
<tr><td>R 180</td><td>22</td><td colspan="2">23</td><td>22,5</td><td>55</td><td></td></tr>
<tr><td>R 240</td><td>8,5</td><td colspan="2">8,5</td><td>8,49</td><td>91</td><td>64</td></tr>
<tr><td>R 300</td><td>-</td><td colspan="2">6,45</td><td>6,44</td><td>>100</td><td>68</td></tr>
<tr><td>R 180**</td><td>66</td><td colspan="2">67</td><td></td><td>55</td><td></td></tr>
<tr><td>R 240**</td><td>25</td><td colspan="2">25</td><td></td><td>91</td><td></td></tr>
<tr><td>F = 600 MJ/m^2</td><td>?</td><td colspan="2">?</td><td>?</td><td>?</td><td>?</td></tr>
<tr><th>D.10</th><th colspan="4">Moment capacity (kNm)</th><th colspan="2" rowspan="2">Penetration of sides (mm)</th></tr>
<tr><th>Fire exposure</th><th colspan="2">500^{o}C</th><th colspan="2">Computer model</th></tr>
<tr><td>F = 800 MJ/m^2</td><td colspan="2">?</td><td colspan="2">?</td><td colspan="2">?</td></tr>
</table>

BEAM E.1-E.2

The thicker lines of the geometry's are the sides exposed to fire			Material properties
E.i	i = 1a, 1b, 1c R-Beam (300x500) 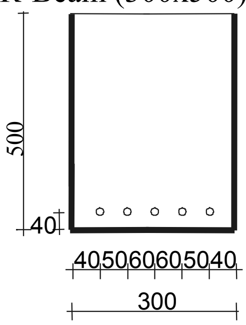 	i = 2a, 2b, 2c R-Beam (400x750) 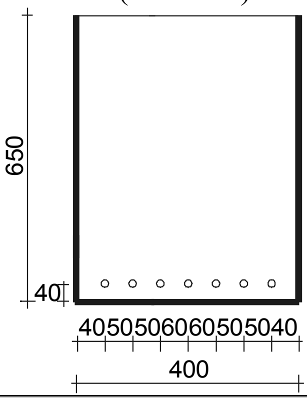 	Concrete: f_{cc} = 29,6 MPa Hot rolled steel : f_y = 370 MPa i = 1a, 2a, ϕ 25 i = 1b, 2b, doubled reinforcement area i = 1c, 2c, tripled reinforcement area

E.1 (R-Beam 300x500)	ISO-834					Fire load at opening factor 0,04m$^{1/2}$		
i = 1a Moment capacity(kNm)	T = 20^{o}C	R 30	R 60	R 90	R 120	200 MJ/m^2	300 MJ/m^2	400 MJ/m^2
strain assumed over 2%	371	368	358	293	217	349	297	224
stress-strain relationship taken into account	371	360	338	272	211	325	278	217
Difference in moment capacity (%)								
	0	2	0	7,5	3	7,5	7	3
Strain (%)								
	0,91	0,85	1,04	1,44	1,44	1,00	1,12	1,39
i = 1b Moment capacity(kNm)								
strain assumed over 2%	650	635	606	517	395	608	525	407
stress-strain relationship taken into account	650	603	503	418	339	504	430	346
Difference in moment capacity (%)								
	0	5	20	24	17	21	23	18
Strain (%)								
	0,28	0,28	0,385	0,51	0,7	0,45	0,54	0,67
i = 1c Moment capacity(kNm)								
strain assumed over 2%	835	801	761	668	535	779	685	549
stress-strain relationship taken into account	753	701	612	510	425	619	529	433
Difference in moment capacity (%)								
	11	14	24	31	26	26	29	27
Strain (%)								
	0,15	0,15	0,21	0,31	0,44	0,26	0,33	0,42
Reinforcement temperature (C^{o})								
1, 7	20	205	443	590	692	468	571	653
2, 6	20	125	287	416	515	329	436	523
3, 5	20	121	265	375	460	295	386	464
4	20	121	260	369	449	291	375	448

E.2 (R-Beam 400x750)	ISO-834					Fire load at opening factor 0,04m$^{1/2}$		
i = 2a Moment capacity(kNm)	T = 20^{o}C	R 30	R 60	R 90	R 120	200 MJ/m^2	300 MJ/m^2	400 MJ/m^2
strain assumed over 2%	707	703	683	600	472	677	605	485
stress-strain relationship taken into account	707	697	657	579	469	657	586	481
Difference in moment capacity (%)								
	0	1	4	4	1	3	3	1
Strain (%)								
	1,24	1,17	1,19	1,33	1,67	1,31	1,38	1,65
i = 2b Moment capacity(kNm)								
strain assumed over 2%	1278	1262	1222	1086	875	1225	1098	896
stress-strain relationship taken into account	1278	1221	1065	920	772	1068	935	789
Difference in moment capacity (%)								
	0	3	15	18	13	15	17	14
Strain (%)								
	0,45	0,44	0,53	0,64	0,81	0,61	0,66	0,80
i = 2c Moment capacity(kNm)								
strain assumed over 2%	1712	1644	1617	1458	1206	1643	1480	1233
stress-strain relationship taken into account	1712	1549	1339	1149	983	1352	1176	1002
Difference in moment capacity (%)								
	0	6	21	27	23	22	26	23
Strain (%)								
	0,18	0,18	0,30	0,40	0,52	0,36	0,42	0,51
Reinforcement temperature (C^{o})								
1, 7	20	205	443	590	692	468	571	653
2, 6	20	125	287	416	515	329	436	523
3, 5	20	121	265	375	460	295	386	464
4	20	121	260	369	449	291	375	448

BEAM F.1-F.2

The thicker lines of the geometry's are the sides exposed to fire		Material properties
F.i	R-Beam (280x500) i = 1a, 1b i = 2a, 2b, 2c 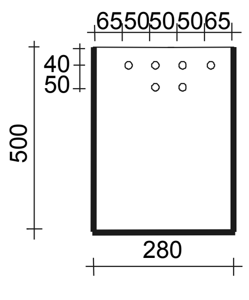	Concrete: f_{cc} = 35,4 MPa Cold worked steel: f_y = 370 MPa i = 1a, ϕ 12 i = 1b, ϕ 17 Prestressing steel: $f_{0,2\%}$= f_y =1670 MPa i = 2a, ϕ 8 i = 2b, ϕ 10 i = 2c, ϕ 13

F.1 (R-Beam 280x500)	ISO-834						
i = 1a Moment capacity(kNm)	R 30	R 60	R 90	R 120	R 180	R 240	R 300
strain assumed over 2%	201	193	182	168	151	130	101
stress-strain relationship taken into account	201	193	181	166	148	125	92
Difference in moment capacity (%)							
	0	0	0	1	2	4	10
Strain (%)							
	1,94	1,69	1,48	1,31	1,02	0,90	0,73
i = 1b Moment capacity(kNm)							
strain assumed over 2%	376	357	332	304	265	224	165
stress-strain relationship taken into account	375	354	325	288	248	201	138
Difference in moment capacity (%)							
	0	1	2	6	7	11	20
Strain (%)							
	0,84	0,71	0,61	0,55	0,44	0,31	0,28
Reinforcement temperature (C^o)							
1, 4	54	118	188	258	371	464	544
2, 3, 5, 6	23	43	75	108	176	268	354

F.2 (R-Beam 280x500)	ISO-834						
i = 2a Moment capacity(kNm)	R 30	R 60	R 90	R 120	R 180	R 240	R 300
strain assumed over 2%	202	190	175	157	122	91	58
stress-strain relationship taken into account	202	190	171	152	116	87	56
Difference in moment capacity (%)							
	0	0	2	3	5	4,5	3,5
Strain (%)							
	1,93	1,73	1,58	1,49	1,42	1,5	1,55
i = 2b Moment capacity(kNm)							
strain assumed over 2%	276	260	238	213	165	123	79
stress-strain relationship taken into account	273	250	220	192	145	108	70
Difference in moment capacity (%)							
	1	4	8	11	14	14	13
Strain (%)							
	1,27	1,18	1,12	1,07	1,03	1,09	1,13
i = 2c Moment capacity(kNm)							
strain assumed over 2%	473	441	398	353	270	203	130
stress-strain relationship taken into account	399	353	309	265	200	153	99
Difference in moment capacity (%)							
	19	25	29	33	35	33	31
Strain (%)							
	0,72	0,69	0,65	0,63	0,60	0,63	0,64
Reinforcement temperature (C^o)							
1, 4	54	118	188	258	371	464	544
2, 3, 5, 6	23	43	75	108	176	268	354

B. COLUMNS, PARAMETER SETUP AND RESULTS

PARAMETER SETUP

	Column number				
	1	**2**	**3**	**4**	**5**
Concrete cross-section (mm^2)	300x300				
Reinforcement diameter (mm)	4ϕ25	4 ϕ16	4 ϕ12	4ϕ25	4ϕ25
Geometrical reinforcement ratio	0,022	0,010	0,005	0,022	0,022
Concrete cover (mm)	40				
Column length (mm)	8000			12000	4000
Initial slenderness	27	27	27	40	13
Initial out of straightness, e_a (mm)	20				
Structural boundary condition (α).	1				
Fire exposure	ISO-834				
Boundary conditions for temperature analysis	4-sided exposure				
Time of maximum load (minutes)	30, 60, 90 and 120				

Table B.1 Geometrical and structural parameters for column calculations.

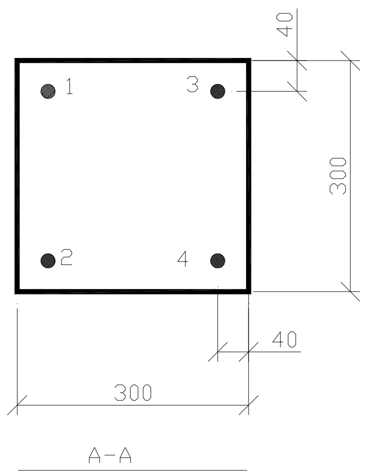

(mm)

Concrete:
f_{cc} = 29,6 MPa
f_{ct} = 0 MPa

Reinforcement:
f_y = 370 MPa

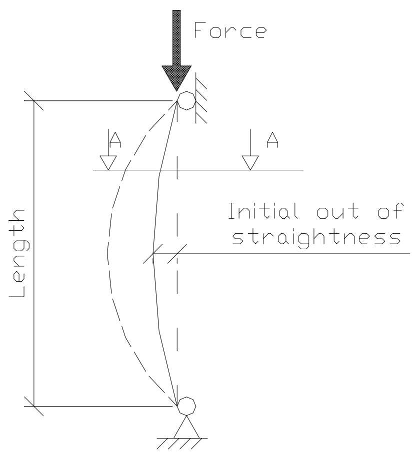

Figure B.1 Boundary condition for heat flow analysis and topology of reinforcement.

Figure B.2 Structural boundary conditions, whole line shows the initial conditions and the dashed line the deflections.

CALCULATED LOAD CAPACITIES

Column 1

A = 300x300 mm^2, L = 8 m, Number of bars = 4, ϕ = 25 mm. λ_0 = 27 λ_{120}=38.							
Load-bearing capacity (kN) at	Computer model	BKR	BKR (Steel area reduced with 0,5)	EC ϕ_{eff}= 0	EC ϕ_{eff}= 0,9	Hertz's method	Hertz's method combined with EC
R 30	970	770	650	850	475	612	690
R 60	475	605	525	585	330	263	370
R 90	350	405	375	415	215	123	200
R 120	170	190	175	290	165	43	100

Column 2

A = 300x300 mm^2, L = 8 m, Number of bars = 4, ϕ = 16 mm. λ_0 = 27 λ_{120}=38.							
Load-bearing capacity (kN) at	Computer model	BKR	BKR (Steel area reduced with 0,5)	EC ϕ_{eff}= 0	EC ϕ_{eff}= 0,9	Hertz's method	Hertz's method combined with EC
R 30	700	600	550	800	450	317	600
R 60	260	475	450	560	320	117	230
R 90	190	355	350	390	200	53	100
R 120	110	165	160	280	155	20	45

Column 3

A = 300x300 mm^2, L = 8 m, Number of bars = 4, ϕ = 12 mm. λ_0 = 27 λ_{120}=38.							
Load-bearing capacity (kN) at	Computer model	BKR	BKR (Steel area reduced with 0,5)	EC ϕ_{eff}= 0	EC ϕ_{eff}= 0,9	Hertz's method	Hertz's method combined with EC
R 30	630	545	515	540	355	199	530
R 60	200	435	420	375	255	68	185
R 90	140	330	320	255	170	30	75
R 120	85	150	145	270	155	10	30

Column 4

A = 300x300 mm^2, L = 12 m, Number of bars = 4, ϕ = 25 mm. λ_0 = 40 λ_{120}=57.							
Load-bearing capacity (kN) at	Computer model	BKR	BKR (Steel area reduced with 0,5)	EC ϕ_{eff}= 0	EC ϕ_{eff}= 0,9	Hertz's method	Hertz's method combined with EC
R 30	430	415	340	400	220	327	450
R 60	290	270	205	255	155	125	240
R 90	200	200	170	190	110	58	110
R 120	80	120	100	140	80	20	50

Column 5

A = 300x300 mm^2, L = 4 m, Number of bars = 4, ϕ = 25 mm. λ_0 = 13 λ_{120}=19.							
Load-bearing capacity (kN) at	Computer model	BKR	BKR (Steel area reduced with 0,5)	EC ϕ_{eff}= 0	EC ϕ_{eff}= 0,9	Hertz's method	Hertz's method combined with EC
R 30	1900	1725	1600	2000	1510	1545	1500
R 60	1050	1335	1325	1500	1080	1075	1125
R 90	650	1080	1050	1125	760	670	520
R 120	290	700	700	825	520	289	290

C. CONFIRE, DISPLACEMENTS AND STRAINS

REINFORCEMENT TEMPERATURE

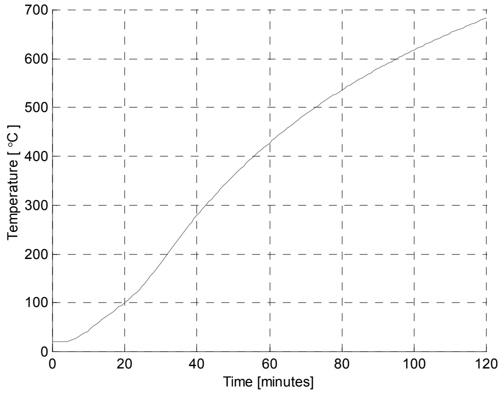

Figure C.1 Reinforcement temperature as a function of time for the analysed columns.

COLUMN 1

	R30	R60	R90	R120
1,2 strain$_{\sigma}$ (promille)	-0,33	-0,41	-0,46*	-0,14*
1,2 $\sigma_{failure}$ (MPa)	-67	-70	-68*	-21*
3,4 strain$_{\sigma}$ (promille)	-2,98	-2,46	-1,26*	-0,4*
3,4 $\sigma_{failure}$ (MPa)	-431	-303	-186*	-60*
$\sigma_{0,5\%\ strain}$ (MPa)	348	270	168	84
Temperature (C^{o})	170	423	580	685

*Table C.1 Stress related strain and stress at failure. *The program could not write to the output file after 73 minutes.*

Failure at 30 minutes

Load = 970 kN

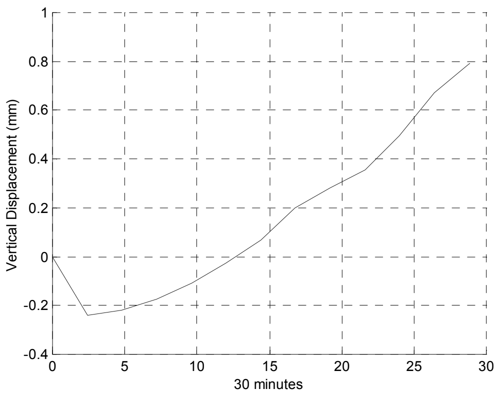

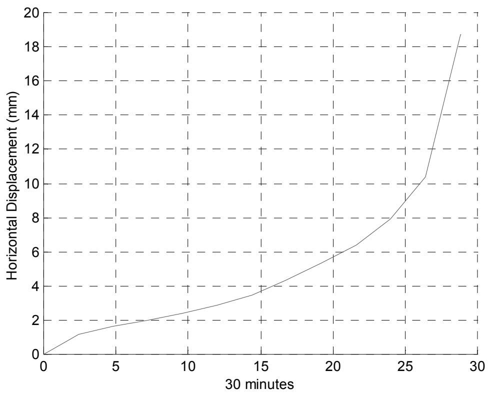

Figure C.2 Vertical and horizontal displacement.

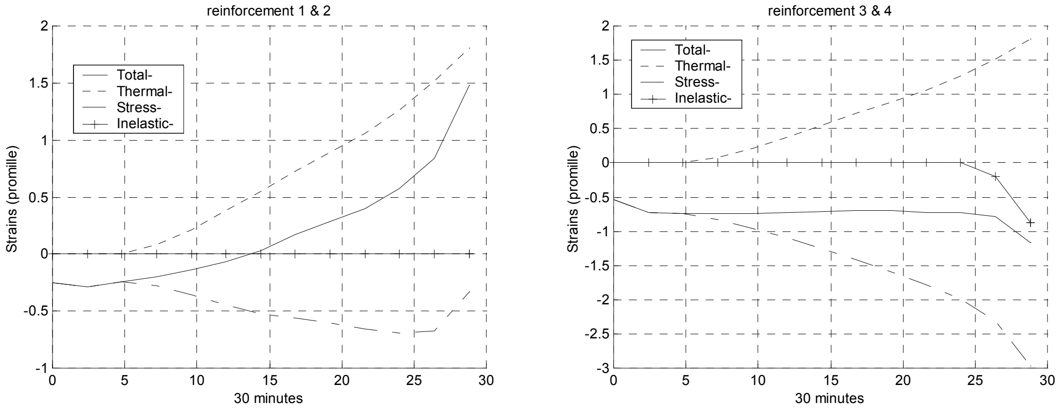

Figure C.3 Strains in reinforcement 1,2 and 3,4.

Failure at 60 minutes

Load = 475 kN

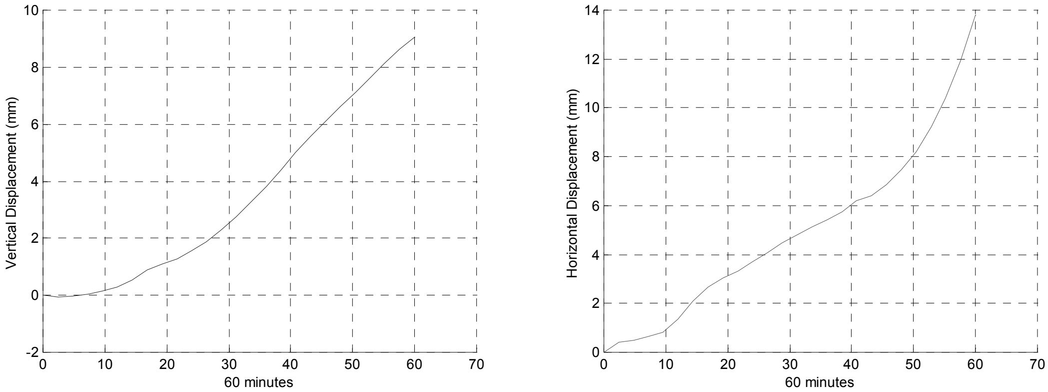

Figure C.4 Vertical and horizontal displacement.

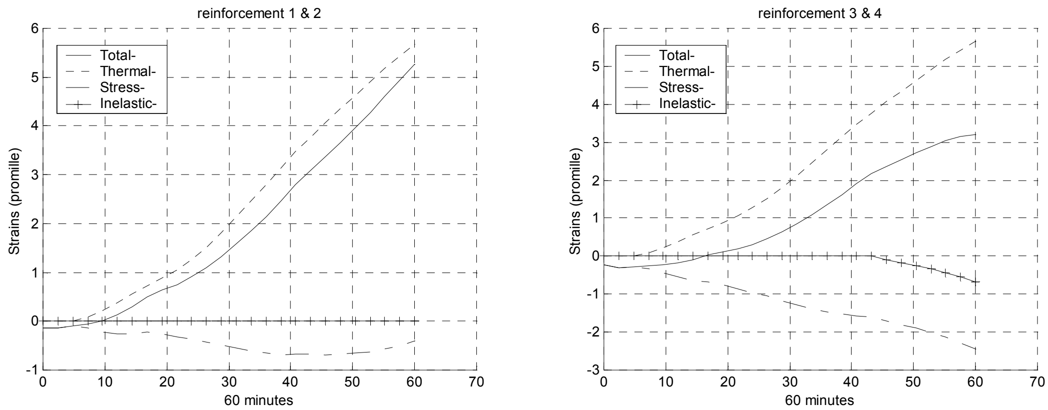

Figure C.5 Strains in reinforcement 1,2 and 3,4.

Failure at 90 minutes

Load = 350 kN

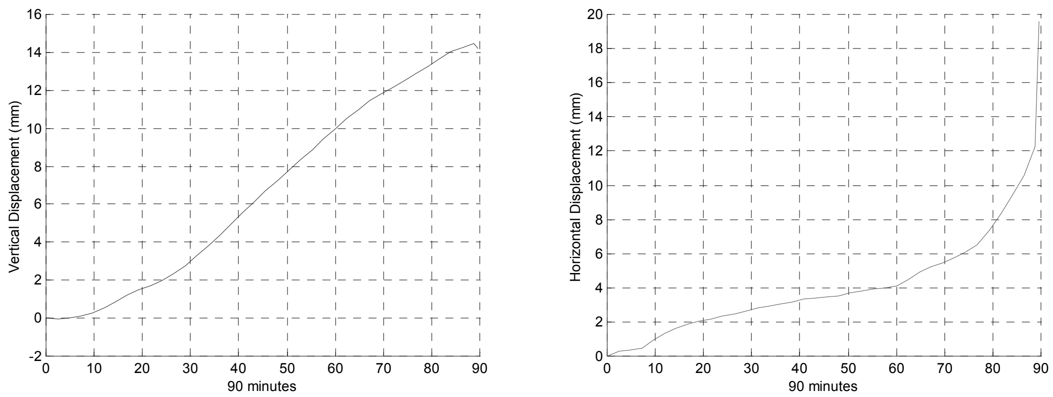

Figure C.6 Vertical and horizontal displacement.

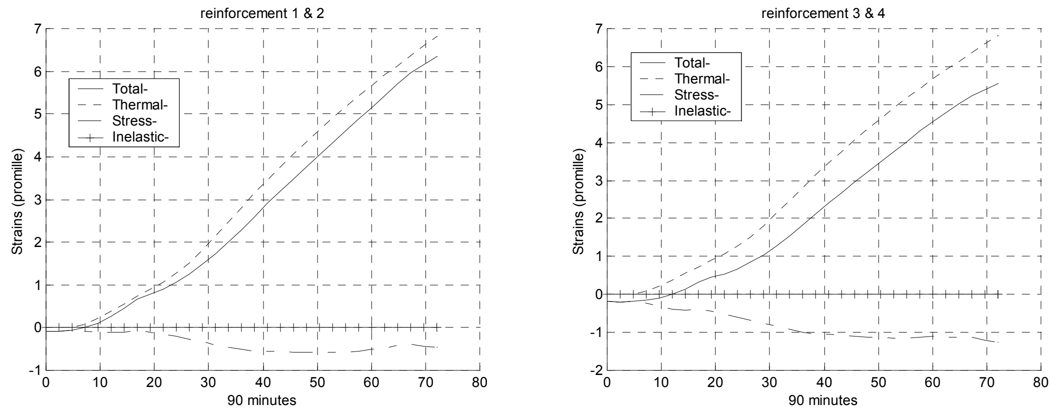

Figure C.7 Strains in reinforcement 1,2 and 3,4.

Failure at 120 minutes

Load = 170 kN

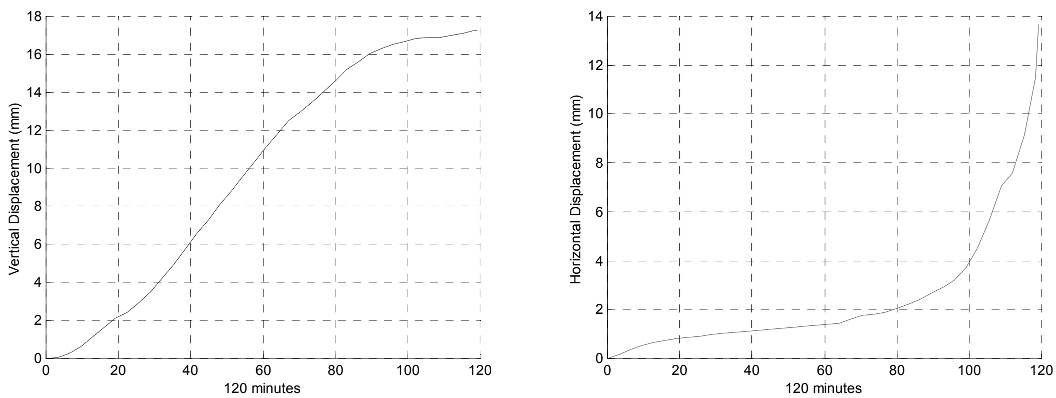

Figure C.8 Vertical and horizontal displacement.

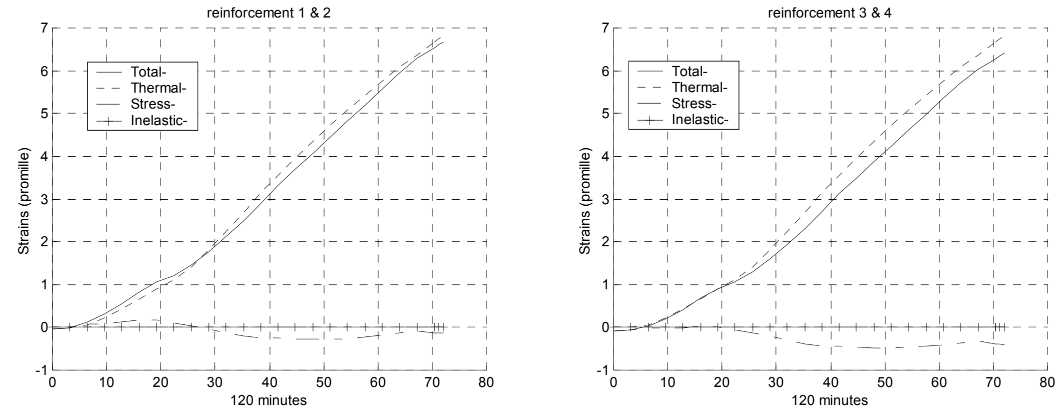

Figure C.9 Strains in reinforcement 1,2 and 3,4.

COLUMN 2

	R30	R60	R90	R120
1,2 strain$_\sigma$ (promille)	-0,41	1,3	-0,16*	0,03*
1,2 $\sigma_{failure}$ (MPa)	-90	222	-24*	4,8*
3,4 strain$_\sigma$ (promille)	-3,1	-4,58	-1,38*	-0,46*
3,4 $\sigma_{failure}$ (MPa)	-430	-311	-203*	-67*
$\sigma_{0,5\%\ strain}$ (MPa)	348	270	168	84
Temperature (C^o)	170	423	580	685

*Table C.2 Stress and stress related strain at failure. *The program could not write to the output file after 73 minutes.*

Failure at 30 minutes

Load = 700 kN

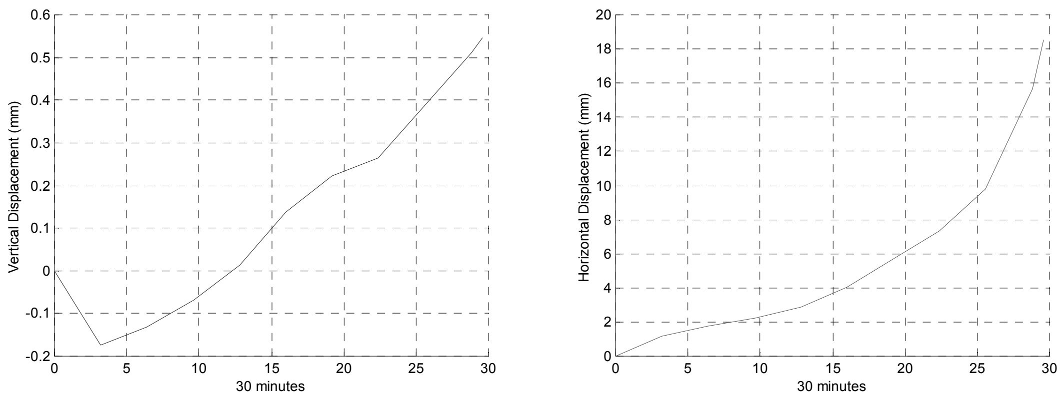

Figure C.10 Vertical and horizontal displacement.

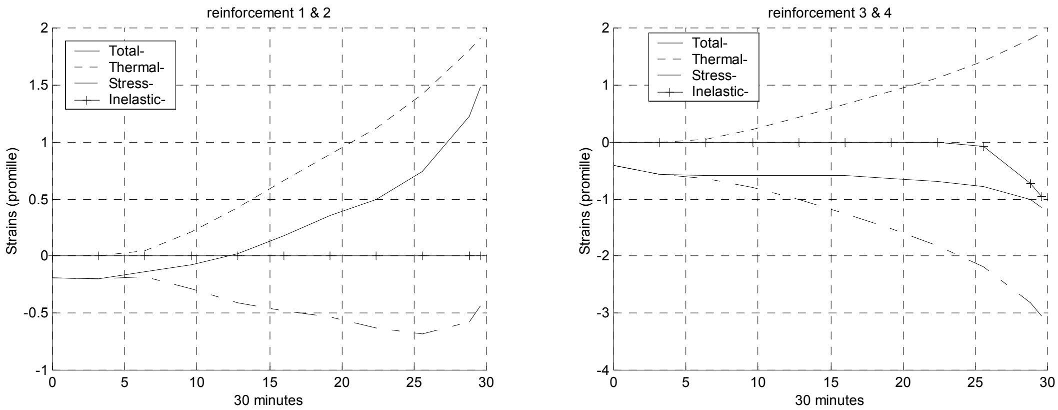

Figure C.11 Strains in reinforcement 1,2 and 3,4.

Failure at 60 minutes

Load = 260 kN

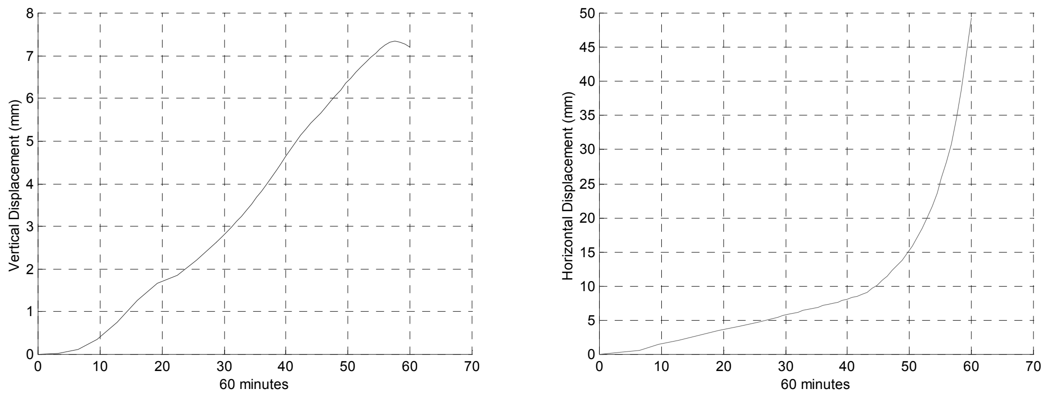

Figure C.12 Vertical and horizontal displacement.

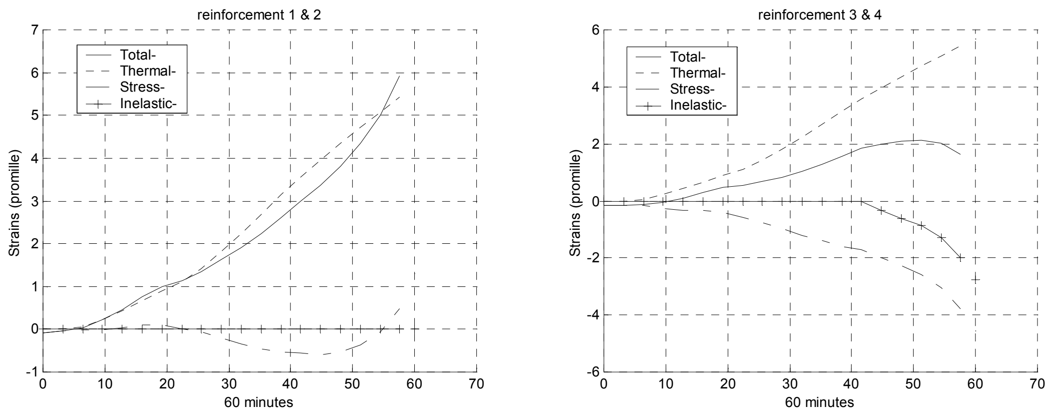

Figure C.13 Strains in reinforcement 1,2 and 3,4.

Failure at 90 minutes

Load = 190 kN

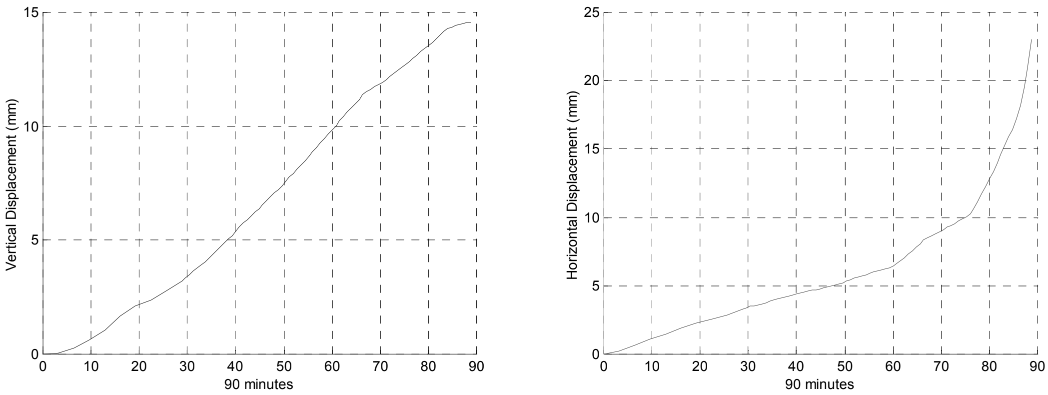

Figure C.14 Vertical and horizontal displacement.

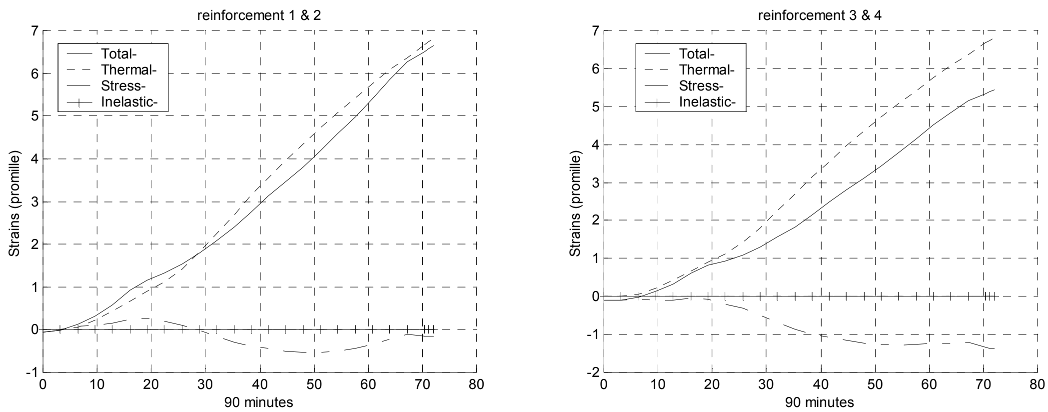

Figure C.15 Strains in reinforcement 1,2 and 3,4.

Failure at 120 minutes

Load = 110 kN

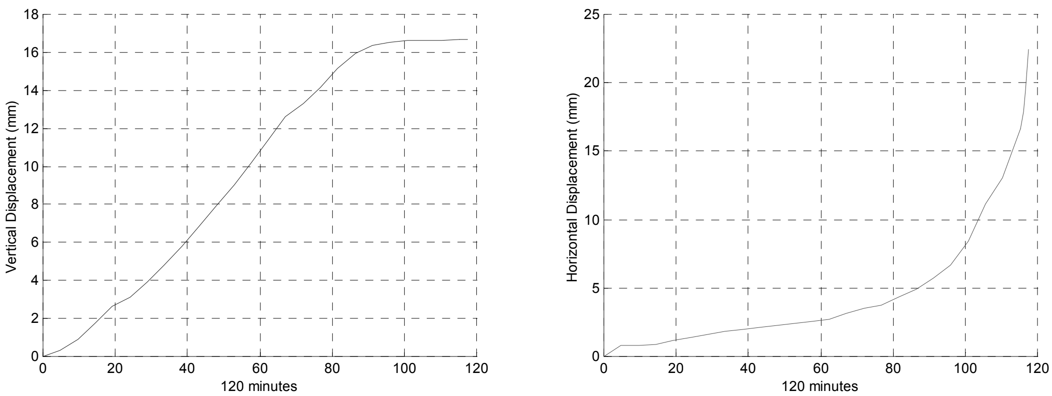

Figure C.16 Vertical and horizontal displacement.

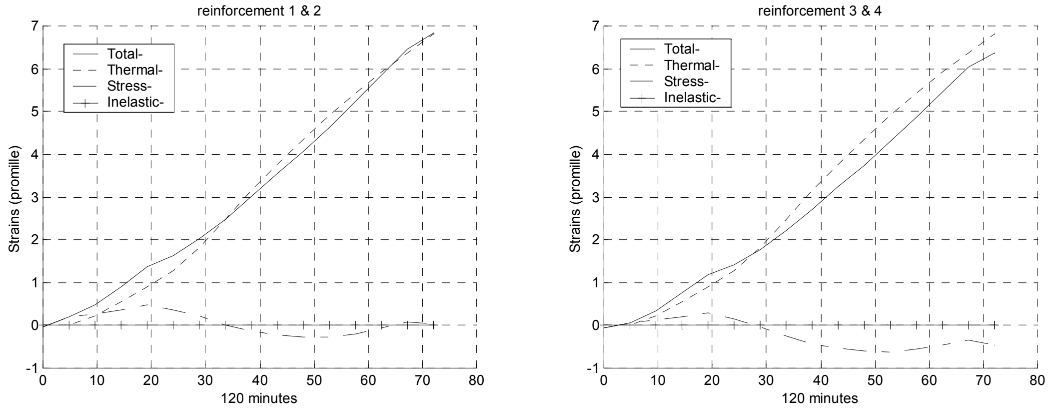

Figure C.17 Strains in reinforcement 1,2 and 3,4.

COLUMN 3

	R30	R60	R90	R120
1,2 strain$_\sigma$ (promille)	-0.43	1,64	-0,19*	0,33*
1,2 $\sigma_{failure}$ (MPa)	-87	283	28*	48*
3,4 strain$_\sigma$ (promille)	-3,1	-4,3	-1,35*	-0,30*
3,4 $\sigma_{failure}$ (MPa)	-430	-313	-199*	-44*
$\sigma_{0,5\% \text{ strain}}$ (MPa)	348	270	168	84
Temperature (C^o)	170	413	580	685

*Table C.3 Stress and stress related strain at failure. *The program could not write to the output file after 73 minutes.*

Failure at 30 minutes

Load = 630 kN

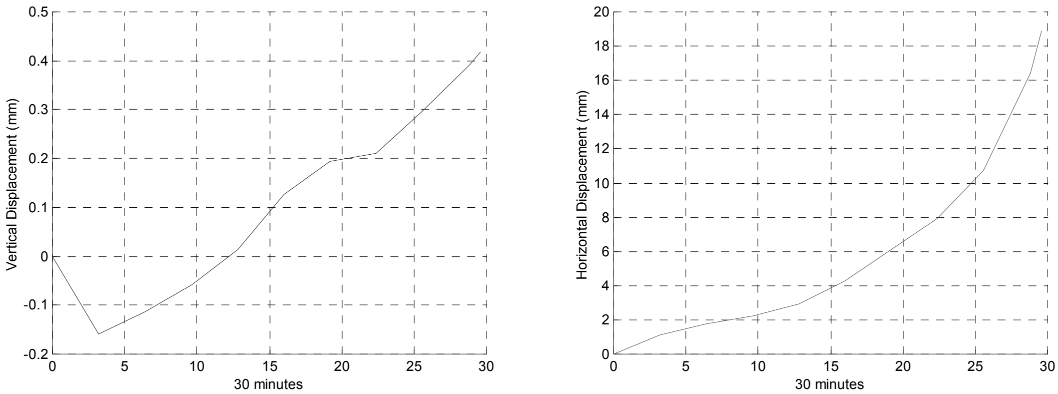

Figure C.18 Vertical and horizontal displacement.

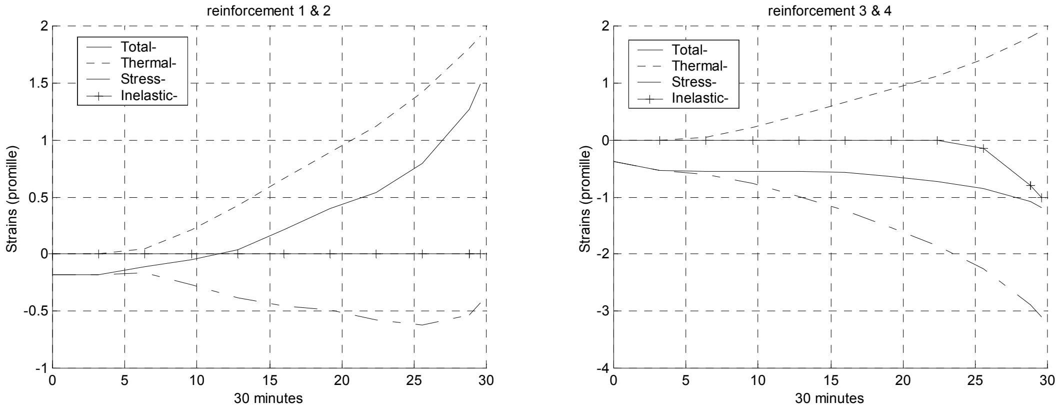

Figure C.19 Strains in reinforcement 1,2 and 3,4.

Failure at 60 minutes

Load = 200 kN

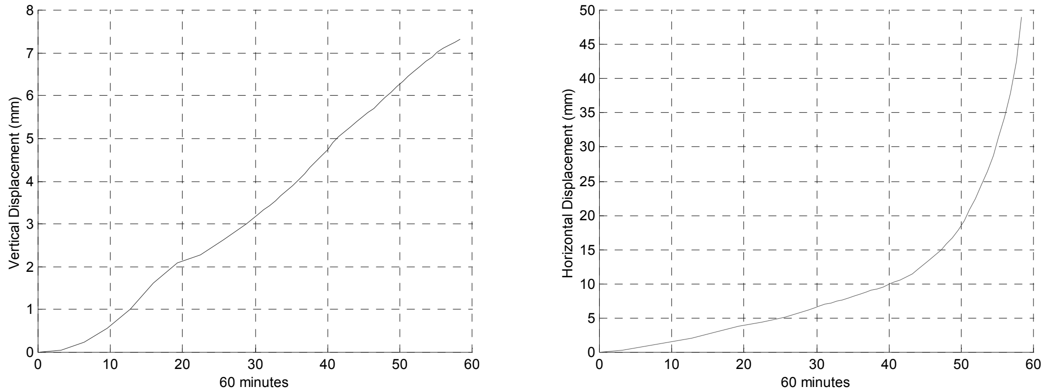

Figure C.20 Vertical and horizontal displacement.

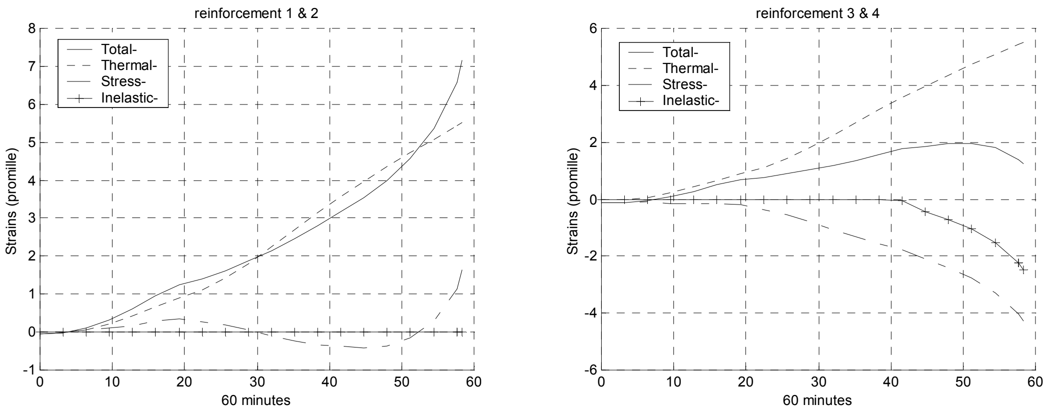

Figure C.21 Strains in reinforcement 1,2 and 3,4.

Failure at 90 minutes

Load = 140 kN

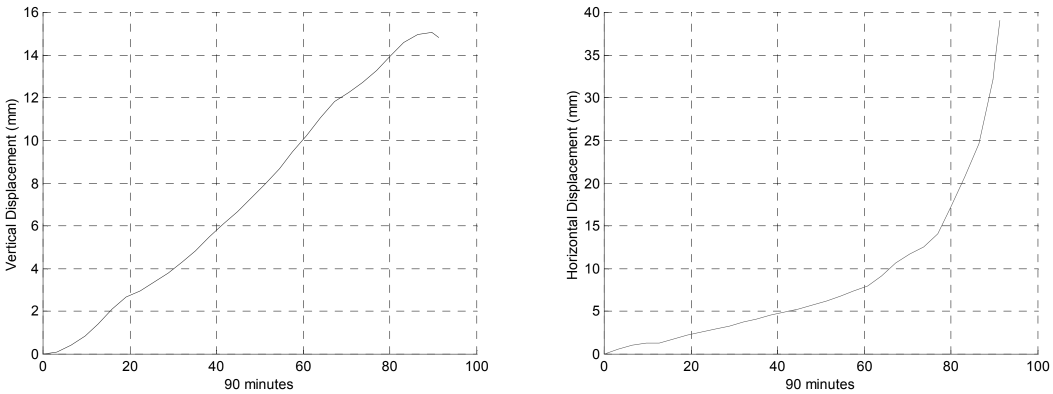

Figure C.22 Vertical and horizontal displacement.

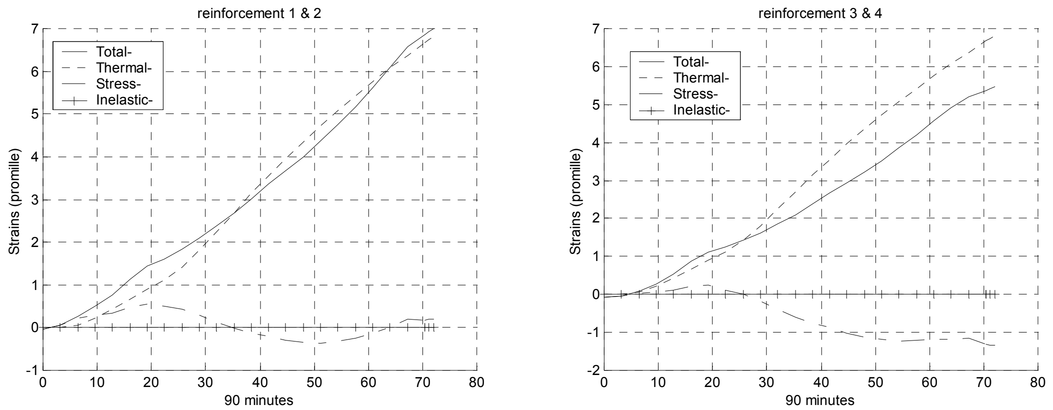

Figure C.23 Strains in reinforcement 1,2 and 3,4.

Failure at 120 minutes

Load = 85 kN

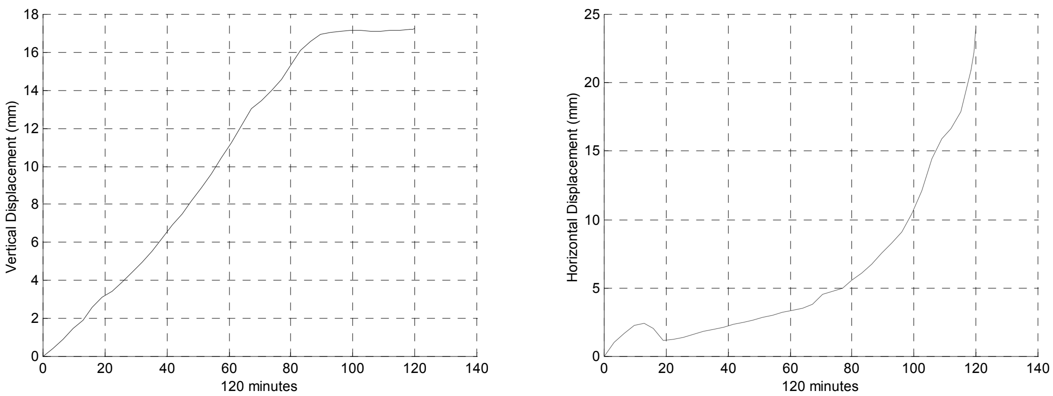

Figure C.24 Vertical and horizontal displacement.

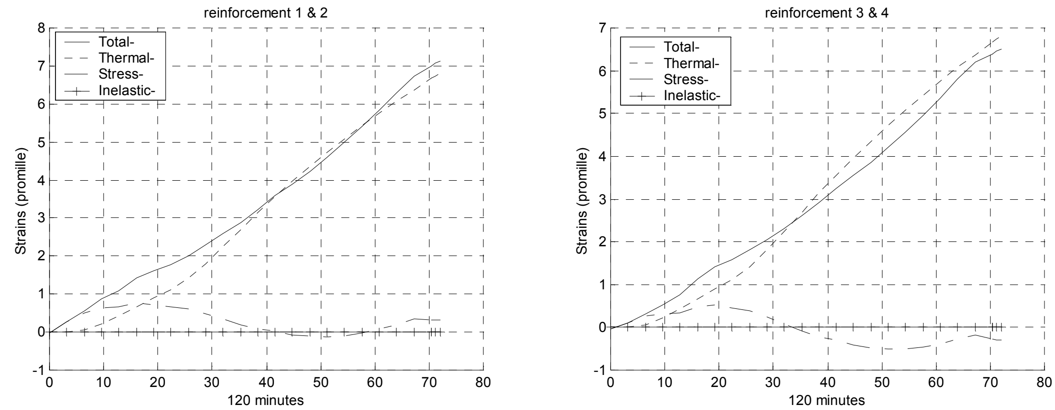

Figure C.25 Strains in reinforcement 1,2 and 3,4.

COLUMN 4

	R30	R60	R90	R120
1,2 strain$_{\sigma}$ (promille)	1,04	0,54	-0,02*	0,11*
1,2 $\sigma_{failure}$ (MPa)	214	93	3*	16*
3,4 strain$_{\sigma}$ (promille)	-2,1	-1,83	-0,71*	-0,013*
3,4 $\sigma_{failure}$ (MPa)	-422	-304	-106*	-2*
$\sigma_{0,5\%\ strain}$ (MPa)	348	270	168	84
Temperature (C^{o})	162	418	580	685

*Table C.4 Stress and stress related strain at failure. *The program could not write to the output file after 73 minutes.*

Failure at 30 minutes

Load = 430 kN

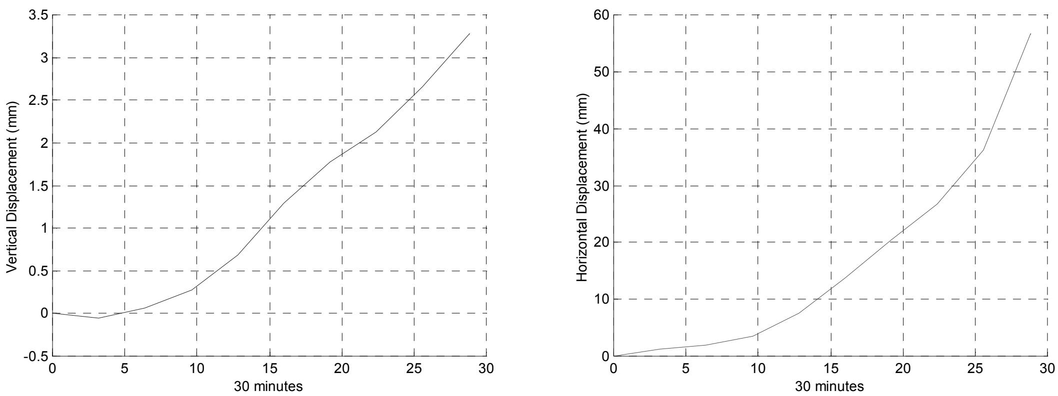

Figure C.26 Vertical and horizontal displacement.

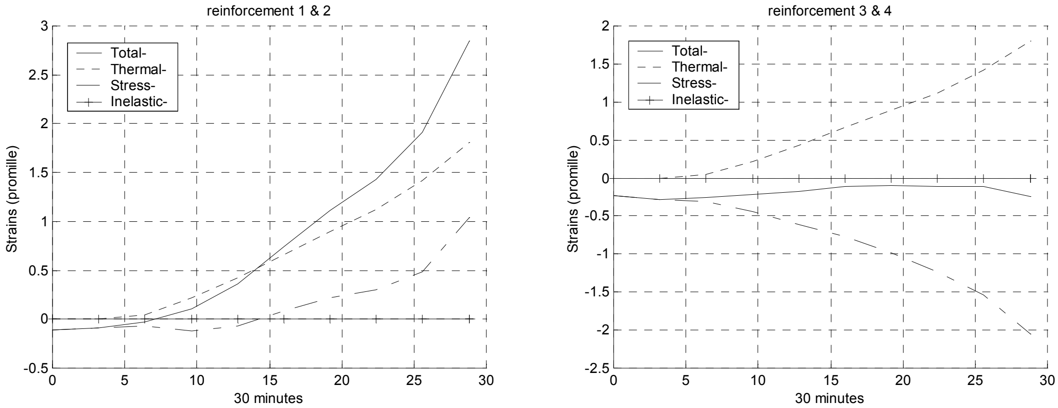

Figure C.27 Strains in reinforcement, 1, 2 and 3, 4.

Failure at 60 minutes

Load = 290 kN

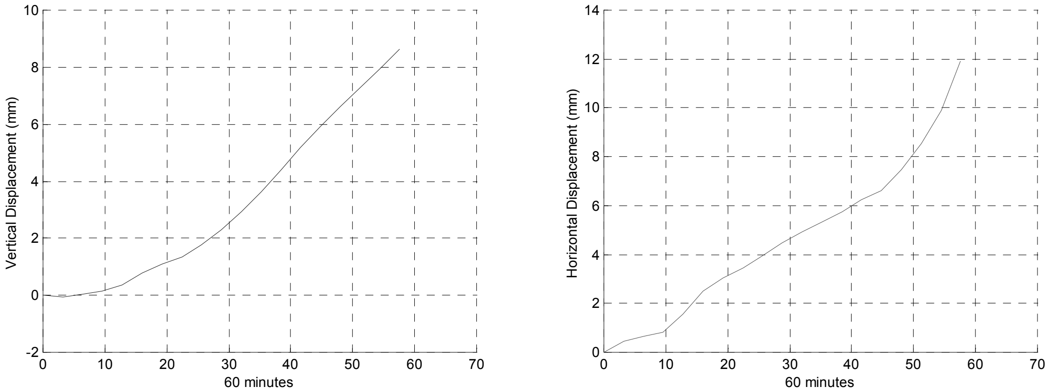

Figure C.28 Vertical and horizontal displacement.

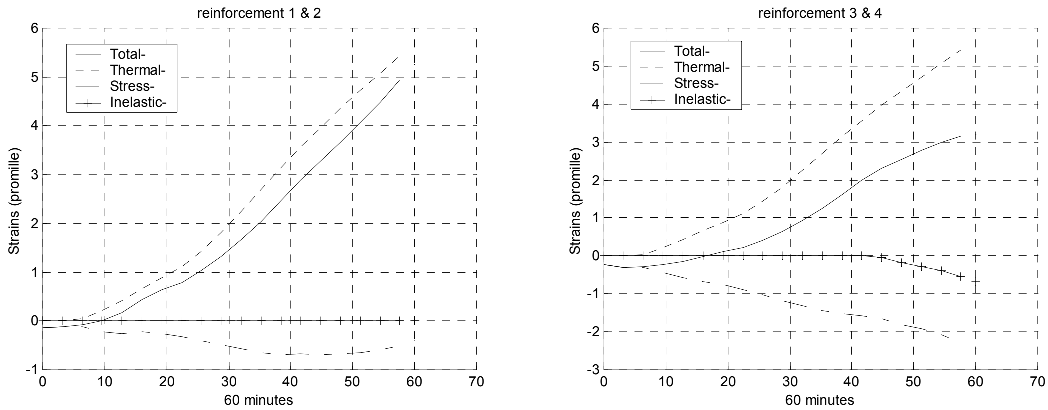

Figure C.29 Strains in reinforcement 1 & 2 and 3 & 4.

Failure at 90 minutes

Load = 200 kN

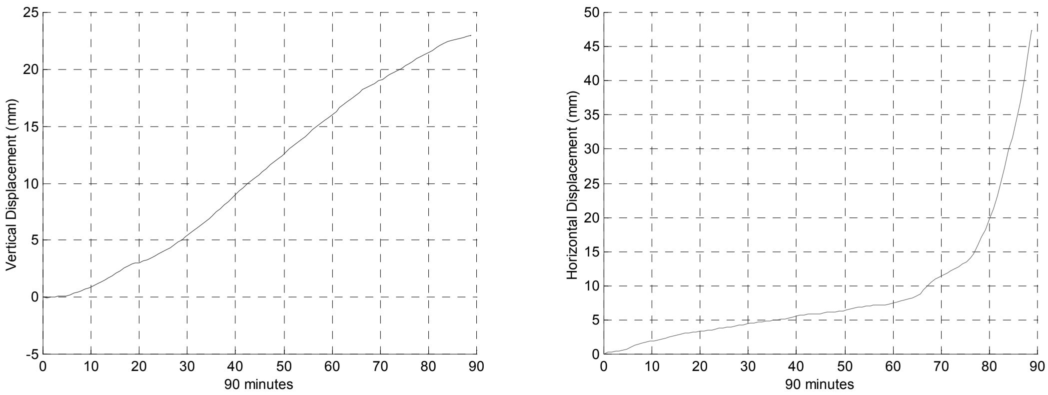

Figure C.30 Vertical and horizontal displacement.

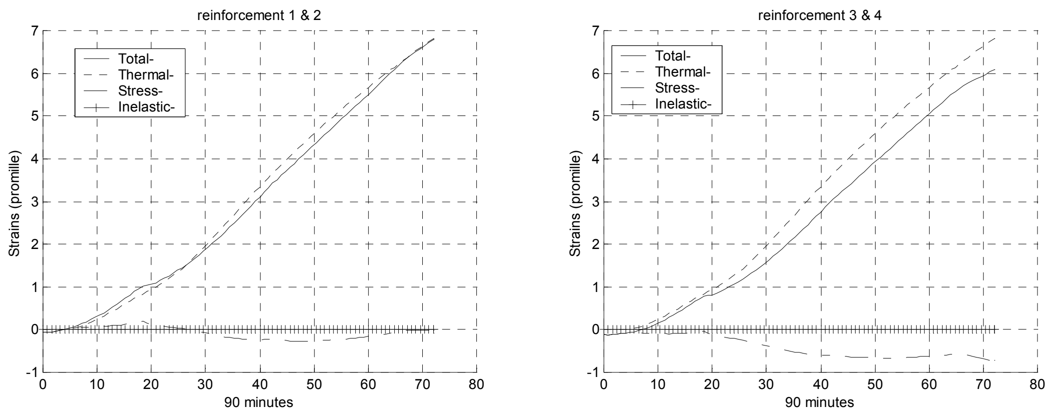

Figure C.31 Strains in reinforcement 1 & 2 and 3 & 4.

Failure at 120 minutes

Load = 80 kN

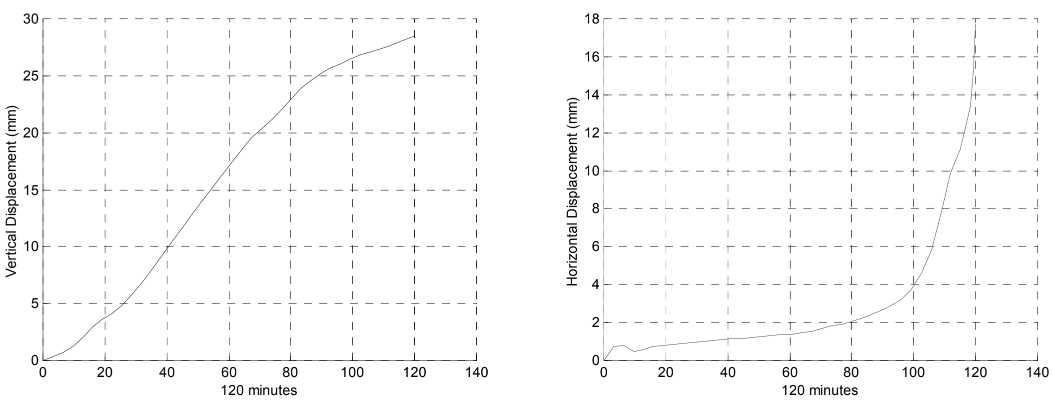

Figure C.32 Vertical and horizontal displacement.

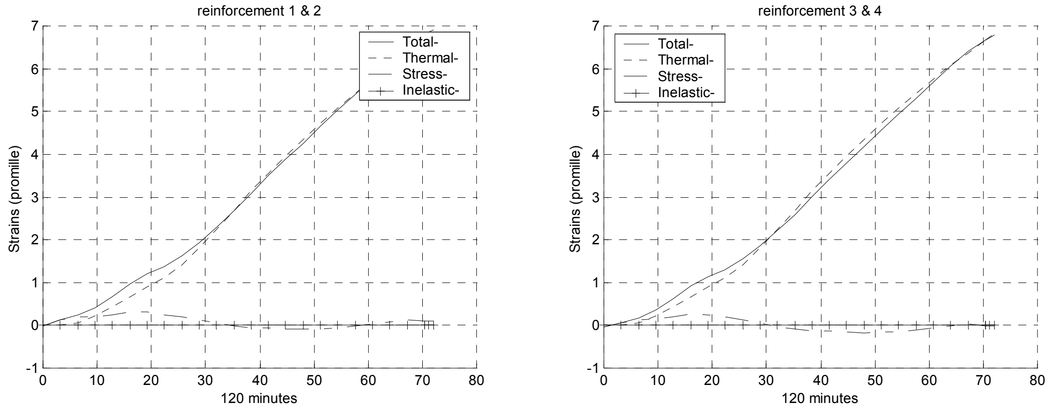

Figure C.33 Strains in reinforcement 1 & 2 and 3 & 4.

COLUMN 5

	R30	R60	R90	R120
1,2 strain$_\sigma$ (promille)	-1,2	0,33	-0,62*	-0,47*
1,2 $\sigma_{failure}$ (MPa)	-247	57	-91*	-69*
3,4 strain$_\sigma$ (promille)	-45,1	-10,3	-6,2*	-0,86*
3,4 $\sigma_{failure}$ (MPa)	-433	-327	-263*	-127*
$\sigma_{0,5\%\ strain}$ (MPa)	348	270	168	84
Temperature (C^o)	162	423	580	685

*Table C.5 Stress and stress related strain at failure. *The program could not write to the output file after 73 minutes.*

Failure at 30 minutes

Load = 1900kN

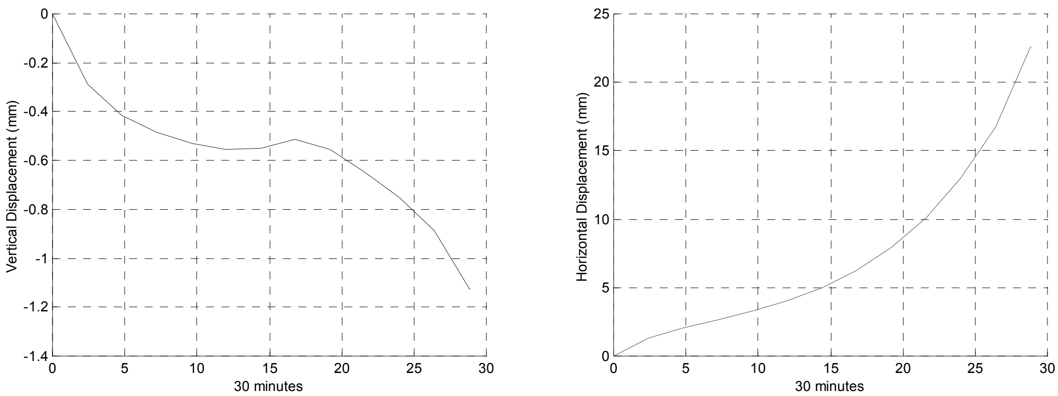

Figure C.34 Vertical and horizontal displacement.

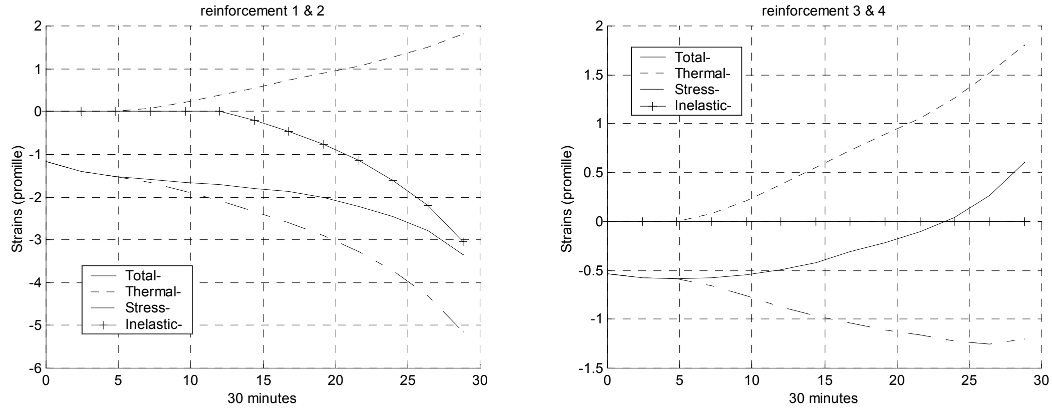

Figure C.35 Strains in reinforcement 1 & 2 and 3 & 4.

Failure at 60 minutes

Load = 1050 kN

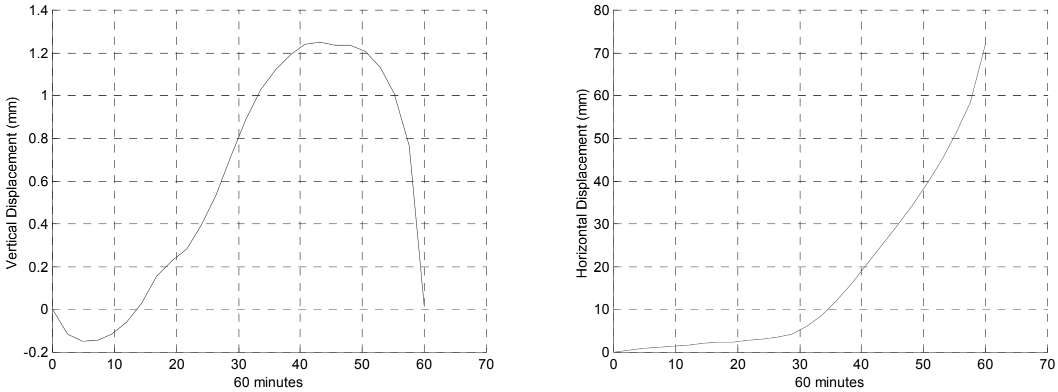

Figure C.36 Vertical and horizontal displacement.

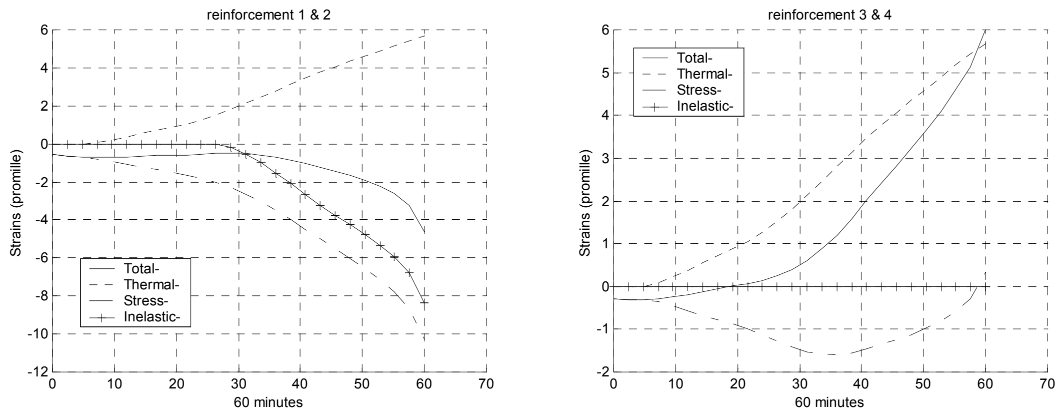

Figure C.37 Strains in reinforcement 1 & 2 and 3 & 4.

Failure at 90 minutes

Load = 650kN

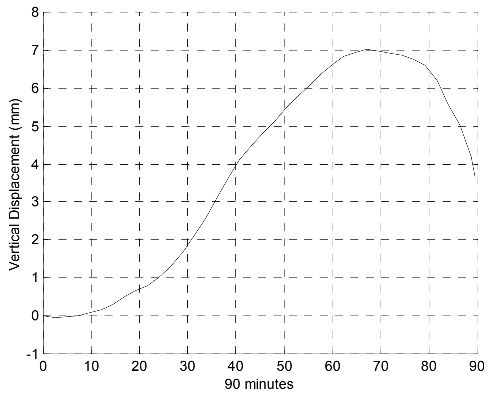

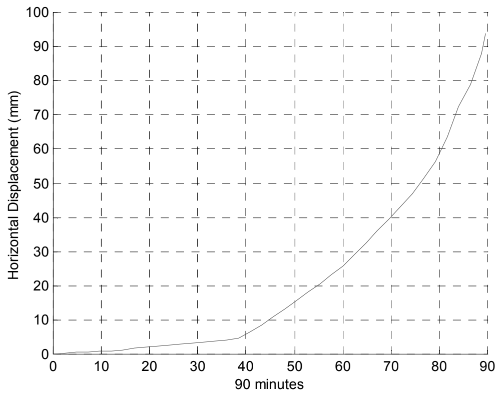

Figure C.38 Vertical and horizontal displacement.

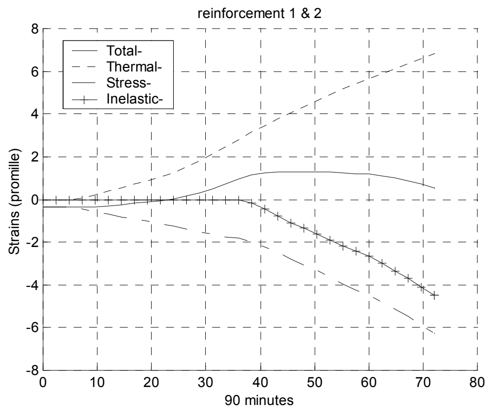

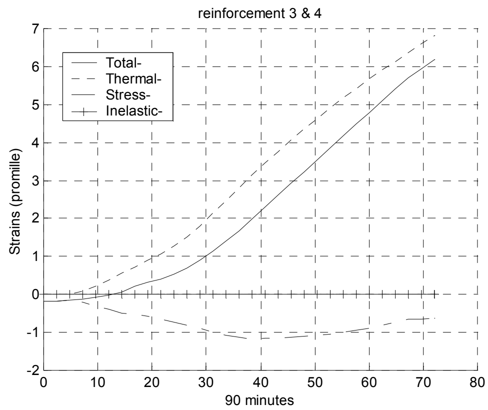

Figure C.39 Strains in reinforcement 1 & 2 and 3 & 4.

Failure at 120 minutes

Load = 290kN

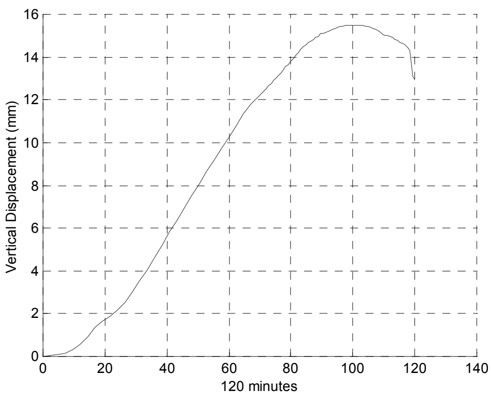

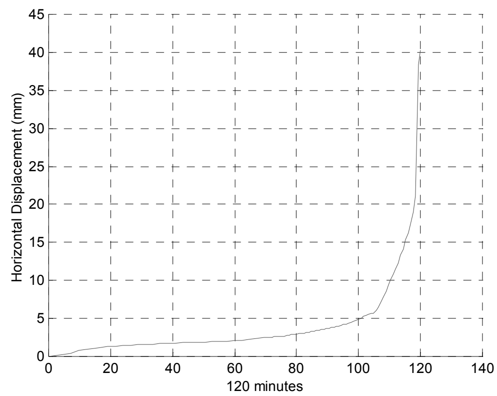

Figure C.40 Vertical and horizontal displacement.

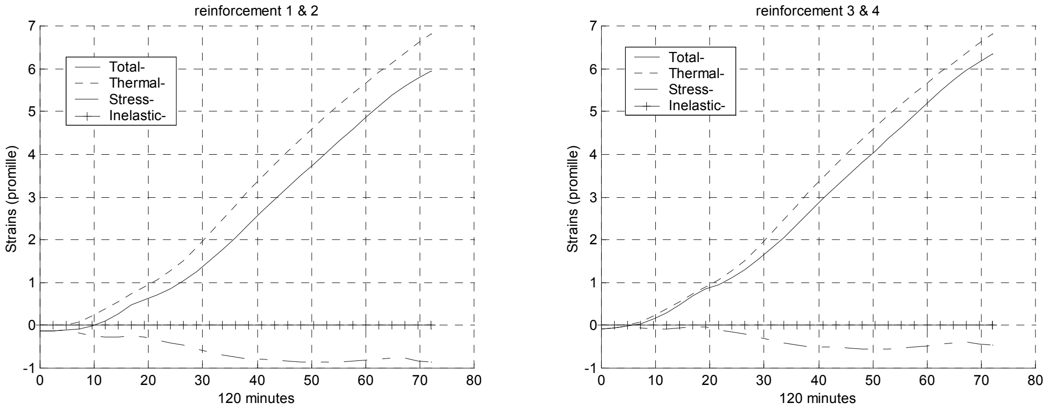

Figure C.41 Strains in reinforcement 1 & 2 and 3 & 4.

D. BKR, INTERACTION DIAGRAMS

COLUMN 1

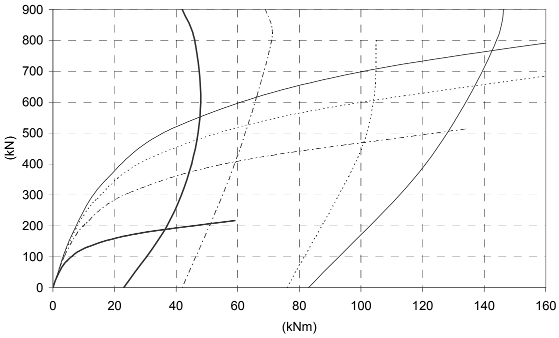

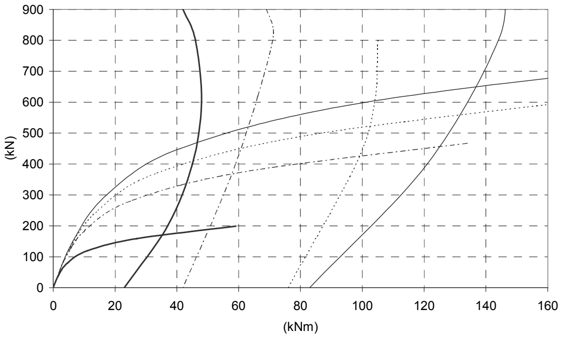

Figure D.1 Load-bearing capacity at 30, 60, 90 and 120 minutes with no reduction of steel area.

Figure D.2 Load-bearing capacity at 30, 60, 90 and 120 minutes with the steel area reduced with 0,5.

COLUMN 2

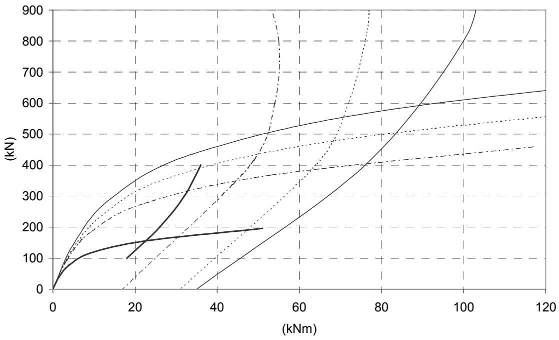

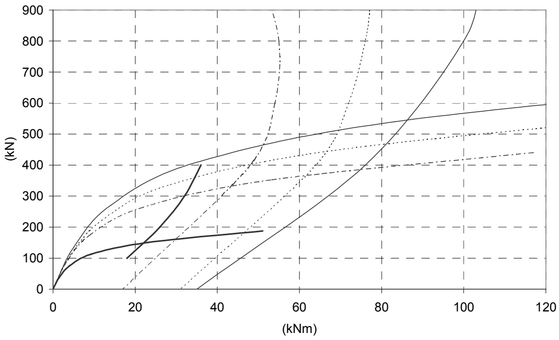

Figure D.3 Load-bearing capacity at 30, 60, 90 and 120 minutes with no reduction of steel area.

Figure D.4 Load-bearing capacity at 30, 60, 90 and 120 minutes with the steel area reduced with 0,5.

COLUMN 3

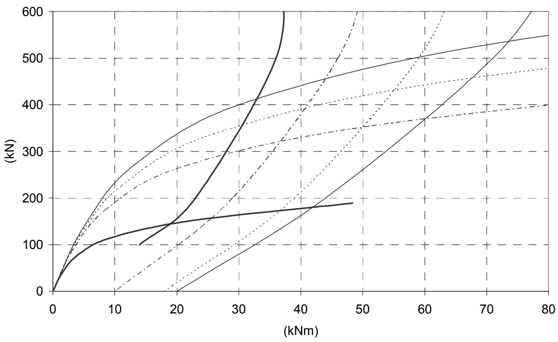

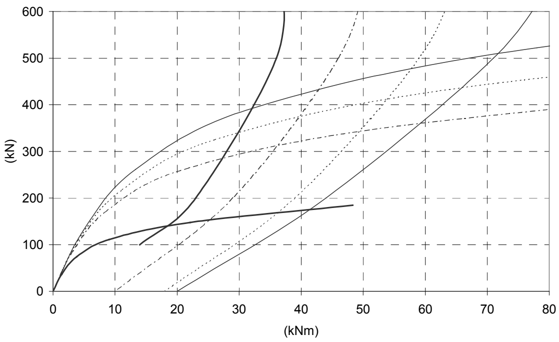

Figure D.5 Load-bearing capacity at 30, 60, 90 and 120 minutes with no reduction of steel area.

Figure D.6 Load-bearing capacity at 30, 60, 90 and 120 minutes with the steel area reduced with 0,5.

COLUMN 4

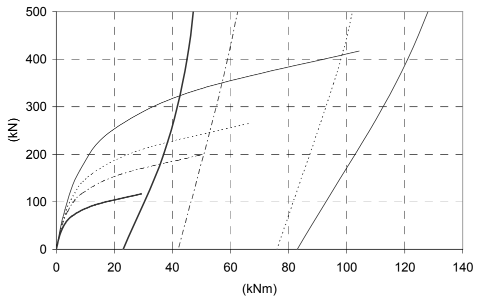

Figure D.7 Load-bearing capacity at 30, 60, 90 and 120 minutes with no reduction of steel area.

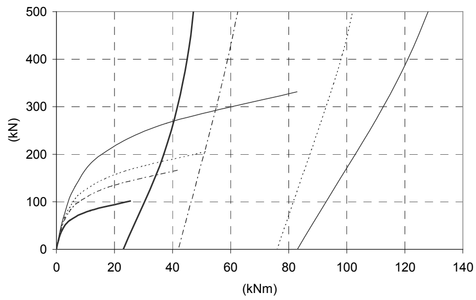

Figure D.8 Load-bearing capacity at 30, 60, 90 and 120 minutes with the steel area reduced with 0,5.

COLUMN 5

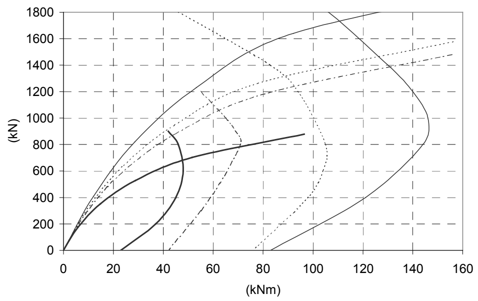

Figure D.9 Load-bearing capacity at 30, 60, 90 and 120 minutes with no reduction of steel area.

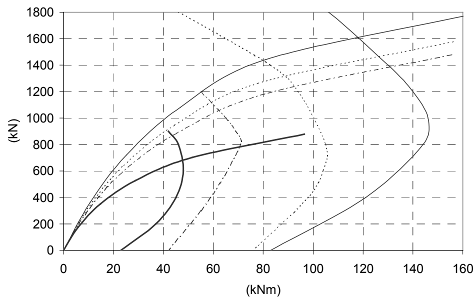

Figure D.10 Load-bearing capacity at 30, 60, 90 and 120 minutes with the steel area reduced with 0,5.

E. EUROCODE, INTERACTION DIAGRAMS

COLUMN 1

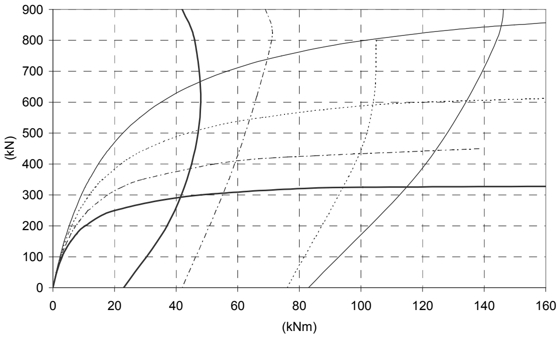

Figure E.1 Load-bearing capacity at 30, 60, 90 and 120 minutes with ϕ_{eff}= 0.

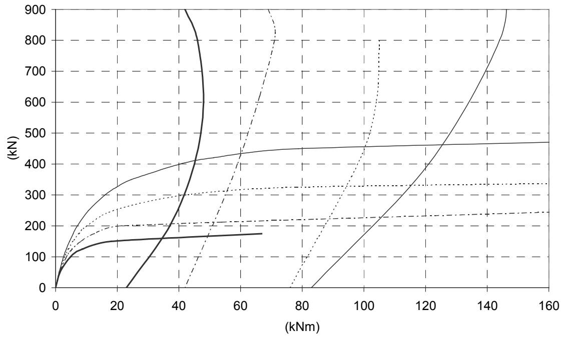

Figure E.2 Load-bearing capacity at 30, 60, 90 and 120 minutes with ϕ_{eff}= 0,9.

COLUMN 2

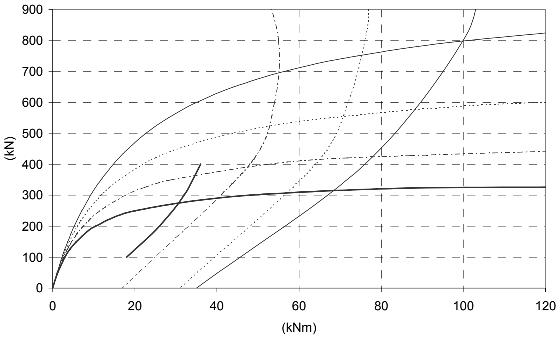

Figure E.3 Load-bearing capacity at 30, 60, 90 and 120 minutes with ϕ_{eff}= 0.

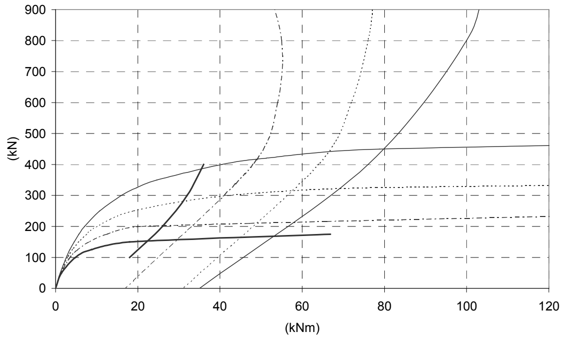

Figure E.4 Load-bearing capacity at 30, 60, 90 and 120 minutes with ϕ_{eff}= 0,9.

COLUMN 3

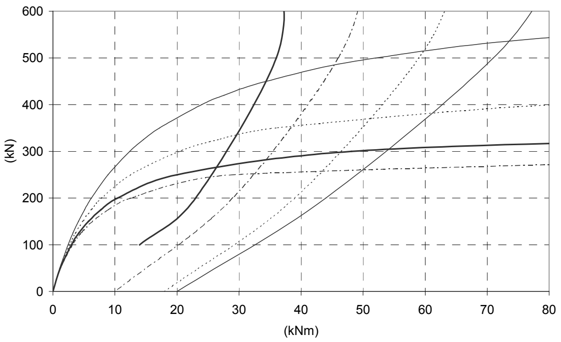

Figure E.5 Load-bearing capacity at 30, 60, 90 and 120 minutes with ϕ_{eff}= 0.

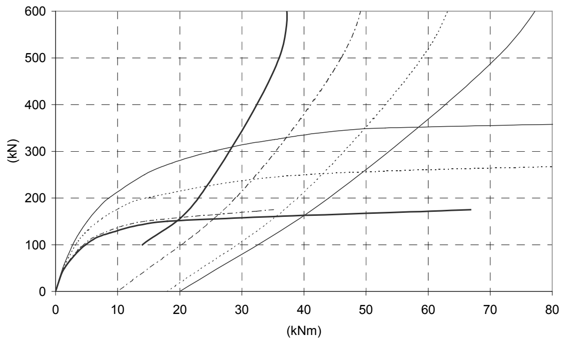

Figure E.6 Load-bearing capacity at 30, 60, 90 and 120 minutes with ϕ_{eff}= 0,9.

COLUMN 4

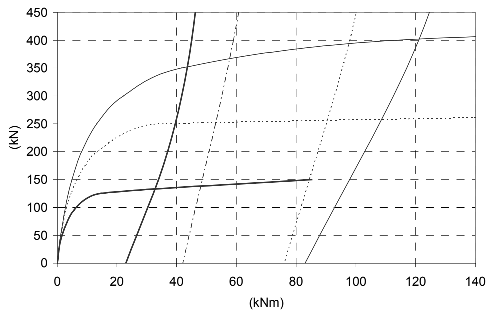

Figure E.7 Load-bearing capacity at 30, 60, 90 and 120 minutes with ϕ_{eff}= 0.

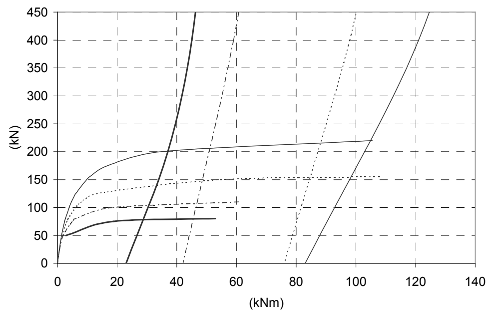

Figure E.8 Load-bearing capacity at 30, 60, 90 and 120 minutes with ϕ_{eff}= 0,9.

COLUMN 5

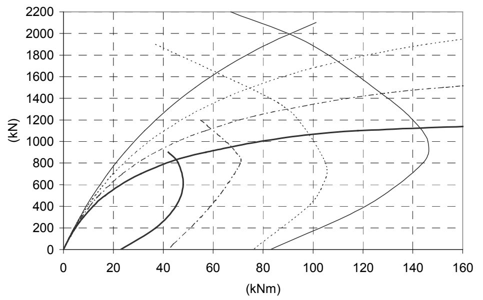

Figure E.9 Load-bearing capacity at 30, 60, 90 and 120 minutes with ϕ_{eff}= 0.

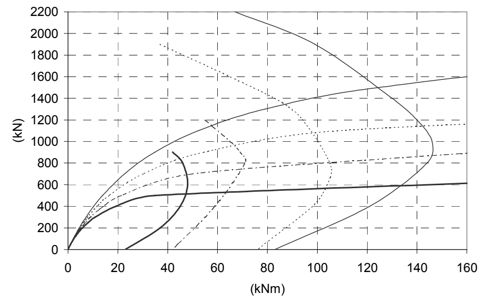

Figure E.10 Load-bearing capacity at 30, 60, 90 and 120 minutes with ϕ_{eff}= 0,9.

F. COMPUTER PROGRAMS

TEMPERATURE CALCULATION AND DESIGN

The computer software TCD, *Temperature Calculation and Design*, is a tool for thermal analysis of fire exposed structures. The three main parts are

- Graphical User Interface for pre- and postprocessing
- SUPER-TEMPCALC
- Fire Design

the graphical user interface of the current TCD version is a MATLAB-toolbox, compatible with MATLAB v5.2 or higher.

SUPER-TEMPCALC is a 2-dimensional, fire-dedicated finite element program, which have been under continuously development since 1985. The differential equation for 2-dimensional heat flow is derived from conservation of energy, describing the fact that total inflow per unit time equals the total outflow per unit time. The constitutive relation invoked is Fourier's law of heat conduction, which describes heat flow within the material. The spatial and time domains are discretized by the weighted residual approach. Boundary conditions implemented include convective and radiative heat flow and heat exchange within enclosures. 4-node rectangular and 3-node triangular finite elements are used. Thermal properties of materials are described as temperature dependent. The heat transfer system can be solved in rectangular, cylindrical or polar coordinate systems. The Tempcalc engine is a standalone executable WIN32 application.

Fire Design is a fire-dedicated tool for calculating

- Bending moment capacity of steel beams (S-Beam)
- Bending moment capacity of reinforced concrete beams (C-Beam)
- Bending moment capacity of composite steel and concrete beams (Beam)
- Compression resistance, critical Euler buckling capacity and design load capacity of steel, concrete or composite steel and concrete columns (Compress).

TCD has been developed by Fire Safety Design.

CONFIRE

CONFIRE is a program for analysing plane concrete frames subjected to inplane loading and temperatures varying with time. The analysis is based on a non-linear displacement formulation of the finite element method using two dimensional beam elements. The non-linear geometric effects are taken into account by updating the nodal coordinates of the structure during deformation. In the material model the total strain, ε_{tot}, is restricted to vary linearly in the lateral (Bernoulli-Navier hypothesis) and longitudinal directions for each element. Furthermore the strain is restricted to be constant over the width of the cross-sections. The program requires several kinds of input data; cross-sectional measures, cross-sectional temperature filed as a function of time, mechanical data for concrete and reinforcement, load and eccentricities, structural data including topology, boundary conditions including information on supports as well as about the incremental iteration process and time increments. A principal model of the analysed columns in CONFIRE is shown in figure F.1.

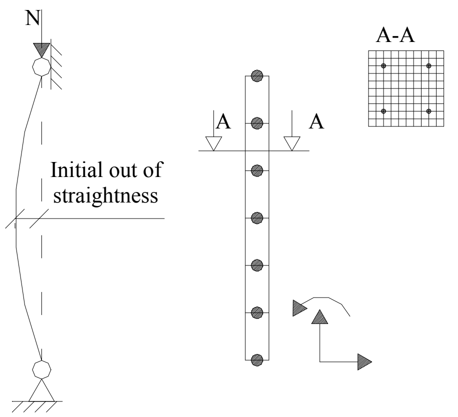

Figure F.1 Simplified structure model and cross-section used in CONFIRE.

CONFIRE has been developed by Nils-Erik Forsén, Multiconsult AS, Oslo.